ARR No. 3I11

NATIONAL ADVISORY COMMITTEE FOR AERONAUTICS

WARTIME REPORT

ORIGINALLY ISSUED
September 1943 as
Advance Report 3I11

WIND-TUNNEL VIBRATION TESTS OF DUAL-ROTATING PROPELLERS

By Mason F. Miller

Langley Memorial Aeronautical Laboratory
Langley Field, Va.

NACA

WASHINGTON

NATIONAL ADVISORY COMMITTEE FOR AERONAUTICS

ADVANCE [redacted] REPORT

WIND-TUNNEL VIBRATION TESTS OF DUAL-ROTATING PROPELLERS

By Mason F. Miller

SUMMARY

Vibration tests of six- and eight-blade tractor and seven- and eight-blade pusher dual-rotating propellers were conducted in the Langley Memorial Aeronautical Laboratory 16-foot high-speed tunnel chiefly to determine the severity of vibrations excited by blade passages, A pusher design with a wing located ahead of the propellers and displaced 50 percent of the propeller radius below thrust-axis level was simulated. Measurements of vibratory stresses of the propellers were made for engine-speed ranges at low, intermediate, and high engine powers,

Few propeller vibrations caused by blade passages were detected; those vibrations found were not serious. Although there were indications of vibrations excited by the wing, the vibratory stresses generally were at satisfactorily low levels, The responses of the front and the rear blades to engine excitation were similar; the stresses of the rear blades were generally higher, probably because the rear propeller was more rigidly coupled to the engine than the front propeller, Some indications of vibrations excited by propeller-shaft whirl caused by gas forces were found, The engine-excited vibratory stresses increased with engine brake mean effective pressure and sometimes reached high values,

INTRODUCTION

It was anticipated that dual-rotating propellers would be subject to vibrations excited aerodpaamically by blade passages, Because reactionless types of vibration for certain dual-rotating propellers can occur with this excitation, it vas expected that some of the vibrations could be serious,

INTRODUCTION

It was anticipated that dual-rotating propellers would be subject to vibrations excited aerodynamically by blade passages, Because reactionless types of vibration for certain dual-rotating propellers can occur with this excitation, it was expected that some of the vibrations could be serious,

Although previous torcue-stand tests indicate that vibrations excited by blade passages are not serious, it was decided to perform a series of tests with ground-adjustable propellers in a wind tunnel where not only a high airspeed can be attained but also the airspeed can be varied to hold the engine brake mean effective pressure constant over a wide range of engine speed,

Vibration tests were conducted in the LMAL 36-foot high-speed tunnel, Six- and eight-bfade dual-rotating propellers were operated as tractors, and seven- and eight-blade dual-rotating propellers were operated as pushers; the pusher condition was simulated by mounting a full-scale wing ahead of the propellers, Measurements of propeller stress were made for engine-speed ranges at low, intermediate, and high engine powers, with a range of airspeeds up to 280 miles per hour,

The vibration staffs of Hamilton Standard Propellers and the Curtiss-Wright Corporation Propeller Division collaborated In conducting the tests and in analyzing the records.

GENERAL DISCUSSION OF PROPELLER VIBRATIONS

Modes of vibration.- A propeller blade may vibrate in any one of several modes; examples of mode shapes are given in figure 1, The airplane engine enforces a node at the propeller center, although the center mag actually have an amplitude of displacement of the order of thousandths of an inch, The amplitudes of the tips are of the order of tenths of an inch, If the node enforced by the engine is not counted, the number of nodes for figure 1 *is* m - 1, where m is the number of the mode, The vibratory frequency increases somewhat with the number of tha mode, The frequencies of the various modes of a blade may be determined by vibrating the blade with some driving oscillator, If the damping of the

blade is very small, the frequency for a maximum response is a natural frequency of vibration; whereas, if the damping is appreciable, the frequency for maximum response is somewhat less than the natural frequency. Centrifugal force increases the natural frequencies for the various nodes and shifts the positions of all the nodes except the node enforced by the engine (reference 1). The nodes can also be shifted by changing the blade angle of the propeller, The shift of node positions can be several Inches.

Types of vibrations.- A propellor vibration may be flatwise, edgewise, or torsional. A vibration is considered flatwise if the vibratory motions of the sections of the blade are primarily in a direction perpendicular to the blade chords. For an edgewise vibration, the motions of the blade sections near the shank are primarily along the blade chords, while the motions near the tips are more flatwise. The flatwise motion of the tips for an edgewise resonance occurs because of the blade twist. Experiments show that, if tho natural frequency for one of the higher flatwise nodes is near the natural, frequency for the first edgewise mode, the motions near the blade tip during edgewise resonance are so flatwise that it is difficult to tell from the stress distribution along the blade whether tho vibration is flatwise or edgewise (reference 2). The stress distribation around the blade shank, however, shows which vibration is occurring. The blade motion for edgewise resonance generally is such that the two maximum-stress positions on the shank are in line with the leading edge and the trailing edge at approximately three-fourths the propellor radius. The maximum-stress positions for flatwise resonance are shifted 90° from the maximum-stress positions for edgewise resonance. For torsional vibration of a blade, the blade twists periodically about a longitudinal axis within the blade. The frequency of this vibration is relatively high, however, and only the fundamental mode is ever encountered. This viljration occurs infrequently in comparison with the flatwise and edgewise vibrations.

Stress distribution on blade.- For flatwise vibration, the maxiam-stress positions along the blade correspond to the positions of maximum c/ρ where c is the perpendicular distance of the extreme fiber from the neutral axis and ρ is the radius of curvature of the neutral axis. Far the first mode, the minimum radius of curvature is somewhere near the propeller hub (fig. 1); whereas, for the higher modes, the positions of minimum radius of curvature are between the nodes, For a given blade section, maximum c occurs at maximum blade thickness.

For edgewise resonance the positions of maximum stress again correspond to positions of maximum c/ρ. For this vibration, however, c is not generally a maximum at maximum blade thickness, because the motions of the blade sections are more edgewise.

For flatwise and edgewise vibration, the distribution of surface-fiber stress around the propeller shank is sinusoidal because the perpendicular distance of the surface fiber from the neutral axis of the vibration considered varies sinusoidally in a circular section.

Classification of types of vibration.- The flatwise and edgewise vibrations of a single-rotating propeller may be grouped under three general headings according to the vibratory bending moments and the vibratory fore-and-aft forces acting on the propeller shaft. The three classes of vibration are as follows: (1) Propeller vibrations with a vibratory fore-and-aft force but no vibratory bending moment acting on the propeller shaft; (2) propeller vibrations with a vibratory bending moment but no vibratory fore-and-aft forces acting on the propeller shaft; and (3) propeller vibrations with neither a vibratory bending moment nor a vibratory fore-and-aft force acting on the propeller shaft. These vibrations are often called symmetrical, unsymmetrical, and reactionless, respectively. For the symmetrical vibrations, all the blades vibrate in phase; for the unsymmetrical vibrations, the blades vibrate out of phase (120° for a three-blade single-rotating propeller); and, for the reactionless vibrations, the blades vibrate out of phase. The engine may afford some damping for either the symmetrical or the unsymmetrical vibration but obviously cannot supply damping for the reactionless vibration.

The classification of vibrations given is academic; a propeller vibration is frequently a combination of two classes and quite feasibly can be a combination of all three classes.

It is evident that the reactionless vibration receives its excitation from aerodynamic forces instead of from engine forces. Because an analysis shows that reactionless vibrations of single-rotating propellers can occur for all frequencies other than 1, kB, and kB ±1 times propeller speed, where k is any integer and B is the number of blades, it is observed that a propeller must have more than three blades to vibrate in a reactionless manner. (See reference 3.) As will be seen later, reactionless vibrations between propellers of a dual-rotating unit can

occur at frequencies of kB times the propeller speed, if the two propellers have equal numbers of blades,

Determination of static natural frequencies.— The natural frequencies for a nonrotating propeller can be measured by vibrating the blades and taking oscillograph records of strain, using electrical strain gages for pickups; the frequencies of the strain variations can be accurately determined by comparing the traces of strains with a trace produced by an accurately calibrated electrically excited tuning fork. The modes can be distinguished from each other by the records showing strain distribution along the blade, The records showing strain distribution around. the shank can be used Lo distinguish between flatwise and edgewise vibrations, The static natural frequencies of a propeller are appreciably affected by the looseness of blade retention, It is therefore desirable when determining the static natural frequencies to have a blade retention corresponding as nearly as possible to the retention obtained with propeller rotation.

The natural frequencies used for estimating the engine speed for the first two classes of vibration are obtained by vibrating the blades with a mechanical exciter, that is, a rotating unbalanced mass, mounted at the propeller hub, If the propeller is suspended with an elastic sling, the natural frequencies of the propeller proper are determined; these natural frequencies are somewhat different from those determined with the propeller coupled to the engine. It is therefore desirable to determine the natural frequencies with the propeller coupled tc the engine that is to drive the propeller.

Tho natural frequencies of reactionless vibrations can be determined with excitation supplied ai; a blade tip. The propeller mag rest on its hub, which need not be restrained, because for a reactionless vibration tho vibratory bending moments and the forces of tha various blades cancel at the hub. For raactionless vibrations of dual-rotating combinations composed of two propellers each having fewer than four blades, the static frequencies are found by measuring those of a single-rotating four-blade propeller having blades of the same design,

Especially for flatwise vibrations of solid blades, the positions of maximum stress with rotation can be determined fairly well by finding the positions with the propeller not rotating and than applying suitable corrections for centrifu-

gal force, In order to determine the maximum-stress positions for a hollow steel blade, records from strain gages mounted at many positions on the blade are needed, These records are necessary because the flexural vibration of a hollow steel blade produces a diaphragm vibration! that is, the two faces bend in and out like the head of a drum, Some gages are mounted transversely on the hollow steel blades to record the diaphragm stress,

Fig. 5

Correction of static frequencies for centrifugal force.- The static natural frequencies of vibration are corrected for the effect of centrifugal force by using the accepted formula (reference 1)

$$f^2 = f_o^2 + Kn^2$$

where

f_o static natural frequency

K constant for a given node of a given propeller

n propellar speed

f natural frequency at that propeller speed,

The effect of centrifugal force upon the natural frequencies of the first flatwise, the second flatwise, and the first edgewise modes of reactionless vibrations of a typical propeller is shown in figure 2, The values of K used for these mod-es of this propeller are 1.7, 5.6, and 1.12, respectively. The static natural frequencies for the propeller represented by figure 2 were determined with a 'blade retention corresponding as nearly as possible to the retention obtained with the propeller rotating. The line labeled 6n represents a frequency of excitation of six times propeller speed such as would. be expected with blade interferences of two three-blade propellers rotating in opposite directions, The intersections of the line representing the excitation frequency with the lines representing natural frequencies yield the speeds at which the reactionless vibrations are expected,

Vibrations excited by blade passages.- Propeller vibrations can be excited b;~the passage of blades through regions of disturbed air flow caused by obstructions in the air stream

or by another propeller, Dual-rotating propellers are subject to vibrations caused by the passage of blades of one propeller near the blades of the other propeller. The type of propeller vibration produced by blade-passage excitation depends upon the number of blades of each of the two propellers forming the dual-rotating unit, Blade-passnge excitation may produce a raactionless vibration of a dual-rotating unit composed of two propellers having equal numbers of blades. Because the engine absorbs no energy from the reactionless vibration of the dual-rotating propeller, the vibratory stresses are limited only by aerodynamic damping, by hysteresis damping of the blade material, and by damping provided by motion of the blade shanks in their hub sockets,

A reactionless type of vibration for a dual-rotating propeller can occur with blade passages in a slightly different manner from thct for a single-rotating propeller, For the reactionless vibration of the dual-rotating unit composed of two propellers having equal numbers of blades, the vibratory bending moments of the several blades of each propeller cancel at the respective shafts and the fore-and-aft vibratory force acting on the shaft of each of the two propellers cancels with that of tho other; this cancelation occurs through the propeller shafts, the reversing gear, and the thrust bearing. The blades of either propeller vibrate in phase with one another, but the blades of one propeller vibrate 180° out of phase with the blades of the other propeller, The vibration frequencies of the two propellers are equal for the cancelation of hub forces; and the number of blade passages encountered By each blade of one propeller per propeller revolution is equal to twice the number of blades of the other propeller, because the two porpellers rotate at the same speed but in opposite directions, The vibration of a single-rotating propeller (one of the two propellers for the case of dual rotation} at a frequency equal to propeller speed times an integral multiple of the number of its blades is always a vibration with no resultant vibratory moments but with a resultant fore-and-aft vibratory force acting on tho propeller shaft,

If the propellers forming the dual-rotating unit have unequal numbers of blades, each blade of one propeller of the unit encounters a number of blade passages different from that eucountered by each blade of the other propeller, and the front propeller therefore vibrates at a different frequency from the rear propeller, With this dual-rotating propeller having an odd total number of blades, a reaction-less vibration of the propeller unit may occur only when both

the propellers forming the dual-rotating unit individually vibrate in a reactionless manner, A seven-blade dual-rotating unit composed of one three-blade and one four-blade propeller does not vibrate in a reactionless mode with blade-passage excitation because a single-rotating propeller must have more than three blades to vibrate in a reactionless mode, A nine-blade dual-rotating unit composed of a four-blade and a five-blade propeller might possible vibrate in a reactionless mode with blade-passage excitation, the four-blade propeller vibrating at a frequency of 10n and the five-blade propeller vibrating at a frequency of an,

Effect of wing for pusher condition.- A wing mounted ahead, of a dual-rotating propeller to simulate a pusher condition would be expected to provide additional. aerodynamic excitation, and the frequency of this excitation would depend upon the location of the wing, If the wing were located at thrust-axis level, the wake behind the wing would supply sizable excitation at a frequency of 2n, while the downwash behind the wing would supply some excitation at a frequency of 1n,

For a dual-ratntiqg unit with each of the propellers having four or more blades, the sizable excitation provided by the wake at the frequency of 2n can be serious; the strength of this excitation increases considerably with airspeed, The serious condition is present when the frequency of excitation is equal to the natural frequency for a reactionless vibration, Because the airspeed in the wing wake is less than the airspeed well above or below the wing, the excitation frequency of 2n occurs 'because each blade passes through two low-velocity regions per revolution,

The excitation at a frequency of 1n supplied by downwash behind the wing is small for tests performed in a closed-throat wind tunnel, because the tunnel walls limit the downwash, The downwash behind a wing aan cause a propeller to vibrate at a frequency of 1n because the downward component of velocity increases the angle of attack of the blades during one-half revolution and decreases this angle during the remaining one-half revolution,

If the wing ahead of the propeller is displaced 50 percent of the propeller radius from thrust-axis level, the main frequency os" excitation provided by the wake is expected to be at a frequency of 1n; excitation frequencies that are

harmonics of 1 n ara also expected, Because 3n is one of the lower harmonic frequencies, it is possible that the excitation at this frequency may be of sufficient strength to produce a reactionless vibration of a dual-rotating propeller composed of two three-blade propellers. Similarly, tho excitation having a frequency of 4n might possibly excite a reactionless vibration of a dual-rotating propeller composed of two four-blade propellers,

The vibration of a six-blade dual-rotating propeller excited by the wake at a frequency of 3n is reactionless if the vibratory hub forces of the two three-blade propellers cancel, The vibratory hub forces must be equal in magnitude and opposite in phase for complete cancelation, Because the phasing of the two vibratory hub forces can be regulated by the indexing of the two propellers on their shafts, a reactionless vibration excited by the wake can be changed to a nonreactionless vibration if desired, Indexing the two propellers does not control the cancelation of the vibratory hub forces that are Caused by blade passage,

With the wing displaced 50 percent of the propeller radius from thrust-axis level, it is feasible that a harmonic wake excitation of frequency 6n may exist, This frequency is the same as the frequency for a reactionless vibration excited by blade passages of two three-blade propellers, Because the wake and the blade passages are different causes of vibration, the effect of the two excitations of frequency 6n upon each propeller of a dual-rotating unit would depend upon their magnitudes and phase relationship, The phase relationship of the excitations would depend upon the indexing of the propellers, The vibratory hub forces aaused by blade passages would be expected to cancel, Depending upon the indexing of the propellers, the wake-excited vibratory hub forces of the two propellers may or may not cancel,

A harmonic wake excitation of frequency 6n may possibly excite a reactionloss vibration of each of the four-blade propellers composing an eight-blade dual-rotatfng unit, The phase relationship of the blades of one propeller with respect to the other propeller would depend upon the indexing of the propellers,

Effect of propeller on wing for pusher operation.- Because fatigue failures of the wing trailing edge have previously occurred with pusher designs, the spacing between *tho*

wing and the propeller is important, A pressure field exists about each blade element of all the blades of a rotating propeller, It is expected that the pressures within a radius of about 1 chord of the respective elements are an appreciable source of exaitation for wing vibration, It is therefore desirable that the spacing between the trailing edge of the wing and the various blade elements be greater than 1 blade chord,

The frequency of excitation of the trailing edge for a single-rotating propeller is Bn. For a dual-rotating combination, the main excitation is from the front propeller at a fequency of $B_F n$, where B_F is the number of blades of the front propeller; it is expected that the rear propeller would have relatively little effect upon the wing because it is customarily located more than 1 blade chord behind the front propeller, If the frequency of a sufficient excitation coincides with the natural frequency of either the wing as a unit or any of its parts, such as the two surfaces and trailing edge of the wing, the respective vibration systems will vibrate.

No vibrations of the wing were detected for the tests reported in refereace 4; the blade sections at three-fourths the propeller radius operated at approximately twice their chords behind the trailing edge of the wing,

Engine-excited vibrations.- As will be seen in the results for these tests, propeller vibratory stresses excited by the airplane engine can be high, A basic discussion of the important frequencies expected with engine excitation is therefore of interest, although the determinatioa of aerodynamically excited vibratory stresses was the primary purpose of the present test,

An important symmetrical propeller vibration is caused by the torsional oscillation of the propeller shaft, that is, the periodic twisting of the propeller shaft about its axis of rotation, With this excitation all the propeller blades vibrate in phase because each blade receives the same excitation from the propeller shaft; the frequency of vibration of the blades is the same as that for the shaft, The torsional oscillation of the shaft. is produced chiefly by gas forces: the important frequency is

$$\frac{KX}{2} N$$

where

κ integer

x number of cylinders of the radial-engine bank

N engine speed.

Whirl of the propeller shaft can be produced by gas forces and often results in high vibratory stresses of propellers. A point on the proyeller-shaft axis traces an orbit when the shaft whirls, The frequencies expected from theoretical consideration are $\left(\frac{\kappa x}{2} \pm 1\right) N$ (reference 3). The plus sign indicates forward whirl, that is, in the same direction as engine-shaft rotation, and the minus sign indicates reversal whirl. When κ is zero, only the plus sign is used, inasmuch as tho analysis shows that a whirl of frequency 1 N is only forward,

The frequency of vibration of the propeller blades differs from the frequency of whirl of the propeller shaft by the propeller speed (reference 5). For a dual-rotating propeller, the two propeller shafts whirl in the same direction but the propellers rotate in opposite directions. The vibration frequency of the propeller rotating in a direction opposite to the whirl of its shaft is higher than the frequency of the propeller-shaft whirl, whereas the vibration frequency of tho other propeller is lower than the frequency of propeller-shaft whirl. The propeller-blade frequencies are accordingly $f_w + N/A$ and $f_w - N/A$, where f_w is the frequency of propeller-shaft whirl in terms of engine speed, N/A represents the propeller speed, and A is the ratio of engine-shaft speed to propeller-shaft speed,

Inertia whirl at frequencies of 1 N and 2N can also cause a propeller to vibrate; these whirls are caused by unbalanced, inertia forces of the articulated connecting-rod system. The frequency of propeller vibration resulting from inertia whirl differs from the frequency of inertia whirl by the propeller speed, just as explained Cor whirl caused by gas forces.

Propeller vibrations oaused by propeller-shaft whirls are unsymmetrical,

APPARATUS AND METHODS

Propellers, engine, and nacelle.- The ground-adjustable dual-rotating propellers used for the present test are described in table I, These propellers were driven by a Pratt & Whitney R-2800-12 engine geared 26:15 and mounted on rubber mounts in a full-scale stub-wing nacelle installed in th6 LMAL 16-foot high-speed tunnel. A propeller-engine-nacelle combination is shown in figure 3.

The master rods of the 18-cylinder twin-row engine are located at cylinders 8 and 13, which are the positions for minimum torsional vibration of the engine shaft. The puck damper in the rear-bank crank of the engine damps the torsional vibrations of the engine shaft occurring at a frequency of $4\frac{1}{2}N$. For modern engines the inertial whirl of frequency 1 N is partly balanced out. For this engine, a geared counterbalance is employed to balance out partly the inertia whirl at a frequency of 2N.

The puck damper and geared counterbalance not only reduce the engine-excited propeller stresses but also reduce the vibratory stresses of engine parts.

Simulation of pusher condition.- The pusher condition was simulated by mounting a wing at 0° angle of attack ahead of the propellers (figs. 4 and 5). The inverted wing was displaced 50 percent of the propellor radius above thrust-axis level to simulate an existing design. The wing was inverted and mounted above thrust-axis level in order to locate it as near as possible to the horizontal diameter of the tunnel, the thrust axis being 9 inches below the tunnel cantor line, (See fig. 5.)

Instrumentation.- The method of recording stresses of the propeller blades can be explained with the aid of figure 6. The resistances of the strain gages on the blades, designated R_G, vary with the strains of the gages to produce fluctuating voltages the alternating components of which was applied to the amplifiers, Slip-ring devices are necessary to conduct electrical currents from the rotating propeller to the amplifiers. The amplified voltages are applied to the oscillograph, which records the amplified voltages on photographic paper, The oscillograph traces are proportional to strain and, if stress is proportional to strain, the traces represent stress variations. The steady stress is not measured

Carbon electrical strain gages (small flat sticks of carbon) were mounted on the Curtiss hollow steel blades with a hard grade of deKhotinsky cement; whereas flexible strain gages (carbon deposited on cloth) were mounted on the Hamilton Standard solid aluminum-alloy blades with very hard bakelite cement, A typical strain-gage layout on a blade is shown in figure 7, and a detailed list of strain-gage locations for all the tests appears in table II. All tho strain gages on the aluminum-alloy blades were mounted longitudinally to measure flexural stress variations. At the maximum-stress positions away from the shank, the gages were mounted so as to measure the vibratory stresses at maximum blade thicknesses. Most of the gages on the hollow steel blades were mounted in the same way as on the aluminum-alloy blades. A few of the gages on the hollow steel blades however, were mounted transversely at $-chord positions to detect diaphragm vibrations. All gages were insulated from the propellers by thin pieces of paper and the cements. Separate small wires led from one end of each gage to ths blade shanks; the other end of each gage mas connected to the small common wire leading to the shank. These small iiiaulated wires were securely fastened to the blades with Vulcalock cement. The ends of the small wires at the shanks were connected to relatively heavy stranded wires leading to the rings of one of the slip-ring devices. The heavy insulated wires were wrapped tightly to the blade shanks to prevent them from pulling off the small wires on the blades because of centrifugal force. Gages and wires mounted on a propeller blade are shown in figure 8.

Two types of slip-ring device, the "pineapple" and the flight ring, were used for each test. The pineapple was mounted ahead of the front propeller and was conneated to the gages on the front propeller; whereas, the flight ring was mounted behind the rear propeller and was connected to the gages on the rear propeller. Each of tbe pineapples has 12 silver rings of equal diameter with two silver-graphite brushes, spaced 180°, contacting each ring. The pineapple stator was restrained by a horizontal cable at thrust-axis level ahead of the dual-rotating propellers (fig. 9). One flight ring used has 10 concentric silver rings with two silver-graphite brushes oontacting each ring; the other flight ring used has 13 concentric silver rings with two silver-graphite brushes contacting each ring. The two brushes contacting each ring were connected by wires grouped in a cable. The brushes contacting each of the rings attached to the common wire of each propeller were connected to a battery (fig. 6). The rest of the brushes mere connected

to their respective balancing resistors. Figure 10 shows an inside view of a flight ring,

The resistances designated R_B in figure 6 are called balancing resistances because they must be equal to the strain-gage resistances R_G for maximum alternating-voltage input to the amplifier. The balancing box is composed of variable resistors, and each resistance is capable of adjustment to a value equal to the resistance of a particular strain gage to which it is connected.

A separate attonuator was used with each amplifies (fig, 6). The attenuators are merely potentiometers having several switching points and control the input voltages of the amplifiers to regulate the size of the oscillograph traces.

Three banks of voltage amplifiers, each bank consisting of four amplifiers, were used for each test; a switching arrangement was used in order that more than 12 strain-gage recordings could be made for a given operating condition, The voltage amplification of the amplifiers Is essentially constant over the frequency range from 5 to 2500 cycles per second.

The output voltage of each amplifier mas applied to one of 12 oscillograph elements in an oscillograph. Twelve voltage traces representing strain variations appeared on the photographic paper, and each trace mas often composed of several frequency components. In order to determine the frequencies of vibration in terms of engine speed or of propeller speed, one of the 12 channels was used to record. a periodic induced voltage occurring either with every engine revolution or with every propeller revolution.

An induced voltage with every propeller revolution is obtained by having a small Alnico magnet imbedded in the rotor of the pineapple pass a small coil in the stator with every propeller revolution. The small induced voltage must be amplified, and the amplified voltage is applied to an oscillograph element,

Records of engine speed are obtained by employing a contact in series with a battery and an oscillograph element; the contact makes and breaks with every revolution of the engine shaft. These records may also be obtained by placing a few turns of wire around a spark-plug lead and connecting this small coil to an oscillograph element.

The alternating voltages across some of the balancing resistors were also applied to the input terminals of a wave analyzer to keep constant watch for propeller vibration frequencies corresponding to blade-passage excitation. The frequency dial of the analyzer was set in such a way that the component of voltage at blade-passage frequency would be selected, The response for the frequency selected was indicated by a voltmeter.

Calibration of equipment.- Each strain gage was calibrated in such a way that a known alternating voltage existed across each balancing resistor for a given alternating strain,

The carbon gages (sticks of carbon) were calibrated on a dynamic cantilever bar actuated at the tip with a forcing piston. The tip of the rectangular bar was first statically deflected, and the strains at the gage positions were weasured with a Tuckerman strain gage; the measured strains check closely with those obtained by calculation. The bar was tben vibrated in such a way that the maximum tip amplitude equaled the previous static deflection of the tip, and the alternating voltages across the balancing resistors connected to the strain gages were measured.

The flexible *gages* were statically calibrated on the propeller blades; many of the calibrations before and after the test checked within 1 percent, The static calibration procedure is to deflect the blade and to measure both the strain at maximum blade thickness beside each gage and the percentage change of resistance of each gage. The strains were measured with a Huggenberger strain gage, and the percentage changes of resistance of the gages were measured directly with the use of a bridge circuit. If an alternating strain is considered and if figure 6 is referred to, the peak amplitude of alternating voltage across a balancing resistor far $\Delta R_G/R_G \ll 2$ (the input resistance of the amplifier is high compared with R_G and R_B is considered equal to R_G) is

$$\frac{E}{4}\frac{\Delta R_G}{R_G}$$

where

$\Delta R_G/R_G$ per-unit change of strain-gage resistance corresponding to the peak amplitude of alternating strain

E battery voltage

During a propeller vibration test, $\Delta R_G/R_G$ **ranges** from zero to about 1/2 percent and **E** is usually 45 volts.

A low-frequency oscillator having an output voltage of 60 millivolts was used for calibrating the electrical equipment. At intervals during the testing, the oscillator voltage mas applied simultaneously to all attenuators and sinusoidal traces were produced upon the phobographic paper in the oscillograph, A known relationship between the input voltage to the attenuator and the amplitude of the traces on the photographic paper was therefore determined.

Analysis of records.- Because the strain gages and the electrical equipment were calibrated as explained, the strains at the **various** positions on the propeller blades were readily calculated from the measured amplitudes of the oscillograph **traces.** Each value **of** strain was multiplied by the modulus of elasticity of the blade material to obtain stress values,

The frequencies composing an oscillograph trace **were** determined by counting the number of aeaks of each component **wave** for a considerable number of propeller revolutions (or engine revolutions if the timing wave represented a frequency of 1 N) and dividing by the number of revolutions for which the peaks mere counted. If an oscillograph trace is composed of two frequencies that are nearly equal, a slow beat frequency results which is equal to the difference between the two frequencies; in these cases, one of the frequencies ***was*** determined first and the beats were counted to determine the other frequency.

Test conditions.- The various test conditions are given in table III. **The usual** test **procedure** for **each** blade angle mas to hold the **brake** mean effective pressure constant at values of 100, 150, and 200 pounds per square inch and to vary the engine speed by adjusting the airspeed. Maintenance of aonstant brake mean effective pressure kept the excitation supplied by gas forces constant in order that differences in propeller vibratory stresses would depend as nearly as possible only upon how close the frequency of an exciting force mas to a natural frequency of vibration.

Limitations on airspeeds allowable for these tests prevented covering the full range of engine speed and brake mean effective pressure at all blade angles. The term "propeller load" in table III signifies that the tunnel fans were not running and that airspeed was produced only by the model. In this condition, the brake mean effective pressure varied approximately as the square of the engine speed,

ACCURACY OF MEASUREMENTS

The measurements of strain magnitudes for this test are believed accurate within 5 percent; the main components of frequency for the oscillograph records of strain that represent good resonance are accurately daternined in terms of propeller speed or of engine speed. The stress magnitudes are therefore also believed accurate within 5 percent on the condition that stress is proportional to strain.

Secure bonds of strain gages to the surface of the material are essential for accurate strain measurements. The bonds for these tests were satisfactory, Satisfactory results were obtained with the slip-ring devices located as in figure 6; the effect of imperfect contact between the brushes and. rings was small. Considerable care must be taken, however, that the surfaces of the flight ring, which has rings of considerable diameter, are flat and that the rotor revolves without wobbling.

Transverse as well as longitudinal strain changes the resistance of a strain gage, A strain gage is therefore said to have cross sensitivity. The gages mounted on the blades should have negligible cross sensitivity in order that a gage mounted longitudinally on a blade will respond only to longitudinal strain variations, The exact amount of error introduced by cross sensitivity is not known but, for these tests, the cross sensitivity was about one-half the longitudinal sensitivity and tho important stresses occurred near the blade tips where the vibratory motions are essentially flatwise and therefore introduce negligible transverse stresses of the gages. The gages on hollow steel propellers, however, are strained more in the transverse direction than the gages on solid aluminum-alloy propellers because of the occurrence of diaphragm vibrations.

The Poisson ratio effect, occurring with diaphragm vibrations of the hollow steel propellers, is a source of error of vibratory-stress measurements and can best be explained with the aid of figure 11. A flat metal plate (fig. 11(a)) can be stretched from a length L to a length $L + \Delta L$ by applying a uniform tension F: the width of the plate decreases from W to $W - \Delta W$ because of the Poisson effect. If a uniform transverse force F_t is applied (fig. 11(b)), the uniform tension F must be increased to $F + \Delta F$ to maintain a plate length of $L + \Delta L$. The force F_t therefore destroys tha linear relationship between stress and strain. With vibrations of hollow steel propellers, forces such as F_t occur because of the diaphragm vibrations and act either in a direction the same as or opposite to that shown in figure 11(b). Intensive study by the Curtiss-Wright Corporation Propeller Division (unpublished) indicates that the Poisson ratio effect does not introduce more than an additional 5 percent of uncertainty into flexural-stress determinations on the hollow steel blades used for these tests! Their study also indicates that, because of this phenomenon and also because of the fact that the strain gages used for these tests to measure the diaphragm vibration stresses were thick compared with the rear plates of the blades, the diaphragm-stress determinations were higher than the true stresses by 10 to 30 percent. The strain variations *for* the hollow steel blades were multiplied by the nodulus of elasticity for steel to get approximate stress values.

DISCUSSIOH OB RESULTS

Vibration tests were performed to obtain the vibratory-stress curves shown in figures 12 to 55. The term "stresses" will be used in discussing the tests for hollow steel blades because the more accurate term "strain times modulus" is rather cumbersome. In many of the runs, the engine brake mean effective pressure wag held constant while the engine speed was varied in order to keep constant the excitation supplied by gas forces, as previously discussed, For figures 12 to 19 and 36 to 55, no overlap of ranges of brake mean effective pressure is shown; instead only the highest stress in a region of Overlap is plotted for a given epgine speed. Some of the curves represent maximum composite values of vibratory stress, that is, the experimental points represent the highest stress at any cno of the group of the strain-gage positions at a particular region or the blade

The peaks of the stress curves are labeled with vibration frequencies in terms of propeller speed n and engine speed N - for example, $4\frac{1}{2}N$ and 4n. For stress peaks having more than one component of frequency, the components are given either in order of Importance or as the estimated percentage of the total vibratory stress obtained by inspection of the oscillograph trace.

Test 1; tractor condition; two three-blade Curtiss hollow steel propellers.- The six-blade dual-rotating propeller of test 1 vibrated at a frequency of 6n, which is attributed to blade-passage excitation; this frequency was checked by observing that the oscillograph traces for the blades of either propeller were in phase and that; the blades of one propeller vibrated 180° out of phase with the blades of the other propeller. Figures 12 to 19 show that the engine speeds for vibrations having a frequency of 6n axe 80Q rpm, 850 to 900 rpm, and 950 rpm for blade angles of about 30°, 40°, and 45°, respectively (blade angles are for the 42-in, radius). An explanation of the vibration occurring at different engine speeds is that the natural frequency of propeller vibration increases slightly with blade angle, with the result that higher excitation frequencies are needed for the larger blade angles if a resonant propeller vibration is to occur.

The vibratory stresses far the vibration having a frequency of 6n are highest for blade angles from 40° to 45°. It is expected that the excitation from blade passages would continue to increase far blade angles greater than 40° to 45°. The probable reason that the records do no% show this effect is that, with the limited number of gages and the shifting of maximum-stress position with blade angle, the gages did not record the stress at the maximum-stress position for all blade angles.

The airspeed at which the vibration of frequency 6n occurred was about 40 miles per hour (table III) and the vibratory stresses near the blade tips range up to ±6800 pounds per square inch, The shank stresses at an engine speed in the range of 800 to 950 rpm are shown to be low.

Figures 14 and 15 show that, for vibrations at a frequency of 6n, the vibratory stress of the front propeller is about equal to that of the rear propeller for blade angles of about 40°. Figures 16 and 17 show, however, that only the rear propellar vibrates at a frequency of 6n, sug-

gesting that no reactionless vibration occurred because the vibratory hub forces did nod completely cancel, The difference in response of the two propellers is attributed to the coupling of the two propellers to the engine with different flexibilities because of different shaft sizes and different positions on the shafts. Another plausible explanation for the existance of vibratory stresses at blade-passage frequency for only the rear blades is that the wake effect of the front blades upon the rear blades is important as well as the effect due to tho distortion of potential flow about the blades during blade passages.

The vibration having a frequency of 6n was not serious and the higher modes of vibration at this frequency, expected. at the higher engine speeds, did not appear. Several explanations are given, as follows:

(1) The excitation is probably not strong, The blade sections of the rear blades operated more than 1 blade chord behind the respective Chords of the front blades and the effect of the pressure fields *of* the sections of one propeller upon those of the other during passages was therefore probably quite small, If tho wake effect is considered, a rear blade passes through. tho wake of a front 'blade several blade chords behind a front-blade trailing edge because, it passes through the wake sometime after blade passage.

(2) Damping can result from a loose vibration coupling between the two propellers of the dual-rotating unit. The connection between tho two propellers is one of flexibility and clearances; the clearances are in the bearings and the reversing gear. Because the vibratory hub forces of the two propellers do not completely cancel, there is vibratory motion of the propeller hubs and the engine torque is therefore not applied at a point which is a node for a reaction-loss vibration.

(3) For nodes of propeller-bindo vibration higher than the first mode, tho vibratory velocity of some parts of the blade is 180° out of phase with that at other parts of the blade (fig. 1) and, because a blade passage provides excitation acting in the same sense over tho entire blade length, some parts of the blade absorb energy from tho excitation while the remaining parts dissipate energy. A given excitation is more effective, however, near the blade tip than near the shank; also, the blade-passage excitation near the tip is much greater than near tho shank because the tangential velocity is greater. The cancellation effect ts never-

theless a possible partial, explanation of why no reaction-less vibrations with *a* frequency of 6n occurred at high engine speeds,

The front propeller vibrated at a frequency of 2n. These vibrations, occurring at an engine speed of 1650 rpm (figs. 12, 14, and 16) and at airspeeds ranging from 100 to 200 miles per hour (table III), are attributed to the wake provided by the horizontal cable mounted at thrust-axis level less than 2 feet ahead of the dual-rotating unit (fig. 3), The leads from the pineapple, which are fastened along the cable (fig. 3), would strengthen the wake. An approximate calculation shows that, at 150 miles per hour, a $\frac{3}{8}$ inch cable has one-half the drag of the wing (fig. 5) used to simulate the pusher condition at an angle of attack of 0°. The wake supplied by the cable alone would therefore be quite strong and would provide good excitation to the propellor blades, which were very close behind the cable. The wing on the nacelle had less effect than the cable because its leading edge was about 6 feet behind the dual-rotating unit. It is interesting to note that the wake of the cable affects the front propeller much more than it affects the rear propeller,

A propeller vibration having a frequency of 1 n occurs at an engine speed of 850 rpm (fig. 16). The airspeed was about 200 miles per hour for this vibration (table III). This vibration is attributed to the excitation provided by the wake behind tho half of the horizontal cable to which the leads from the pineapple were attached. The wake behind this half of the horizontal cable would be stronger than the wake provided by the other half.

A prominent engine-excited vibration, having a frequency of $4\frac{1}{2}$N, occurred at an engine speed of 2500 to 2600 rpm (figs, 12 to 15). This vibration is one excited by the torsional oscillstione of tho propeller shaft and, probably because the roar propeller is more tightly coupled to the engine than the front propeller, the vibratory stresses are higher in the rear propeller. Figure 15 shows a vibratory stress at the blade tip of over ±16,000 pounds per square inch. The engine speed for resonance is lower for the front propeller, possibly because the front propeller is coupled to the engine with more flexibility than the rear propeller; the frequency of maximum response of a propeller depends upon the engine-propeller combination.

Figure 14 shows that the front propeller vibrates at a frequency of $4\frac{1}{13}N$ at an engine speed of 2500 rpm. This vibration appears **as** the result of a reverse whirl of the propeller shaft **at** a frequency *of* $3\frac{1}{2}N$. Tho **front** propeller rotates **in** the same direction **as** the engine shaft, that **is**, opposite the direction of whirl, and the frequency of vibration of the **front** propeller **is** therefore $3\frac{1}{2}N + \frac{N}{26/15}$ or $4\frac{1}{13}N$. (See discussion of engine-excited vibrations.) The vibratory frequency that would be expected **fur** the rear propeller is $3\frac{1}{2}N - \frac{N}{28/15}$ **or** $2\frac{12}{13}N$. **This** frequency was not found at an engine speed near 2500 rpm, probably because the frequency $2\frac{12}{13}N$ is **far** different from $4\frac{1}{13}N$ and **is** not equal to a natural frequency of propeller vibration, Also, the whirl of the rear-propeller **shaft may** be **loss** serious than that of tho front-propeller shaft because the rear propeller **is** supported nearer the front-propeller-shaft bearing. **The rear-**propeller shaft, however, whirls at a frequency of 8N at an **engine** speed of 2000 rpm **and causes** tho rear blades to vibrate at a frequency of $7\frac{11}{26}N$ (fig. 17).

Test *2; tractor condition,* two three-blade Hamilton **Standard** aluminum-alloy propellers.- The results of test **2 are** presented in figures 20 to 35, Figures 20 and 21 show that a vibration having a frequency of 6n appeared for an engine speed of 1550 to 1600 rpm. Tho vibratory **stresses** for this frequency appear only for the rear **gro-**peller and are only slightly above ±1000 **pound** per square inch.

vibrations having a frequency of 2n are present for this test; their origin is explained in the results of test 1. Vibrations having a frequency of 4n, however, **are** also present (see, for example, figs. 21, **23,** 25, and *27);* these vibrations probably **are** excited by the wake of the supporting cable because their **frequency** is the second harmonic of 2n. In direct contrast with the results of test 1, the results of test 2 **show** that the wake of the cable affects only the fear propeller,

Engine-excited vibrations having frequencies *of* $4\frac{1}{2}N$ and $4\frac{1}{13}N$ **for** the front propeller and frequencies of $4\frac{1}{2}N$

and $2\frac{12}{13}N$ for the rear propeller are prominent throughout test 2. The vibratory stresses for these frequencies increase considerably with the engine brake mean effective pressure (figs, 20 and 21), are generally higher for the rear propeller, and sometimes reach high values (figs. 20, 21, 26, and 27). The vibrations having a frequency of $4\frac{1}{2}N$ were more prominent than vibrations of frequencies $4\frac{1}{13}N$ and $2\frac{12}{13}N$. A good comparison of the $4\frac{1}{13}N$ component of vibratory stress of the front blades with the $2\frac{12}{13}N$ component of vibratory stress of the rear blades cannot be made, because the $4\frac{1}{2}N$ component appears with both.

Vibratory frequencies corresponding to forward inertia whirl were present for test 2 (figs. 21, 23, 25, and 27). The vibratory frequency is $1\frac{11}{26}N$ for the front propeller and $2\frac{15}{26}N$ for the rear propeller. Stresses at these frequencies were detected only at the shanks of the blades,

In general, the highest vibrations for test 2 occur for blade angles from 30° to 35° (figs. 23 to 27). As explained for test 1, the comparisons of vibratory stresses for various blade angles do not truly show the effect of blade angle upon the stress at the maximum-stress positions because the maximum-stress positions are different for different blade angles.

Test 3; tractor condition; two three-blade Hamilton Standard aluminum-alloy propellers.- The vibrations having blade-passage frequency of 6n appear only for the rear blades (figs. 30, 32, and 33). These stresses are at satisfactorily low levels.

The results of test 3 (figs, 28 to 35) are essentially the same as those of test 2, except that the vibrations occur at different engine speeds because the blades are of different design and therefore have different natural frequencies. The wake of the supporting cable, however, caused vibrations at frequencies of 1 n, 2n, and. 4n for both the front and the rear propellers,

~~Test 4: tractor conditions; two four-blade Curtiss hollow steel~~ propellers.- The blade-passage frequency of vibration for test 4 (figs. 36 to 39) is 8a, inasmuch as the dual-rotating unit consists of two four-blade propellers that rotate in opposite directions, Since such a frequency

was found for the rear blades as shown by figure. 39, it is suggested that a second mode of flatwise vibration was excited by blade passages. For the single case of test 4, the 8n component is only about 30 percent of the total vibratory stress of ±6000 pounds per square inch.

Again, the vibration having a frequency of 2n was found only for the front blades (*fig*, 36).

Engine-excited vibrations appeared and the engine speeds for resonance were lower for the front propeller (figs. 38 and 39). Figures 36 to 38 show that, when longitudinally mounted gages recorded vibrations having a frequency of $4\frac{1}{2}$N, the transversely mounted gages on the hollow steel propeller recorded diaphragm vibrations having a frequency of 9N. The flexural vibration of the blade probably possessed a component having a frequency of 9N as well as one having a frequency of $4\frac{1}{2}$N. The frequency of 9N probably was near the natural frequency of a diaphragm vibration. The natural frequency. of a diaphragm vibration *is* expected to bo high, because the transverse dimension of the blade, that is, the blade chord, is relatively small.

In general, tho results of test 4 verify the results of the first three tests.

Test 5; simulated pusher condition; one three-blade and one four-blade Curtiss hollow steel propeller.- For test 5 (figs. 40 to 45), the blade-passage frequency for the front propeller is 8n and the blade-passage frequency for the rear propeller is 6n. Vibrations of the front blades at a frequency of 8n were found (figs. 40, 42, and 44) for each blade angle, but vibration of the rear blades at a freqency of 6n was detected only once. This fact implies that the wing ahead of the propellers was to some extent responsible for the vibrations of the front blades at a frequency of 8n. The vibratory stresses of the front blades at a frequency of 8n did not exceed ±5000 pounds per square inch.

A vibration of the front propeller at a frequency of 3n was found once at aa engine speed of 1950 rpm (fig. 44); this vibration can be attributed to the presence of the wing, It is noted that no vibration having a frequency of 2n was present. This fact implies that the presence of the wing reduced the excitation provided by the wake of the supporting cable, This condition does not seem likely, however, because the wing was displaced 50 percent of the propeller

radius from thrust-axis level and the horizontal cable was relatively close to the dual-rotating propeller.

The same engine-excited vibrations appeared for test 5 as for the first four tests; the vibratory stresses of frequency $4\frac{1}{2}N$ were somewhat larger for the rear blades. The engine speeds for the resonance at the frequency $4\frac{1}{2}N$ were again lower for the front propeller.

Test 6; simulated pusher condition; two four-blade hollow steel propellers.- No vibrations having the blade-passage frequency of 8n were detected for test 6 (figs. 46 to 49). Also, no important vibrations occurred which can be attributed to the presence of the wing. A vibration of frequency 2n, which has been attributed to the wake of the horizontal cable, was not found.

Engine-excited vibrations occurred as for the first five tests; the $4\frac{1}{2}N$ component of vibratory stress was greater for the rear propeller. The engine speeds for the important vibration of $4\frac{1}{2}N$ were lower for the front propeller by from 50 to 100 rpm.

Test 7; simulated pusher condition; one three-blade and one four-blade Curtiss hollow steel propeller.- For test 7, the blade-passage frequencies are 8n and 6n for the front propeller and for the rear propeller, respectively. Vibrations at these frequencies appeared for the respective propellers (figs. 50 and 51). The flexural vibrations at these frequencies were not serious. Diaphragm stresses of frequency 8n were as high, however, as ±14,000 pounds per square inch for the front blades (fig. 50). Inasmuch as diaphragm stresses of the same frequency occurred at about the same engine speed for the rear blades (fig. 51), it is expected that much of the excitation for vibration of the front blades at a frequency of 8n was caused by the presence of the wing.

The engine-excited vibratory stresses were quite high. The frequency $4\frac{1}{2}N$ appears because of torsioaal oscillation of the propeller shaft; the frequency $4\frac{1}{13}N$ occurs because of the reverse propeller-shaft whirl at a frequency of $3\frac{1}{2}N$; the frequency of $4\frac{12}{13}N$ occurs because of the forward propeller-shaft whirl at a frequency of $5\frac{1}{2}N$.

Test 8; simulated pusher condition; two four-blade Curtiss hollow steel propellers.- The blade-passage fre-

quency for test 8 (figs. 52 to 55) is 8n for both propellers. Vibrations of the front propeller at a frequency of 8n were detected (figs, 52 and 54). Vibrations of the rear propeller at this frequency may also have occurred; few records taken for an engine speed from 1100 to 1200 rpm were analyzed for frequency because the vibratory stresses were low. It is quite possible that the vibration of frequency 8n could be caused by the presence of the wing as well as by blade passages,

For this simulated-pusher test, a vibration of the front propeller at a frequency of 2n was found (fig, 52). This vibration is attributed to the wake provided by the horizontal cable mounted ahead of the dual-rotating unit, For this pusher test, however, it is also feasible that the excitation was provided by the wing.

Engine-excited vibrations were present for test 8 as for tests 1 to 7.

CONCLUSIONS

The results of vibration tests for tractor and simulated pusher conditions of six-, seven-, and eight-blade dual-rotating units composed of propellers with three or four blades and operating in a constricted air stream of 36-foot diameter indicate the following conclusions:

1. Few propeller vibrations caused by blade passages were detected; those vibrations found were not serious for either the tractor or the siinulated pusher conditions of the dual-rotating propellers,

2, Although there were indications of vibrations excited by the wing displaced 50 percent of the propeller radius below thrust-axis level, the vibratory stresses generally were at satisfactorily low levels.

3. The responses of the front and the rear blades to engine excitation were similar; the stresses of the rear blades were generally higher, probably because the rear propeller was more rigidly coupled to the engine than the front propeller.

4. Some indications of vibrations excited by propeller-shaft whirl caused by gas forces were found,

5. The engine-excited stresses increased with engine brake mean effective pressure, and some of these stresses reached high values.

Langley Memorial Aeronautical Laboratory,
National Advisory Committee for Aeronautics,
Langley Field, Va.

REFERENCES

1. Theodorsen,, T.: Propeller Vibrations and the Effect of the Centrifugal Force. NACA T.N. No. 516, 1935.

2. Shannon, J, F., and Forshaw, J. R,; Airscrew Blade Vibration: Nature and Severity of Vibration at Edgewise Resonance as Influenced by Coupling Effects Due to Blade Twist, Bop, No. E.3843, British R.A.E., May 1941.

3. Kearns, Charles M.: Engine-Airscrew Vibrations. Aircraft Engineering, vol. XIII, no. 150, Aug. 1941, pp. 211-215.

4, Miller, Mason F.: Wind-Tunnel Vibration Tests of a Four-Blade Single-Rotating Pusher Propeller. NACA ARR No. 3F24, 1943.

5. Den Hartog, J. P.: Mechanical Vibrations. McGraw-Hill Book Co., Inc., N.Y., N. Y., 2d ed., 1940.

6. Guerke, Ralph M.: Vibration Characteristics of Three- and Four-Blade Propellers for High-Output Engines. SAE Jour., vol. 49, no. 6, Dec. 1941, pp. 544-552.

TABLE I.- DESCRIPTION OF GROUND-ADJUSTABLE DUAL-ROTATING PROPELLERS

Test	Condition	Type	Material	Front propeller			Rear propeller		
				Number of blades	Design	Diameter	Number of blades	Design	Diameter
1	Tractor	Curtiss	Hollow steel	Three	512 Ccl. 5-12	10 ft 0 in.	Three	551 Ccl. 5-15	9 ft $10\frac{5}{8}$ in.
2	Tractor	Hamilton Standard	Solid aluminum alloy	Three	3155-6	10 0	Three	3156-6	10 $2\frac{1}{2}$
3	Tractor	Hamilton Standard	Solid aluminum alloy	Three	43A2-6	12 6	Three	44A2-6	12 $8\frac{1}{2}$
4	Tractor	Curtiss	Hollow steel	Four	512 Ccl. 5-12	10 0	Four	551 Ccl. 5-15	9 $10\frac{5}{8}$
5	Simulated pusher	Curtiss	Hollow steel	Three	512 Ccl. 5-12	10 0	Four	551 Ccl. 5-15	9 $10\frac{5}{8}$
6	Simulated pusher	Curtiss	Hollow steel	Four	512 Ccl. 5-12	10 0	Four	551 Ccl. 5-15	9 $10\frac{5}{8}$
7	Simulated pusher	Curtiss	Hollow steel	Three	614 Ccl. 5-6	11 6	Four	615 Ccl. 5-6	11 $7\frac{5}{8}$
8	Simulated pusher	Curtiss	Hollow steel	Four	614 Ccl. 5-6	11 6	Four	615 Ccl. 5-6	11 $7\frac{5}{8}$

TABLE II.- STRAIN-GAGE LOCATIONS

Location on blade			Blade	
Tip (in. from tip)	Shank (deg from L.E. at 42-in. station)	Side	Front propeller	Rear propeller
Test 1; tractor condition; two three-blade Curtiss hollow steel propellers				
12	———	Front	1,2,3	1,2,3
20	———	Front	1,2,3	1,2,3
40	———	Front	1	1
[a]12	———	Rear	1,2	1,3
———	0	———	1,2	1,2
Test 2; tractor condition; two three-blade Hamilton Standard aluminum-alloy propellers				
5	———	Front	1,2,3	1,2,3
8½	———	Front	1,2,3	1,2,3
12	———	Front	2,3	2,3
15½	———	Front	1,2,3	2,3
———	0	———	1,2,3	1,2,3
———	45	Front	1,2,3	1,2,3
———	90	Front	1,2,3	1,2,3
———	135	Front	1,2,3	1,2,3

[a]Transversely mounted gages.

TABLE II.- STRAIN-GAGE LOCATIONS - Continued

Location on blade			Blade	
Tip (in. from tip)	Shank (deg from L.E. at 42-in. station)	Side	Front propeller	Rear propeller
Test 3; tractor condition: two three-blade Hamilton Standard aluminum-alloy propellers				
5½		Front	1,2,3	1,2
9		Front	1,2,3	1,2,3
12½		Front	1,2,3	1,2,3
16		Front	1,2,3	1,2,3
34		Front	1	1
	0		1,2,3	1,2,3
	45	Front	1,2,3	1,2,3
	90	Front	1,2,3	1,2,3
	135	Front	1,2,3	2
Test 4; tractor condition; two four-blade Curtiss hollow steel propellers				
12		Front	1,2,3,4	1,2,3,4
20		Front	1,2,3,4	1,2,3,4
40		Front	2,3	3
[a]12		Rear	2,3	1
	0		3	1
	45	Rear		
	90	Front	2	
Test 5; simulated pusher condition; one three-blade and one four-blade Curtiss hollow steel propeller				
12		Front	1,2,3	1,2,3,4
20		Front	1,2,3	1,2
40		Front	1	3
[a]12		Rear	1,2	1
	0		1	1
	45	Rear	1	

[a]Transversely mounted gages.

TABLE II.- STRAIN-GAGE LOCATIONS - Continued

Location on blade			Blade	
Tip (in. from tip)	Shank (deg from L.E. at 42-in. station)	Side	Front propeller	Rear propeller
Test 6; simulated pusher condition; two four-blade Curtiss hollow steel propellers				
12		Front	1,2,3,4	1,2,3,4
20		Front	2,3,4	1,2
40		Front	2	3
"12		Rear	2,3	1
	0		2	
Test 7; simulated pusher condition; one three-blade and one four-blade Curtiss hollow steel propeller				
12		Front	1,2	1,2
30		Front	1,2,3	1,2,3
40		Front	1,2	2
[a]12		Rear	1	1
[a]30		Rear	1	1
	0		1,2	2
Test 8; simulated pusher condition; two four-blade Curtiss hollow steel propellers				
12		Front	1,2,3	1,2
30		Front	1,2,3	1,2,3
40		Front	1,2	2
[a]12		Rear	1,2	1
"30		Rear	1	1
	0		1,2	2

[a]Transversely mounted gages.

Blade angles (deg)		Bmep (lb/sq in.)	Engine speed (rpm)	Airspeed (mph)
Front	Rear			
Test 1; tractor condition; two three-blade Curtiss hollow-steel propellers				
29.8	29.4	100	1905 to 2550	103 to 202
		150	2300 to 2700	131 to 189
		200	2550 to 2700	142 to 182
		Propeller load	700 to 2250	37 to 125
39.7	38.7	100	1450 to 2380	106 to 276
		150	1650 to 2500	111 to 270
		200	2555 to 2600	269 to 281
		Propeller load	680 to 1400	[a] 35 to 94
44.6	44.0	100	1850 to 1900	256 to 267
		150	1395 to 2100	104 to 279
		200	2000 to 2245	236 to 288
45.5	44.2	100	1210 to 1900	114 to 266
		Propeller load	700 to 1155	[a] 45 to 90
56.9	55.3	150	1100 to 1420	85 to 271
Test 2; tractor condition; two three-blade Hamilton Standard aluminum-alloy propellers				
20.0	19.9	100	2300 to 2700	105 to 153
		Propeller load	1405 to 2700	63 to 124
30.0	29.6	100	1700 to 2700	104 to 252
		150	2050 to 2700	125 to 226
		200	2350 to 2700	144 to 210
		Propeller load	1200 to 1720	73 to 105
35.0	34.5	100	1445 to 2345	101 to 259
		150	1650 to 2625	114 to 275
		200	1955 to 2700	137 to 273
		Propeller load	1150 to 1400	82 to 98
40.0	39.3	100	1300 to 2195	95 to 269
		150	1470 to 2390	105 to 280
		200	1845 to 2450	160 to 274
		Propeller load	990 to 1690	74 to 126
50.0	48.9	100	1400 to 1500	239 to 267
		150	1400 to 1600	222 to 274
		Propeller load	1000 to 1160	86 to 103
Test 3; tractor condition; two three-blade Hamilton Standard aluminum-alloy propellers				
20.0	19.9	100	1870 to 2695	121 to 202
		150	2255 to 2700	146 to 193
		200	2490 to 2700	167 to 184
		Propeller load	1000 to 2050	66 to 180
25.0	24.8	100	1500 to 2695	117 to 259
		150	1700 to 2700	140 to 249
		200	2000 to 2700	163 to 246
		Propeller load	1200 to 2000	95 to 162
35.0	34.5	100	1200 to 1930	143 to 263
		150	1300 to 2050	148 to 273
		200	1500 to 2120	177 to 280
		Propeller load	1000 to 1240	115 to 133
40.0	39.3	100	1010 to 1690	140 to 270
		150	1020 to 1750	120 to 275

[a] Estimated values.

Blade angles (deg)		Bmep (lb/sq in.)	Engine speed (rpm)	Airspeed (mph)
Front	Rear			
Test 4; tractor condition; two four-blade Curtiss hollow-steel propellers				
26.4	25.9	100	2050 to 2700	98 to 185
		150	2350 to 2800	116 to 155
		200	2600 to 2800	142 to 152
		Propeller load	900 to 2500	57 to 121
38.7	37.9	100	1400 to 2305	124 to 272
		150	1450 to 2450	106 to 276
		200	2000 to 2500	187 to 265
		Propeller load	700 to 1350	49 to 97
Test 5; simulated pusher condition; one three-blade and one four-blade Curtiss hollow steel propeller				
29.8	26.1	100	1950 to 2790	101 to 213
		150	2365 to 2795	127 to 196
		200	2695 to 2790	148 to 173
		Propeller load	1200 to 1950	63 to 107
39.9	37.8	100	1410 to 2310	97 to 270
		150	1600 to 2530	115 to 279
		200	1755 to 2650	119 to 283
		Propeller load	900 to 1410	60 to 99
45.3	42.9	100	1410 to 1950	156 to 264
		150	1460 to 2100	128 to 270
		200	1805 to 2205	202 to 276
		Propeller load	900 to 1440	66 to 108
Test 6; simulated pusher condition; two four-blade Curtiss hollow steel propellers				
26.6	26.3	100	2005 to 2790	109 to 215
		150	2360 to 2790	124 to 189
		200	2640 to 2780	140 to 173
		Propeller load	950 to 2700	47 to 146
38.0	37.5	100	1410 to 2355	106 to 274
		150	1550 to 2465	113 to 270
		200	1710 to 2605	129 to 278
		Propeller load	800 to 1500	57 to 104
Test 7; simulated pusher condition; one three-bled9 and one four-blade Curtiss hollow steel propeller				
36.2	35.0	100	1415 to 2465	109 to 252
		150	1600 to 2600	119 to 254
		200	1803 to 2740	136 to 270
		Propeller load	700 to 1350	51 to 97
Test 8; simulated pusher condition; two four-blade Curtiss hollow steel propellers				
22.1	21.6	100	2155 to 2800	110 to 174
		150	2655 to 2795	137 to 157
		200	2780	146
		Propeller load	550 to 2105	32 to 110
34.8	35.0	100	1410 to 2260	131 to 251
		150	1455 to 2415	118 to 259
		200	1700 to 2510	152 to 268
		Propeller load	700 to 1300	59 to 103

L-405

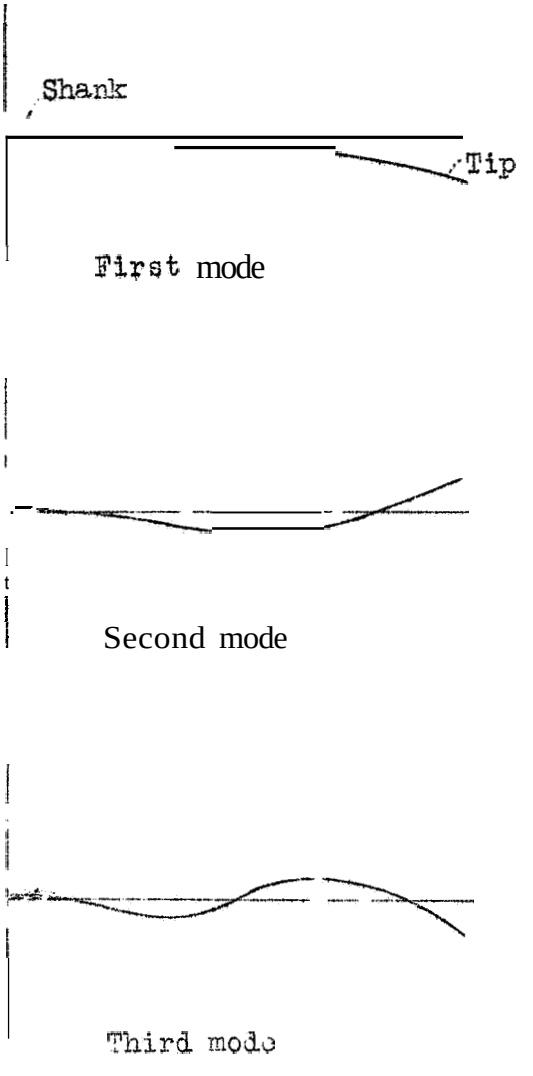

Figure 1.- Mode shapes of vibrating blade.

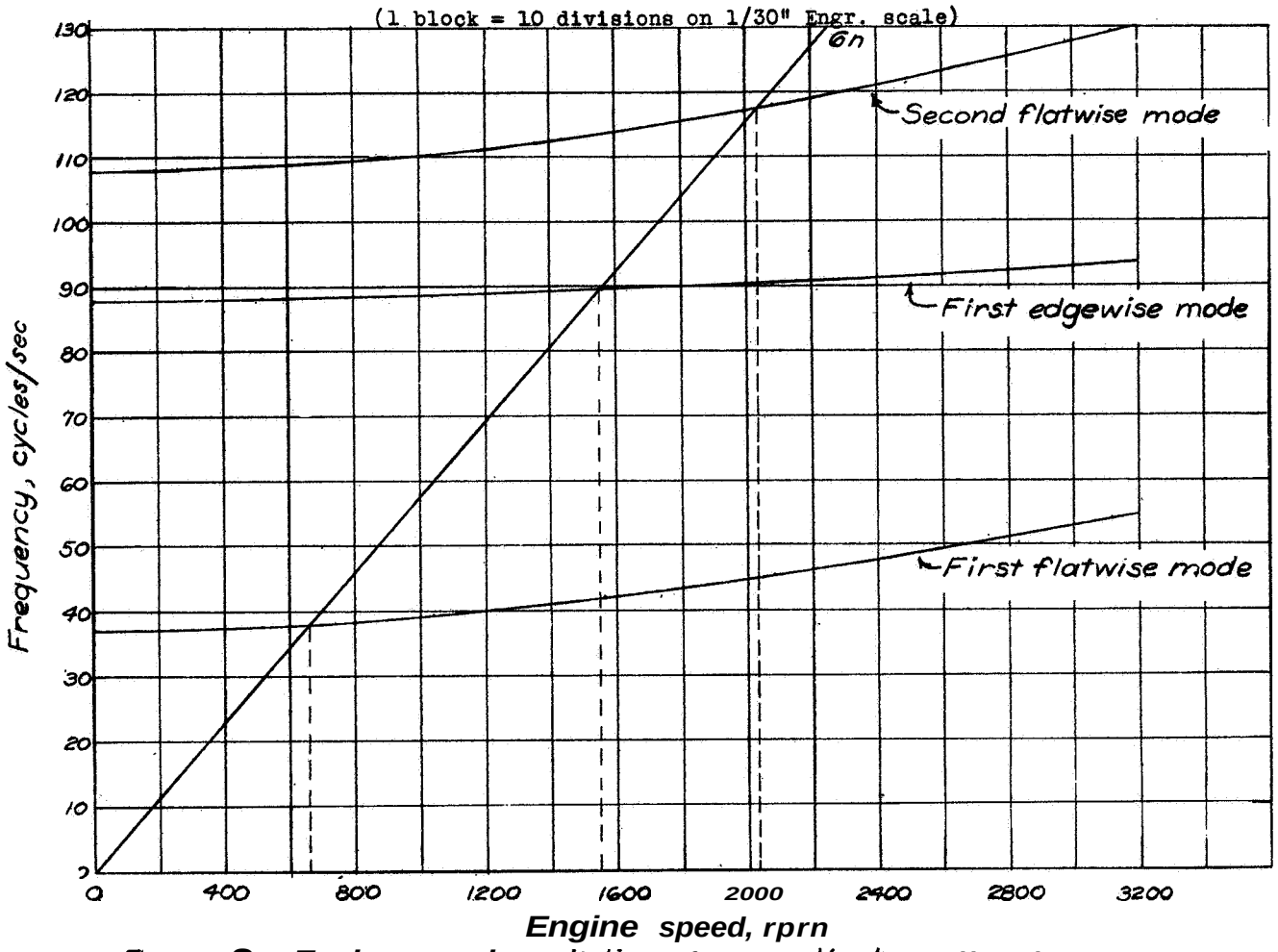

Figure 2 - Engine-speed predictions for reactionless vibrations of two 3-blade Hamilton Standard propellers for test 2.

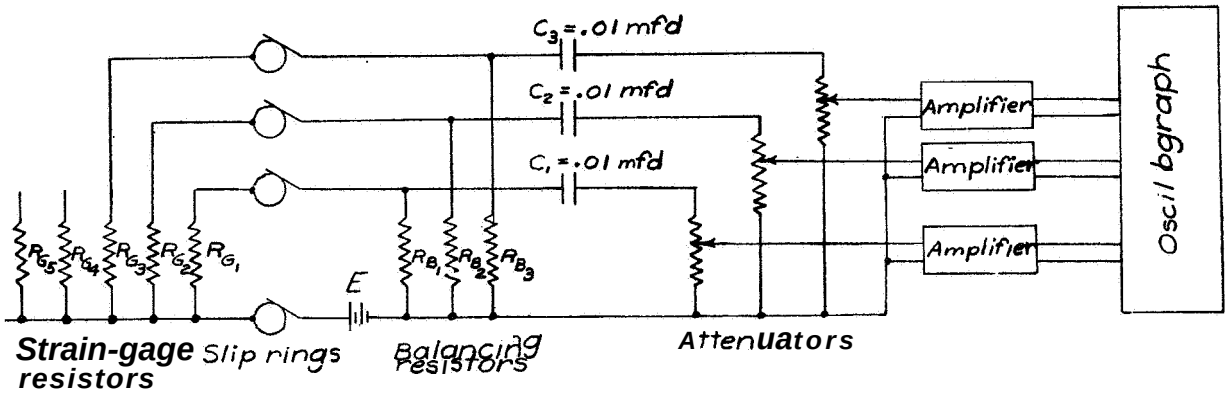

figure 6.- The strain-gage circuit E = 45 volts (approx.); $R_B = R_G = 25{,}000$ ohms (approx.)

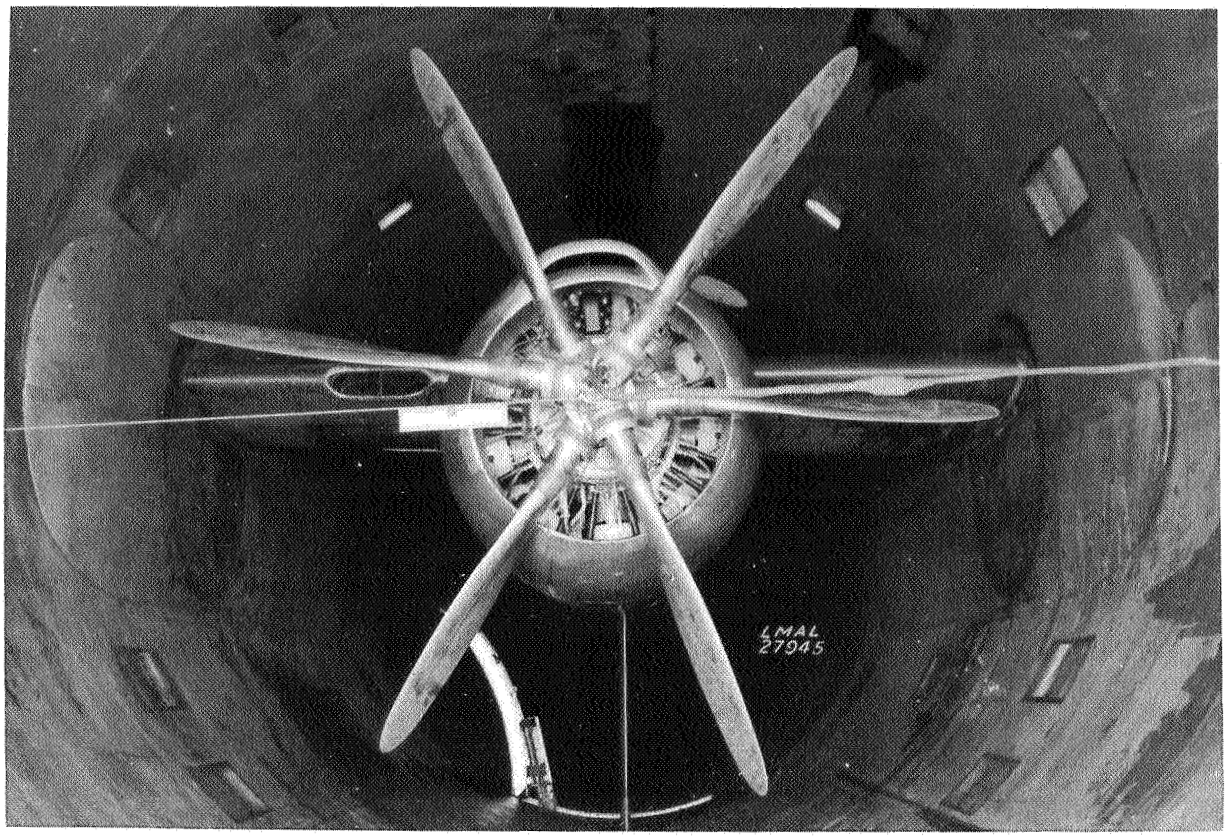

Figure 3.- Engine-propeller -nacelle combination mounted in 16-foot high-speed tunnel.

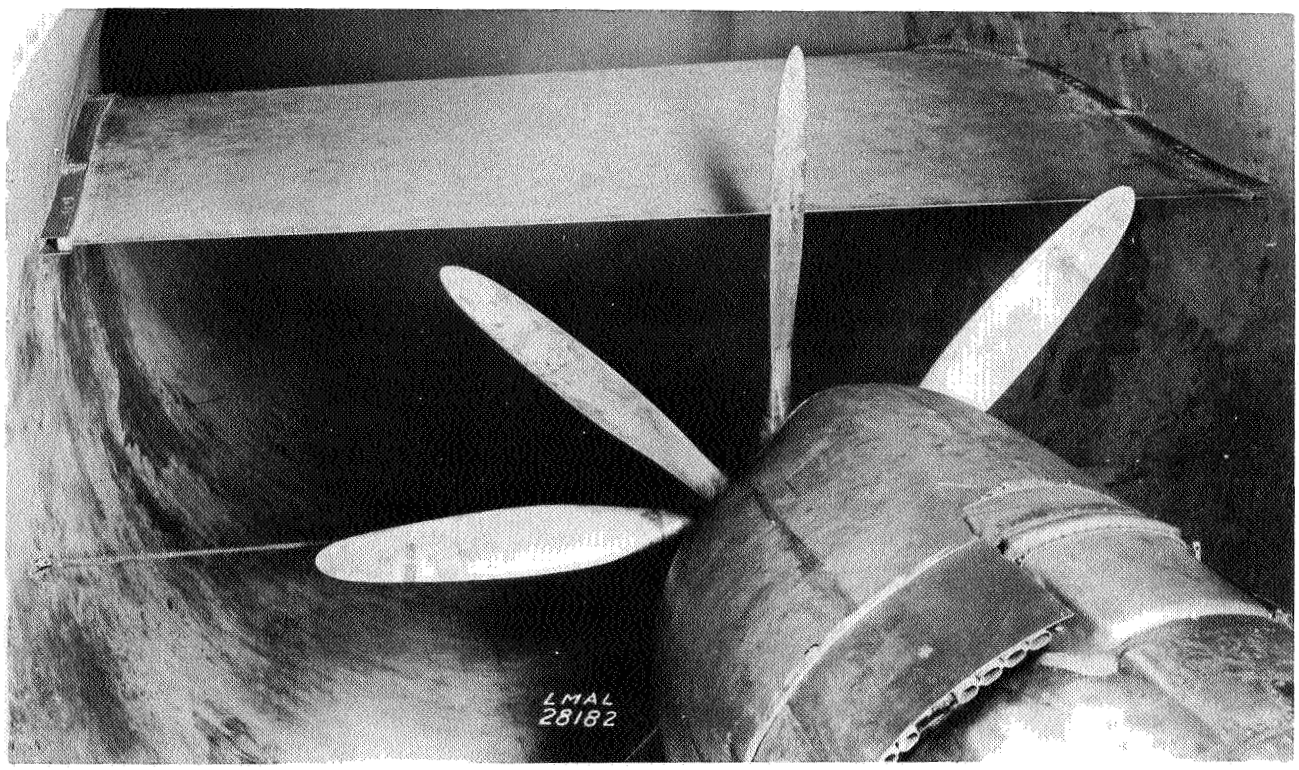

Figure 4.- Inverted wing mounted ahead of eight-blade dual-rotating propeller.

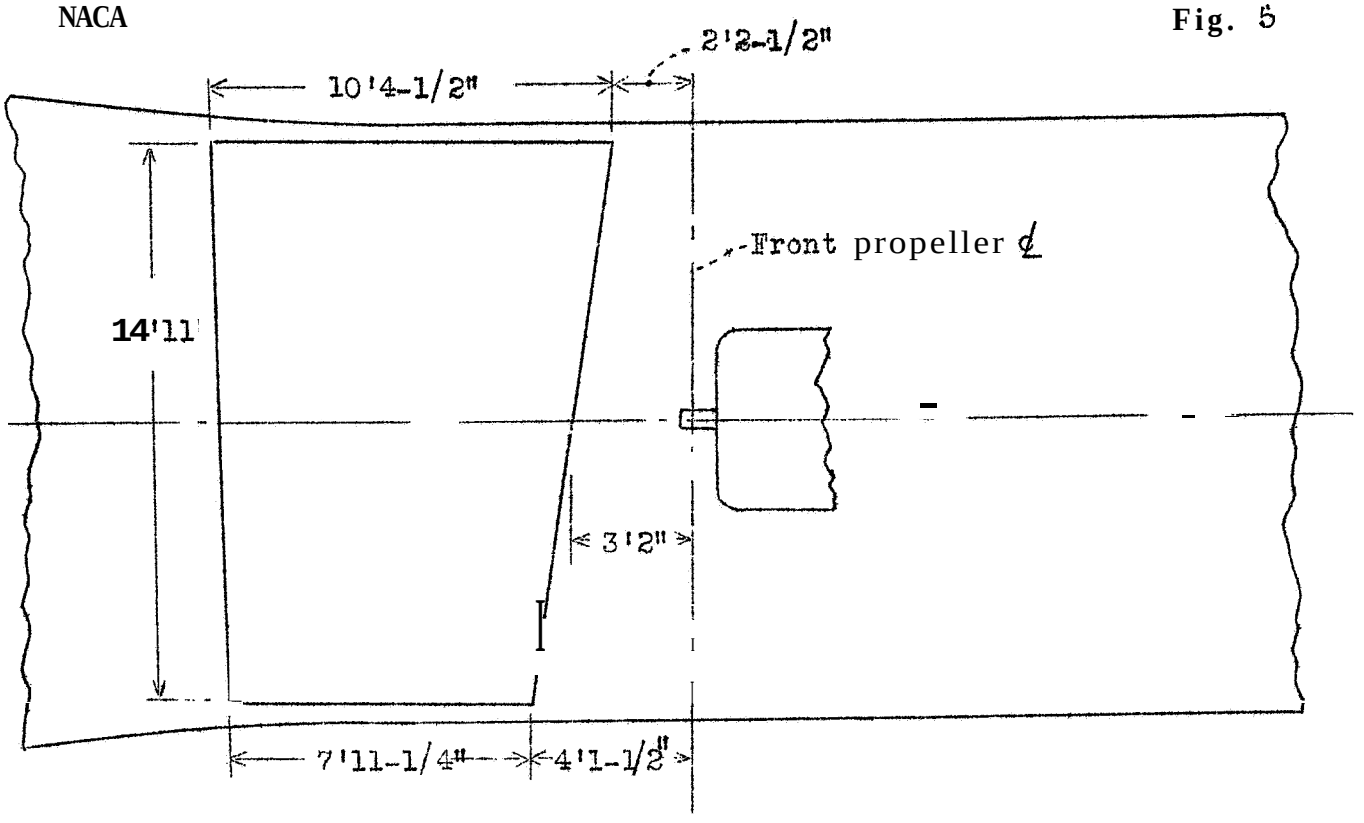

Top view

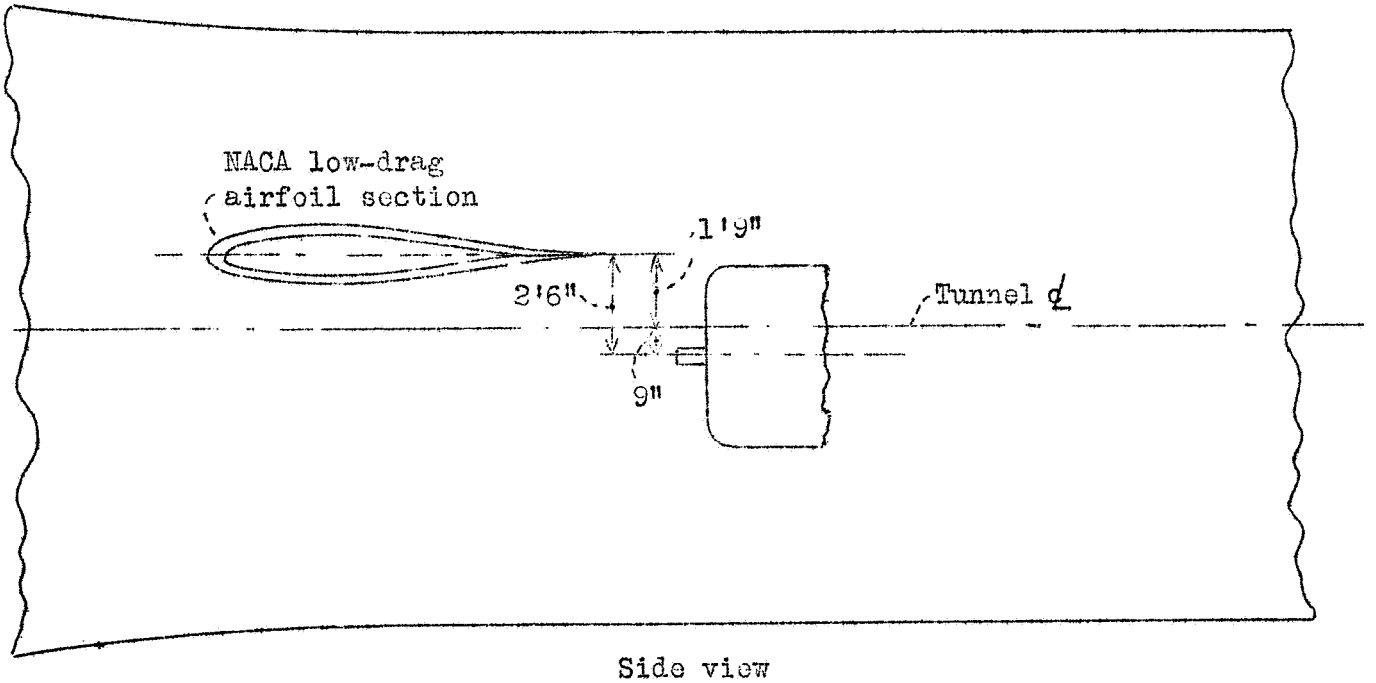

Side view

Figure 5.- Location of inverted wing for pusher-propeller tests.

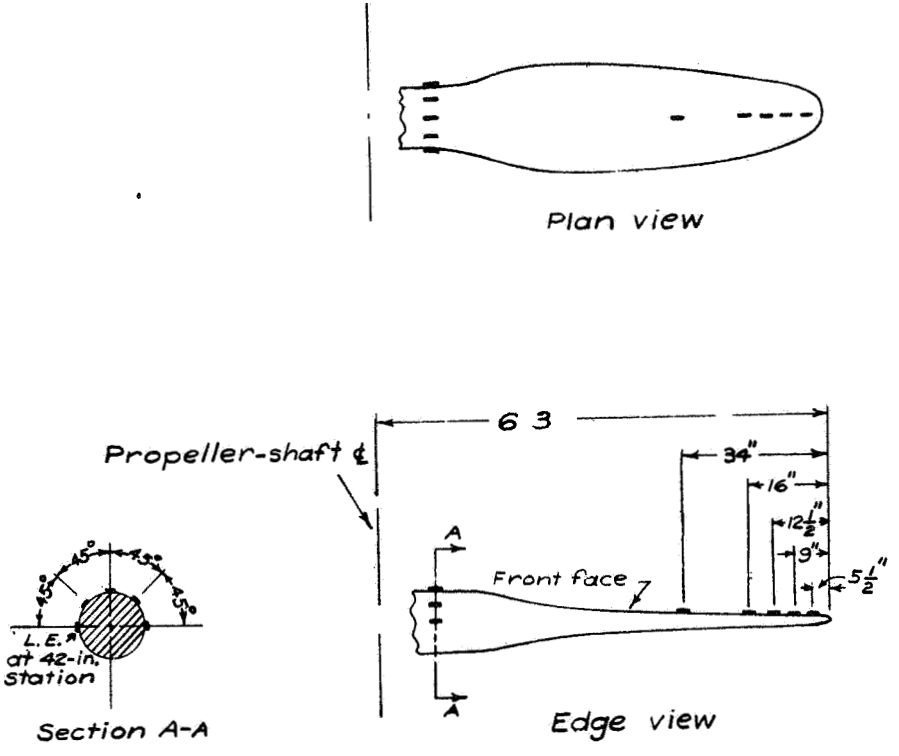

Figure 7.– Strain-gage positions on Hamilton Standard propeller blade, design 43A2-6.

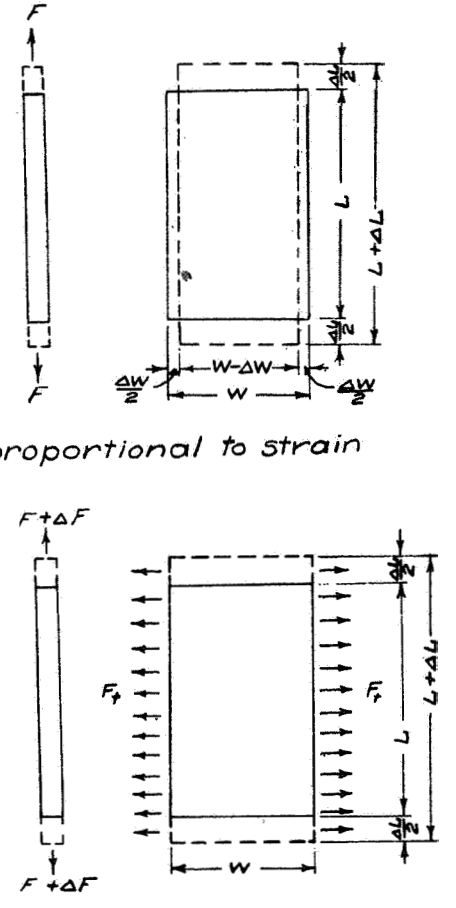

(a) Stress proportional to strain

(b) Stress not proportional to strain

Figure 11 – Illustration of nonlinearity between stress and strain for a metal plate.

L-405

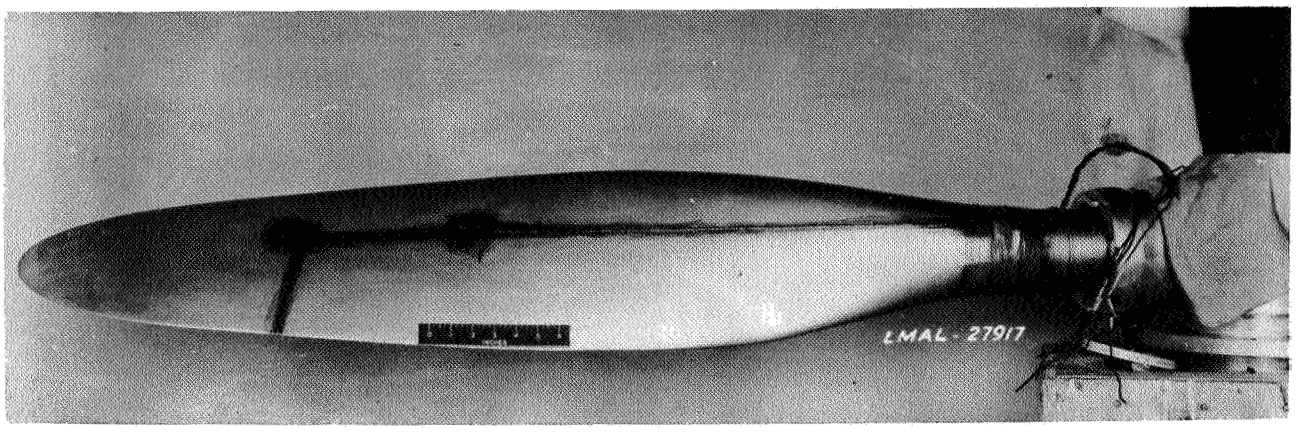

Figure 8.- Gages and wiring on a propeller blade.

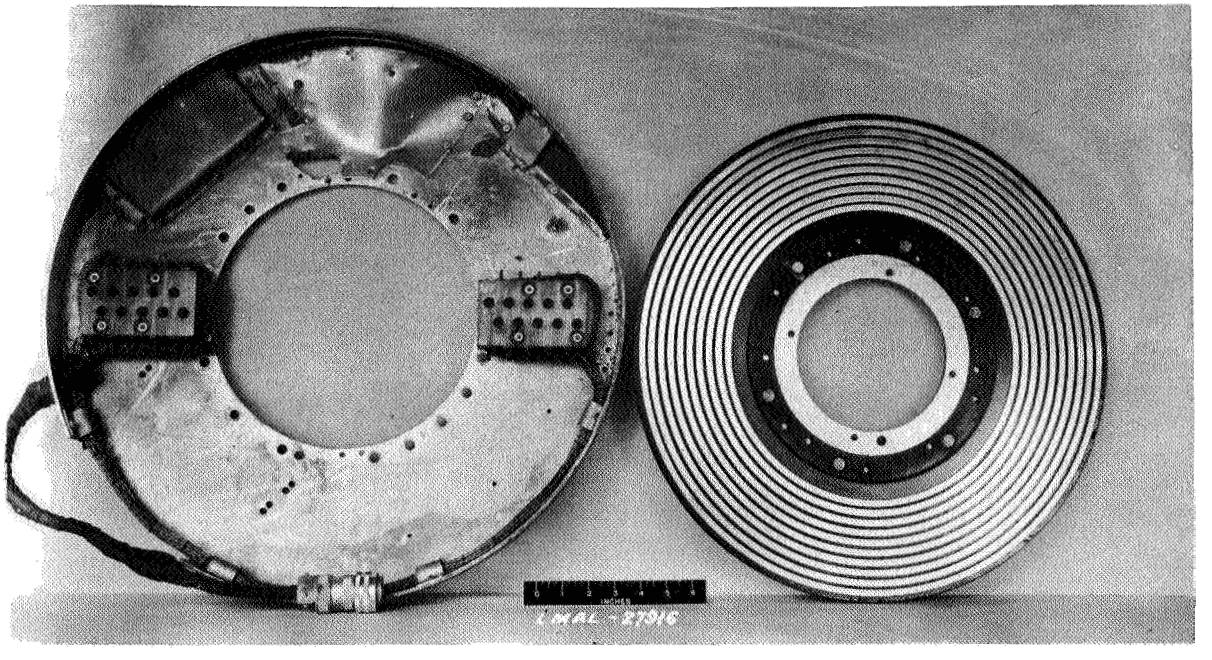

Figure 10.- Inside view of a flight ring.

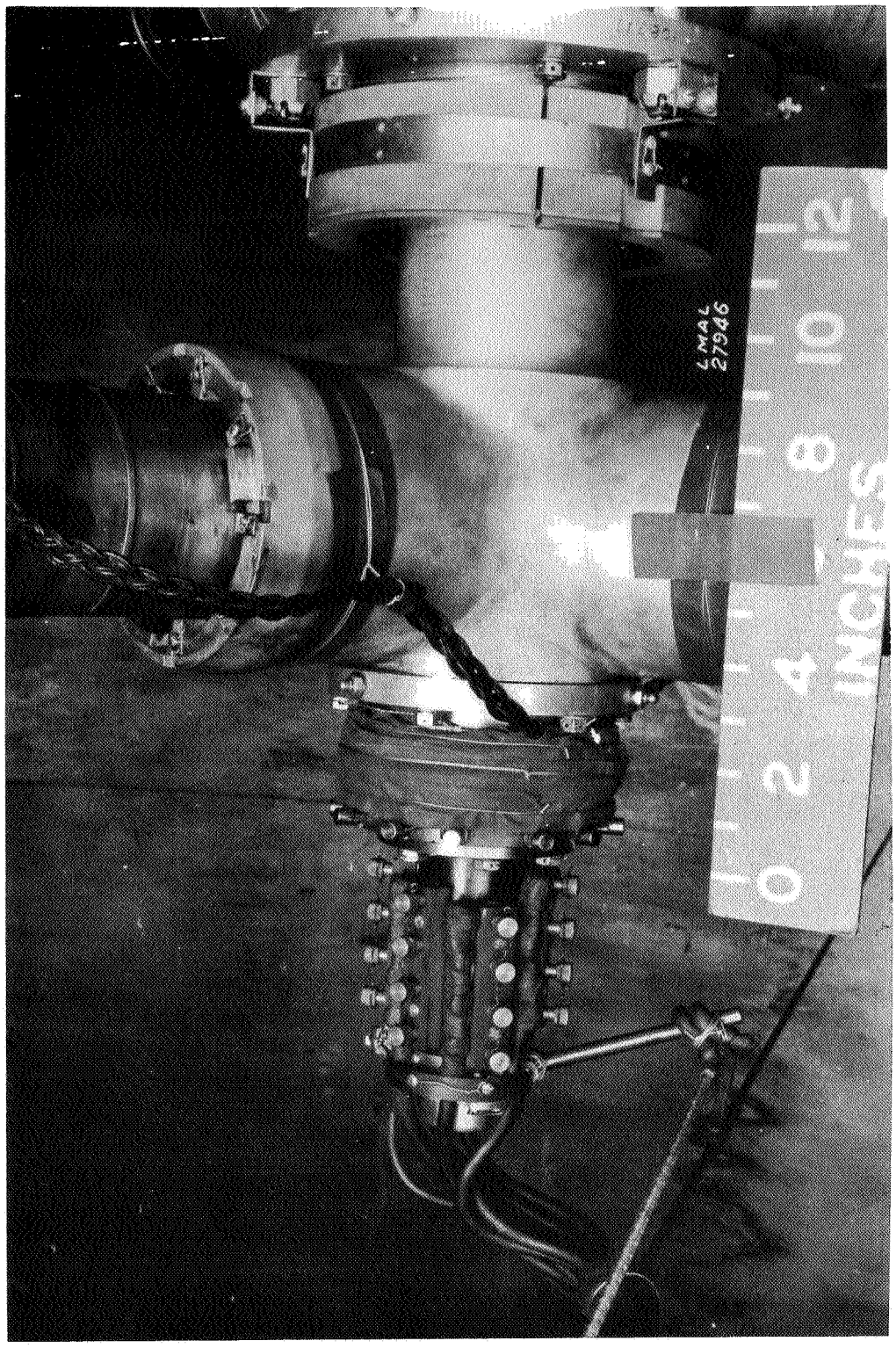

Figure 9.- A pineapple mounted for test.

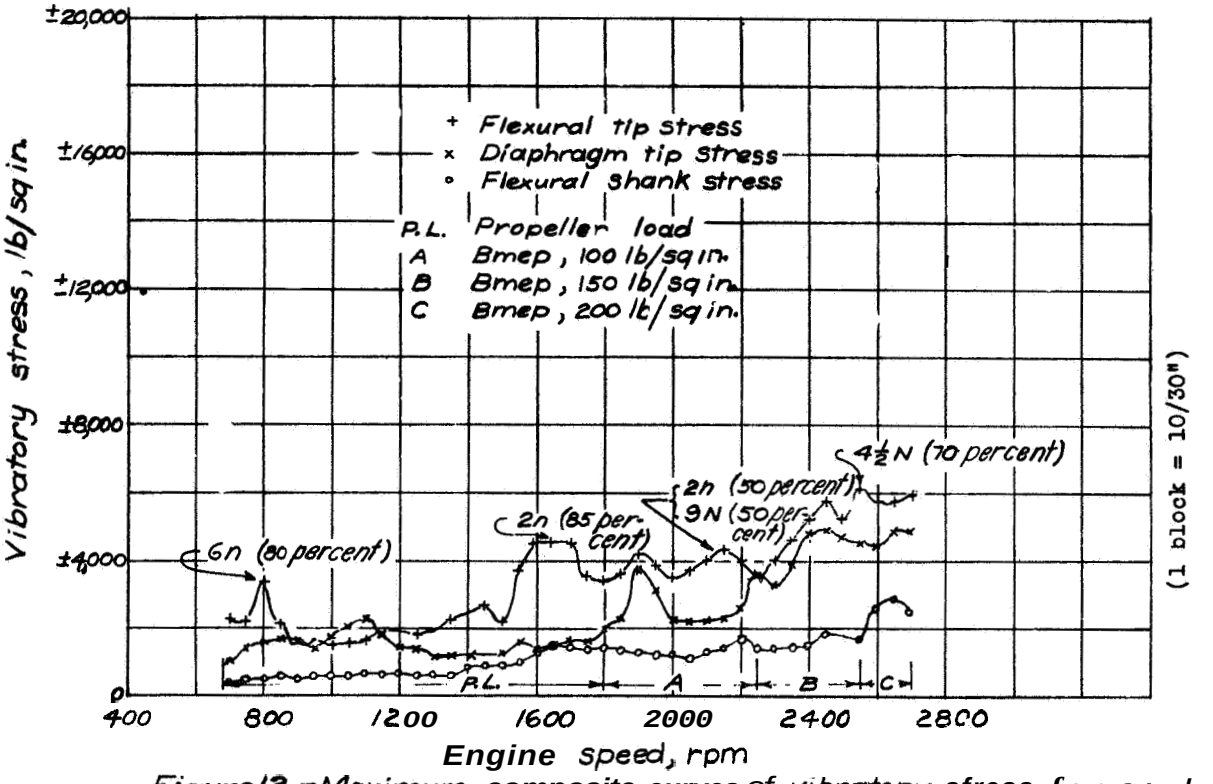

Figure 12.-Maximum composite curves of vibratory stress for test. Tractor; 6 blades; front propeller; hollow steel, β=29.8°

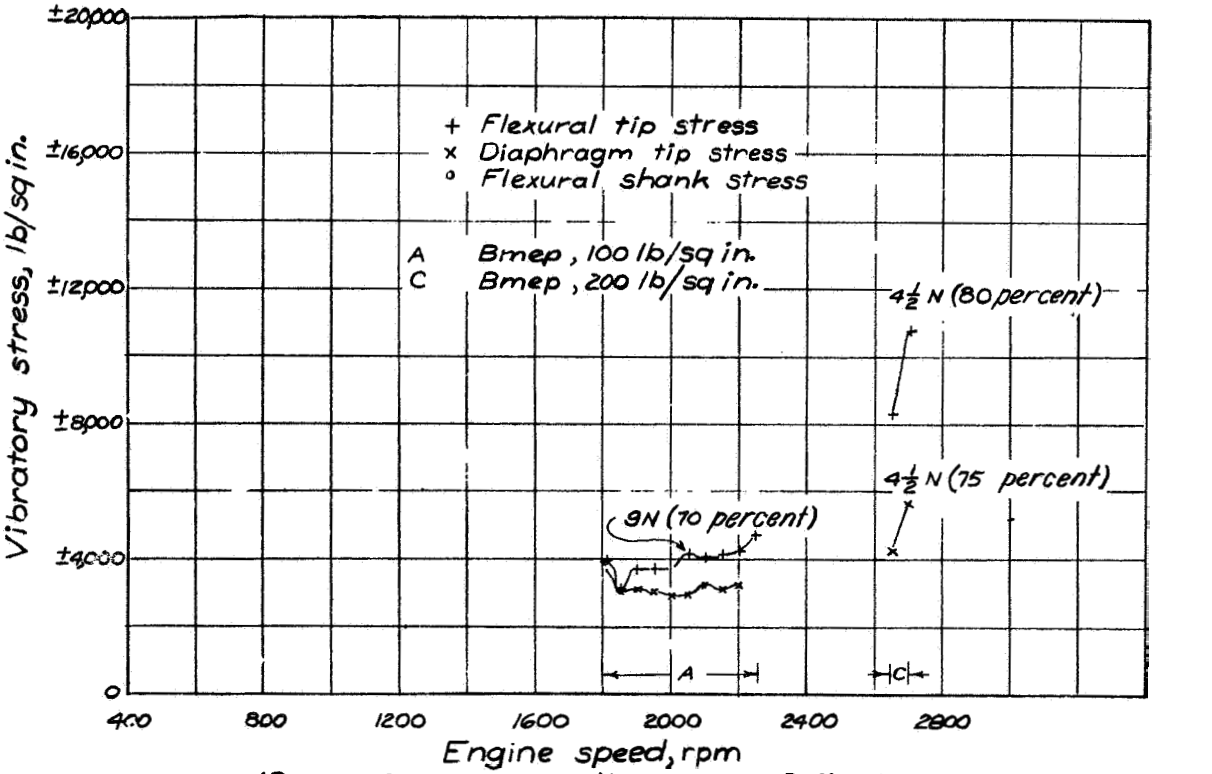

Figure 13.-Maximum composite curves of vibratory stress for test. Tractor; 6 blades, rear propeller; hollow steel; β=29.4°.

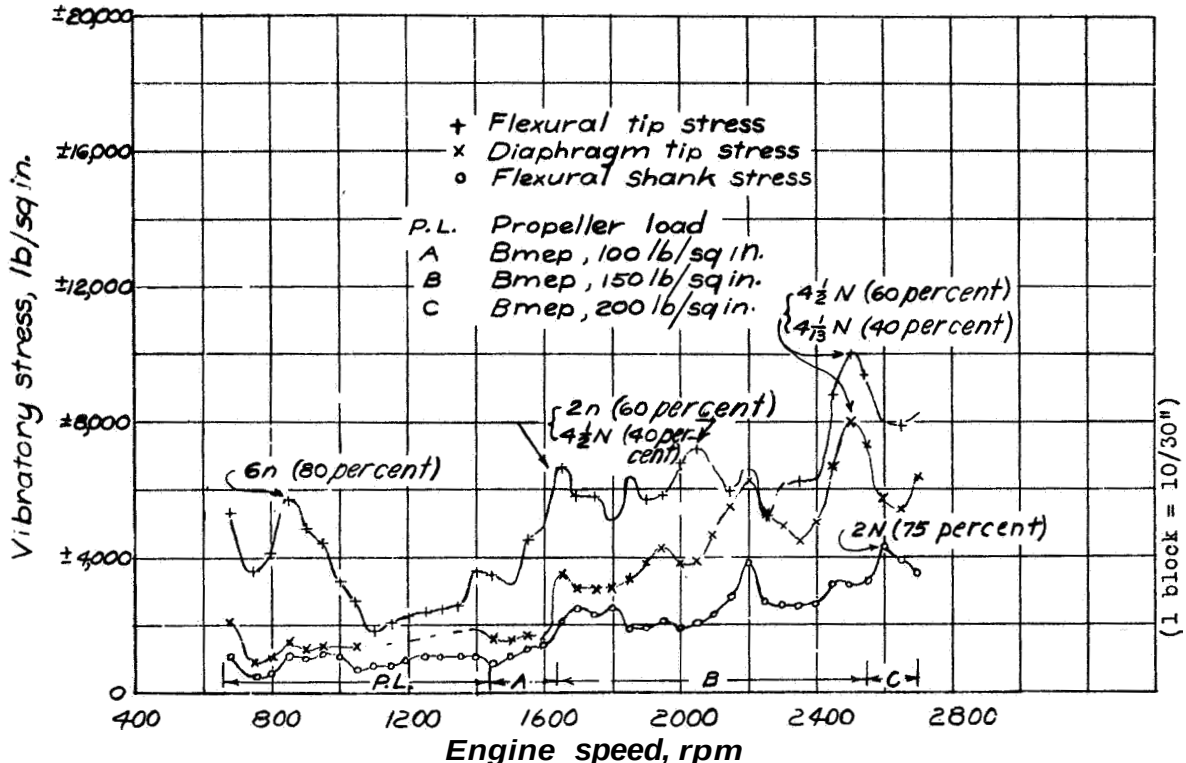

Figure 14.-Maximum composite curves of vibratory stress for test 1. Tractor; 6 blades, front propeller, hollow steel, β=39.7°.

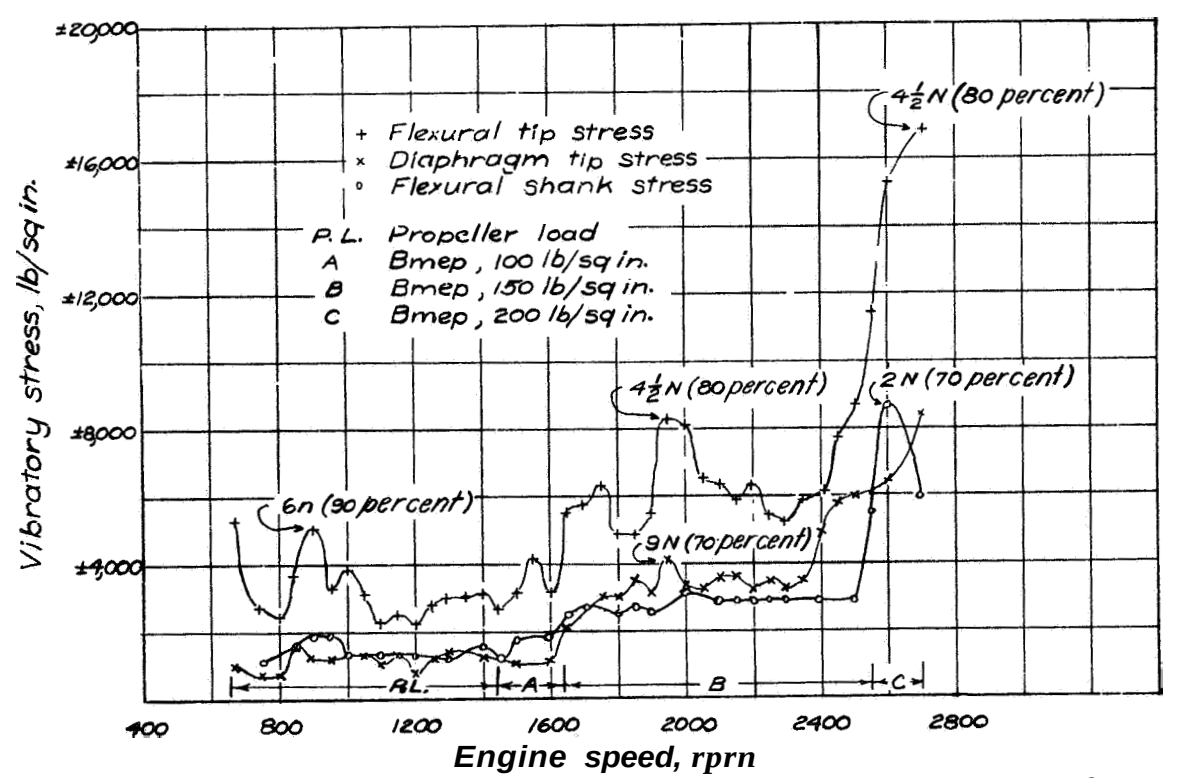

Figure 15.-Maximum composite curves of vibratory stress for test 1. Tractor; 6 blades; rear propeller, hollow steel, β=38.7°

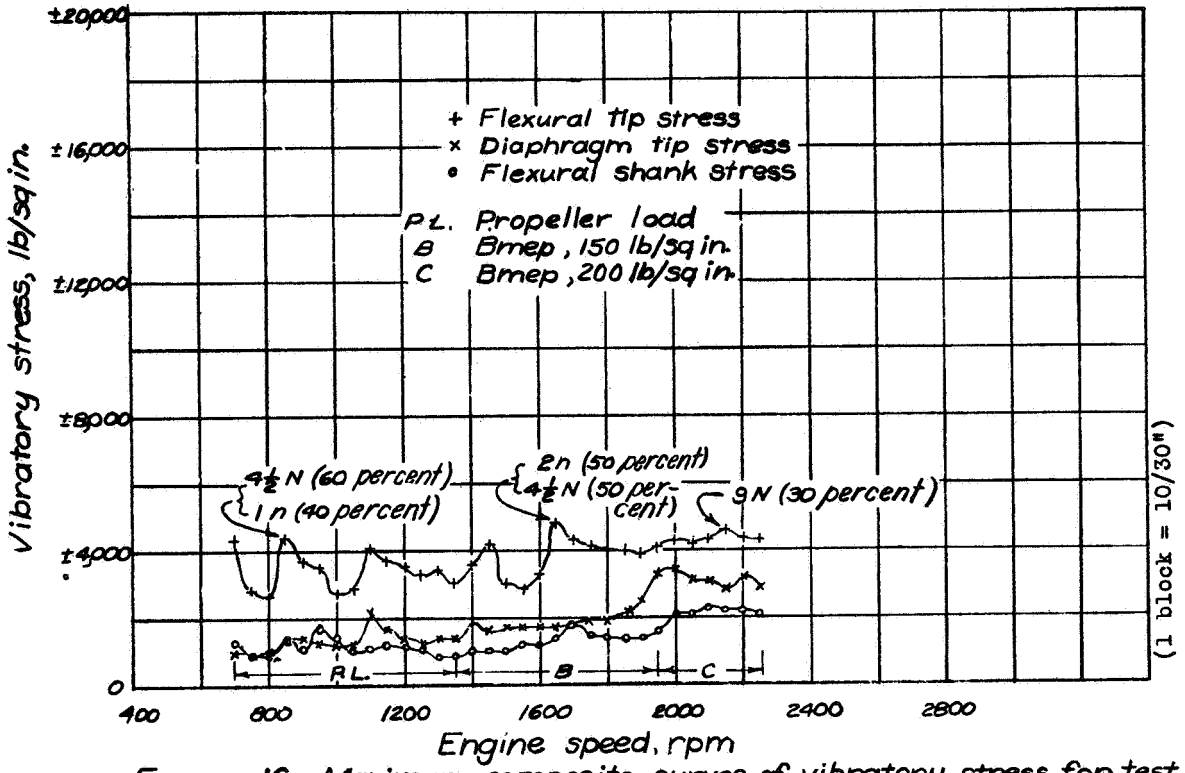

Figure 16.-Maximum composite curves of vibratory stress for test 1. Tractor; 6 blades: front propeller, hollow steel; β=45.5°

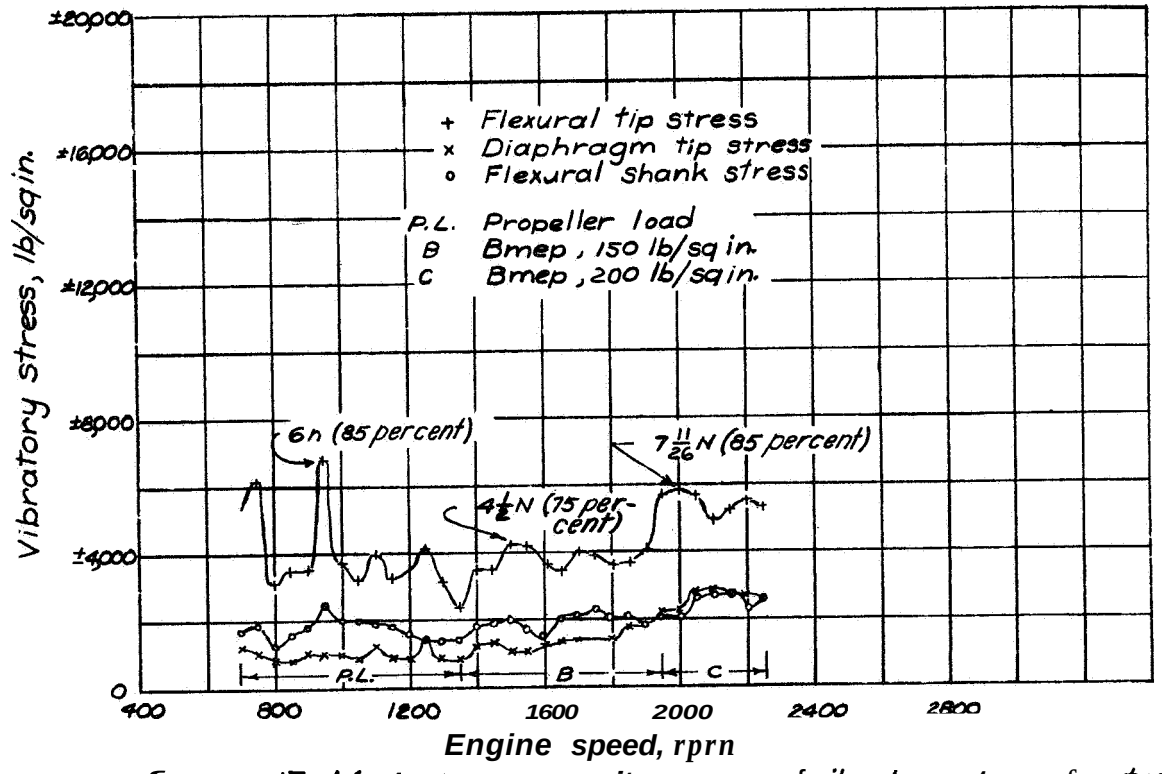

Figure 17.-Maximum composite curves of vibratory stress for test 1. Tractor; 6 blades; rear propeller, hollow steel; β=44.2°.

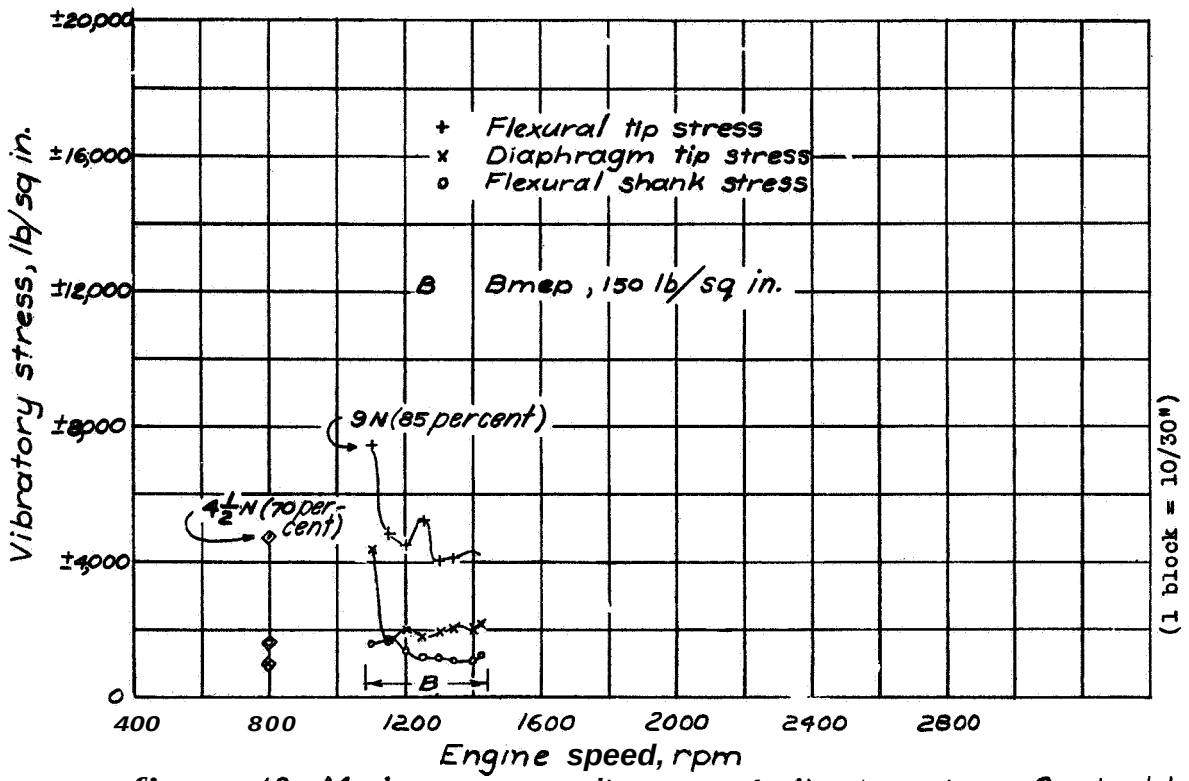

figure 18.-Maximum composite curves of vibratory stress for test 1. Tractor; 6 blades; front propeller, hollow steel; $\beta = 56.9°$.

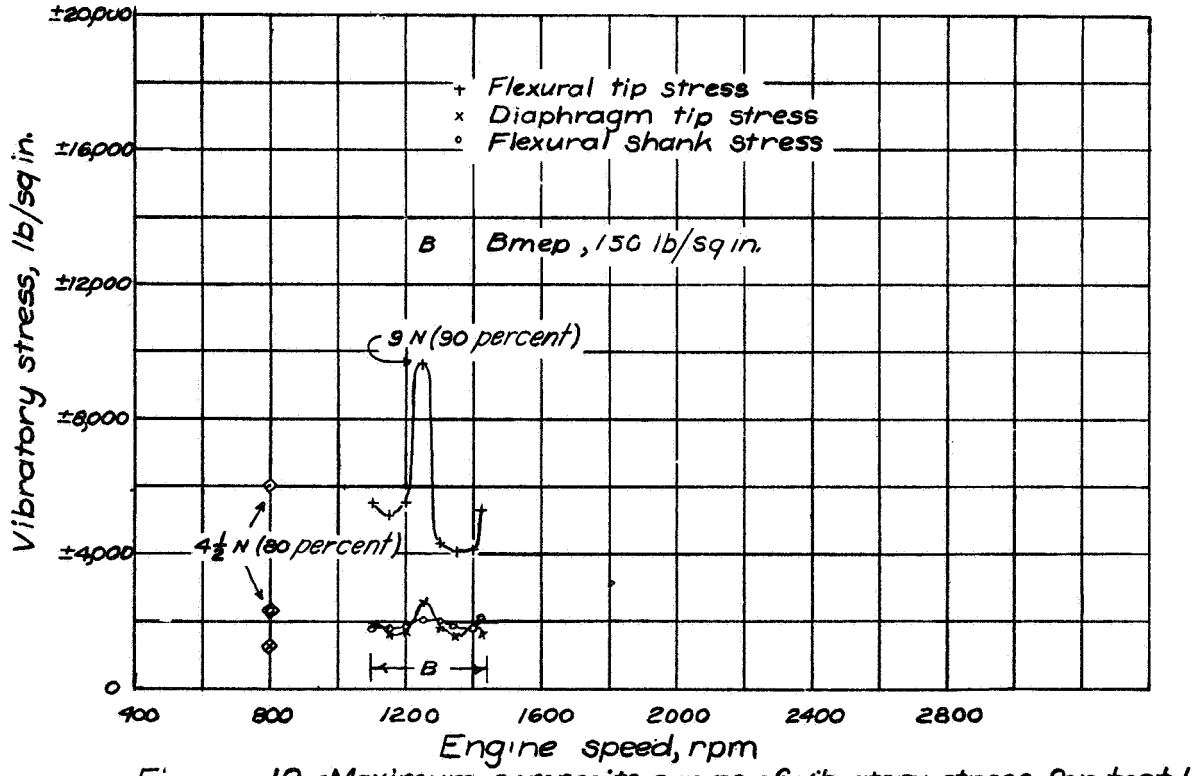

Figure 19.-Maximum composite curves of vibratory stress for test 1. Tractor; 6 blades; rear propeller, hollow steel; $\beta = 55.3°$.

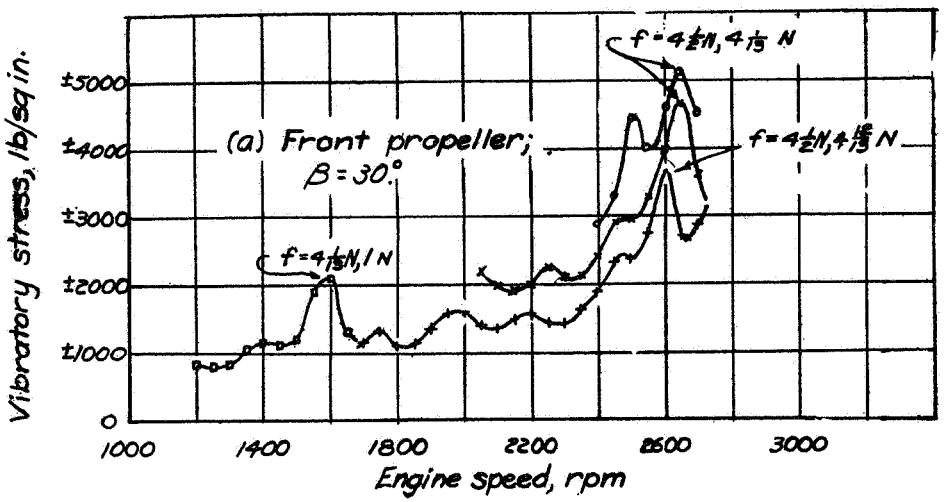

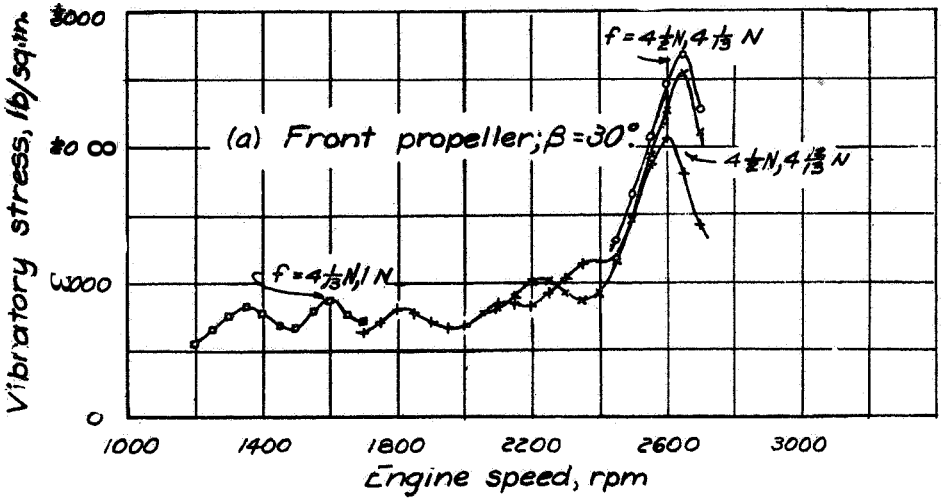

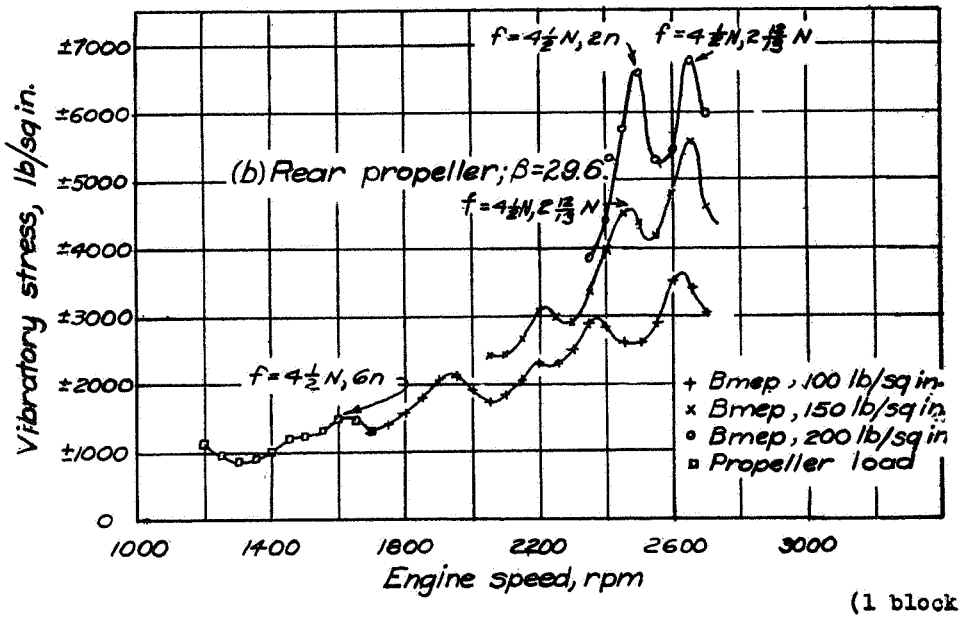

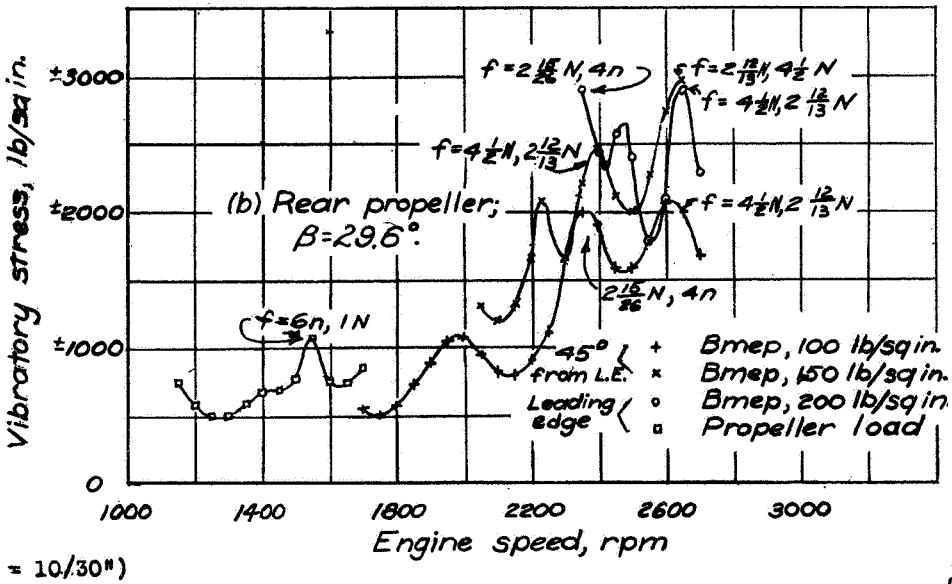

(1 block = 10/30")

Figure 20.-Effect of bmep upon vibratory tip stress, 8½ in. from tip, for test 2. Tractor; 6 blades; aluminum alloy.

Figure 21.-Effect of bmep upon vibratory shank stress for test 2. Tractor; 6 blades; aluminum alloy.

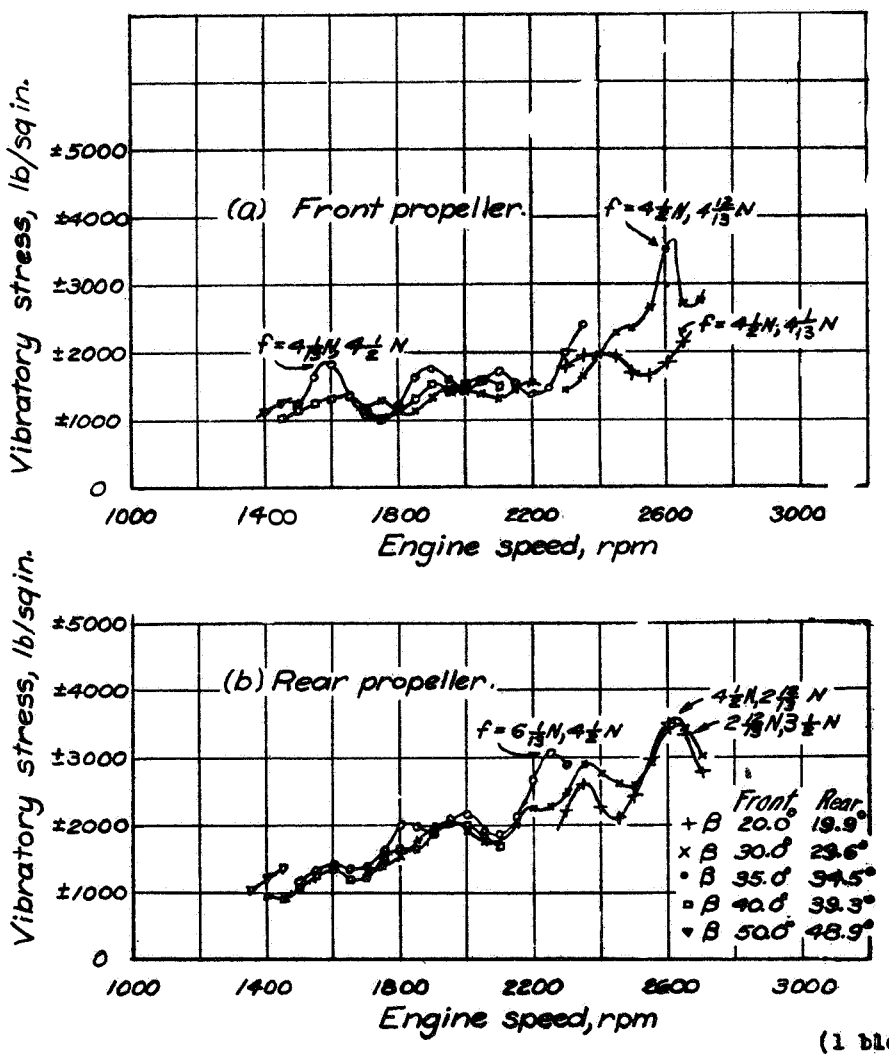

Figure 22.-Effect of blade angle upon vibratory tip stress, 8½ in. from tip, for test 2. Tractor; 6 blades, aluminum alloy; bmep, 100 pounds per square inch.

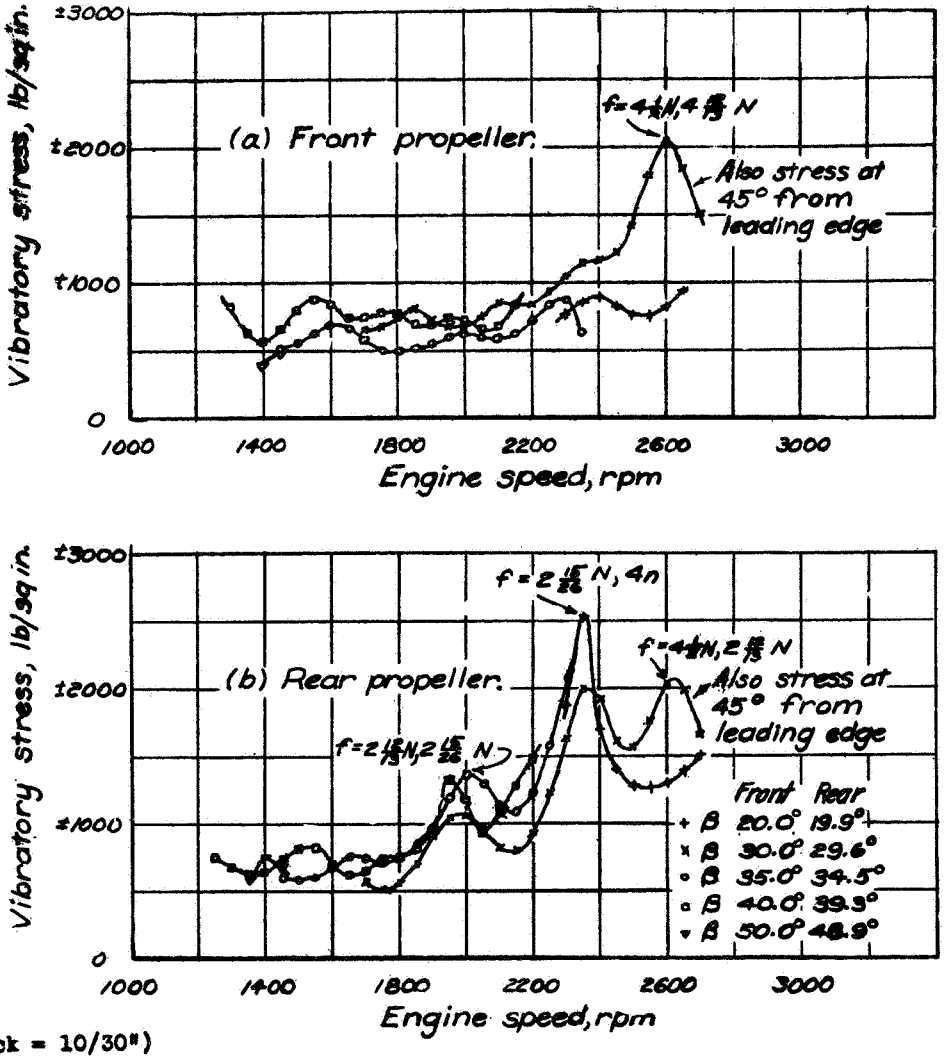

(1 block = 10/30")

Figure 23.-Effect of blade angle upon vibratory shank stress at leading-edge position for test 2. Tractor; 6 blades; aluminum alloy; bmep, 100 pounds per square inch.

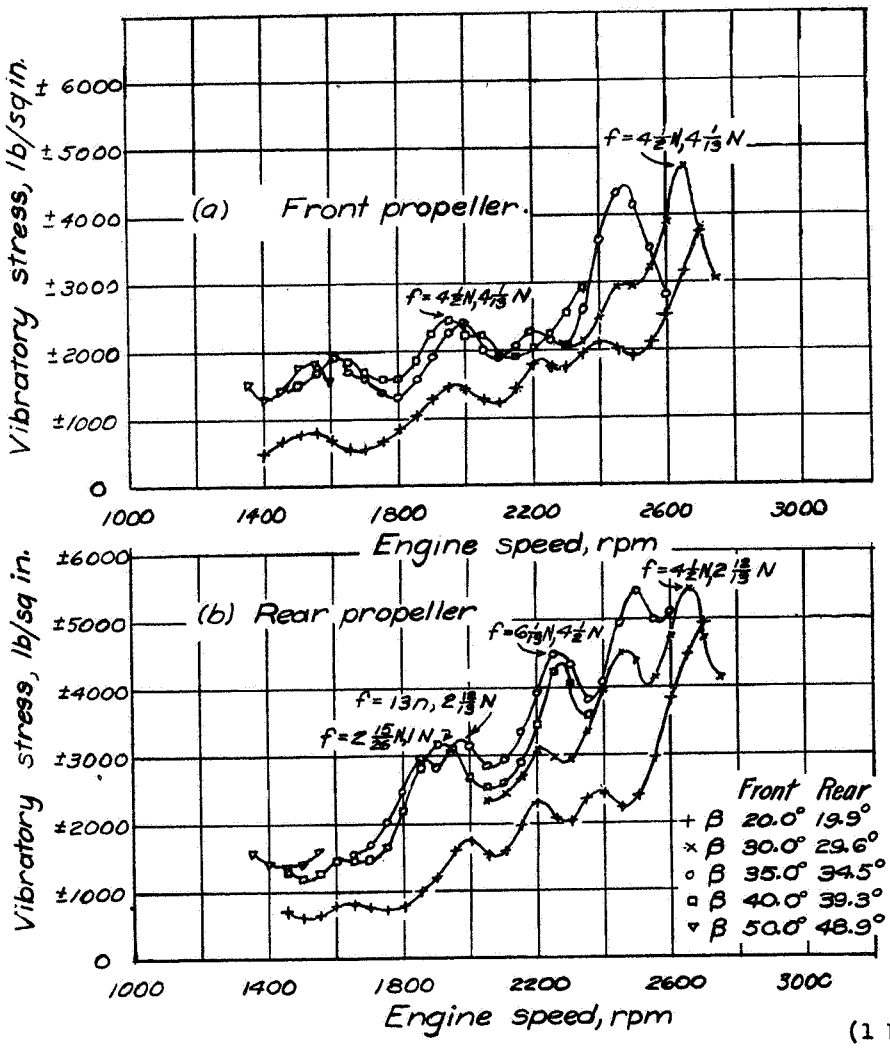

Figure 24.—Effect of blade angle upon vibratory tip stress, 8½ in. from tip, for test 2. Tractor; 6 blades; aluminum alloy; bmep, 150 pounds per square inch.

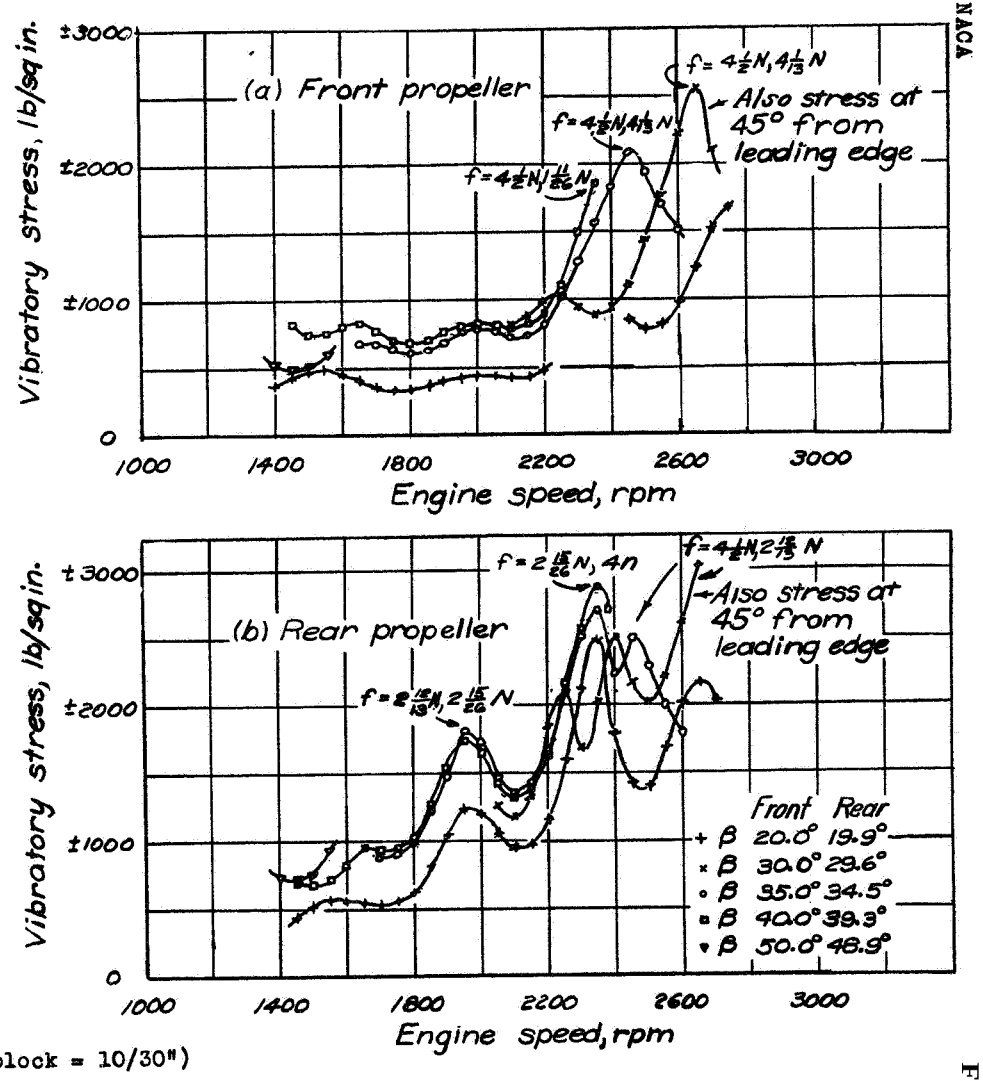

(1 block = 10/30")

Figure 25.—Effect of blade angle upon vibratory shank stress at leading-edge position for test 2. Tractor; 6 blades; aluminum alloy; bmep, 150 pounds per square inch.

NACA

Figs. 24, 25.

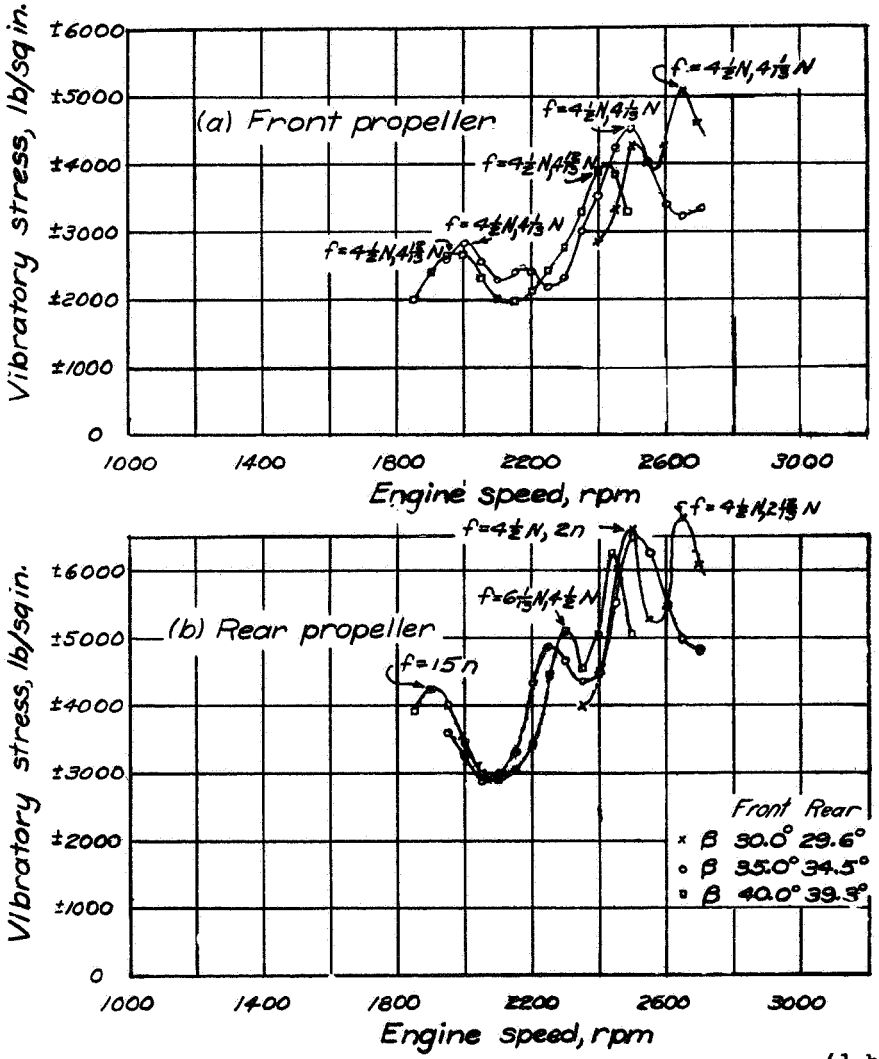

Figure 26.- Effect of blade angle upon vibratory tip stress, 8½ in. from tip, for test 2. Tractor; 6 blades, aluminum alloy; bmep, 200 pounds per square inch.

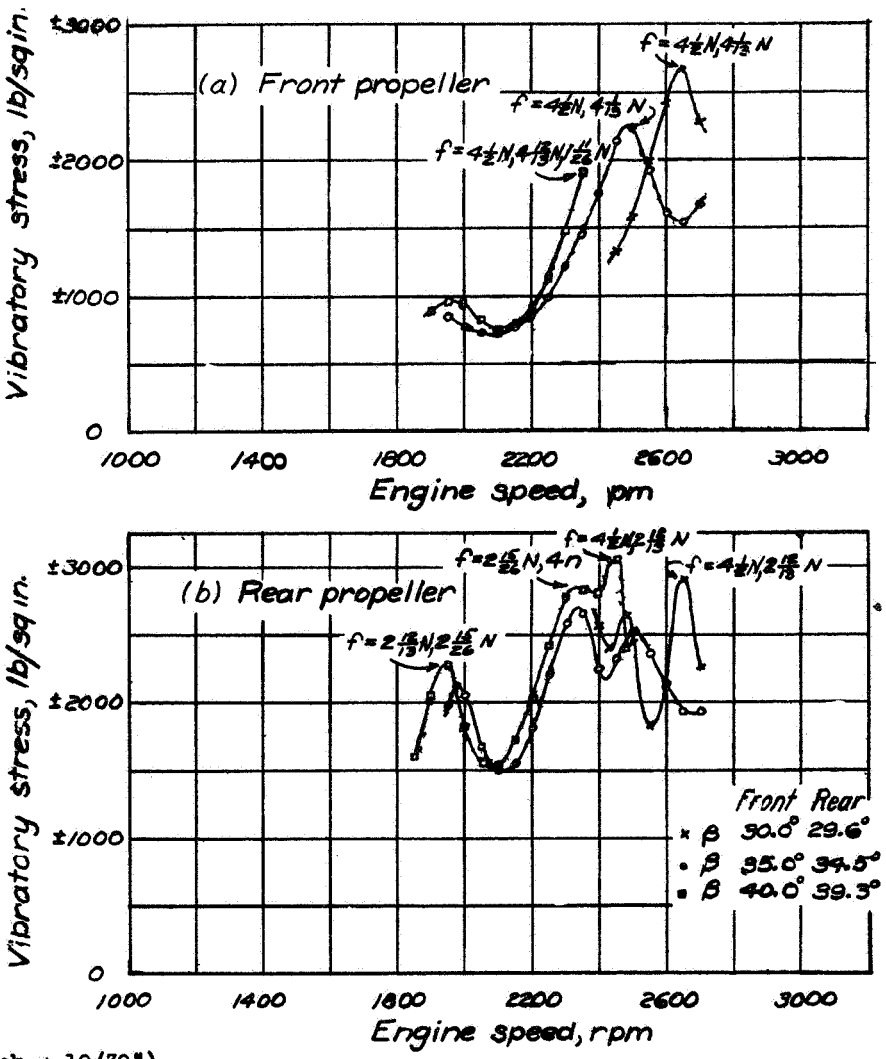

(1 blck = 10/30")

Figure 27.- Effect of blade angle upon vibratory shank stress at leading-edge position for test 2. Tractor; 6 blades; aluminum alloy; bmep, 200 pounds per square inch.

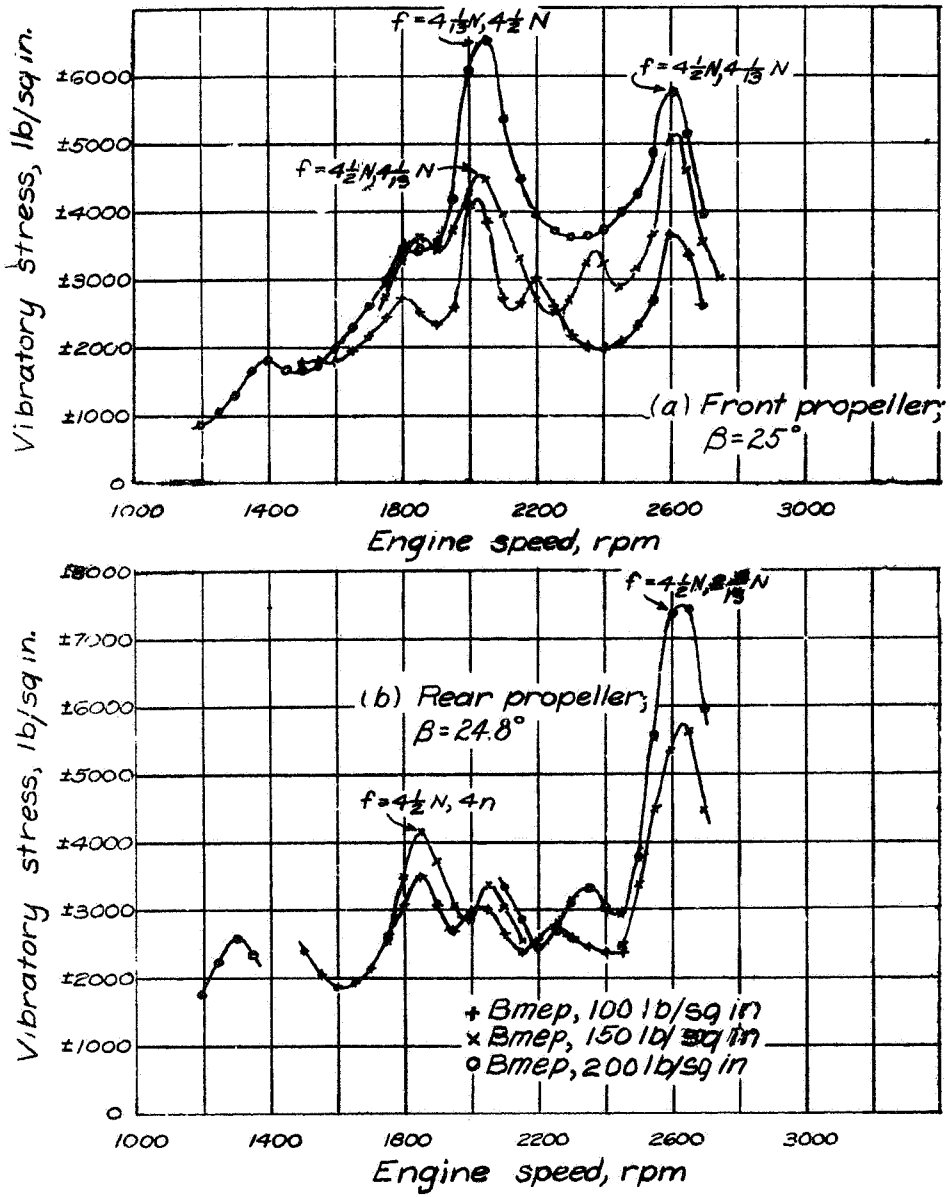

Figure 28.—Effect of bmep upon vibratory tip stress, 9 in. from tip for test 3. Tractor; 6 blades; aluminum alloy

(1 block = 10/30")

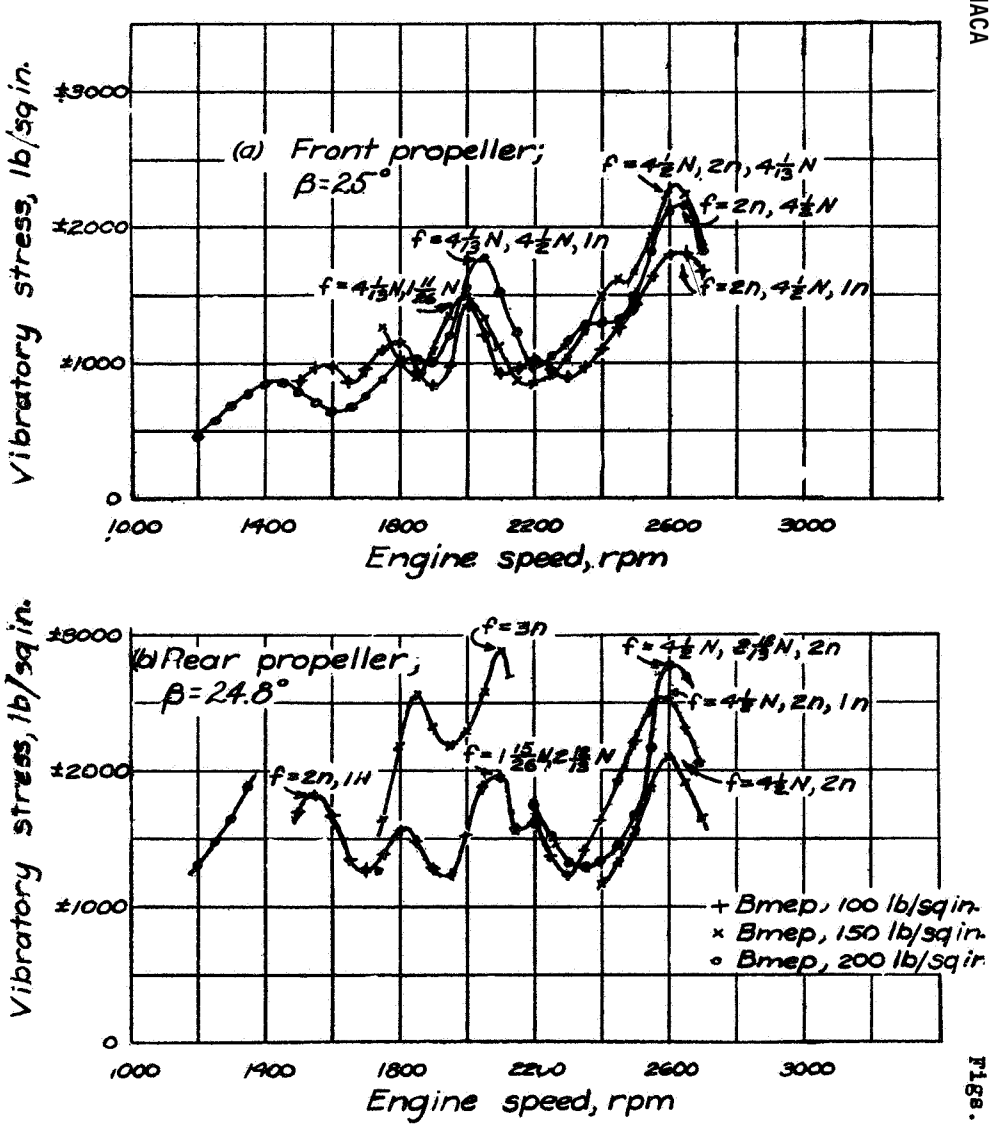

Figure 29.—Effect of bmep upon vibratory shank stress at leading-edge position for test 3. Tractor; 6 blades; aluminum alloy.

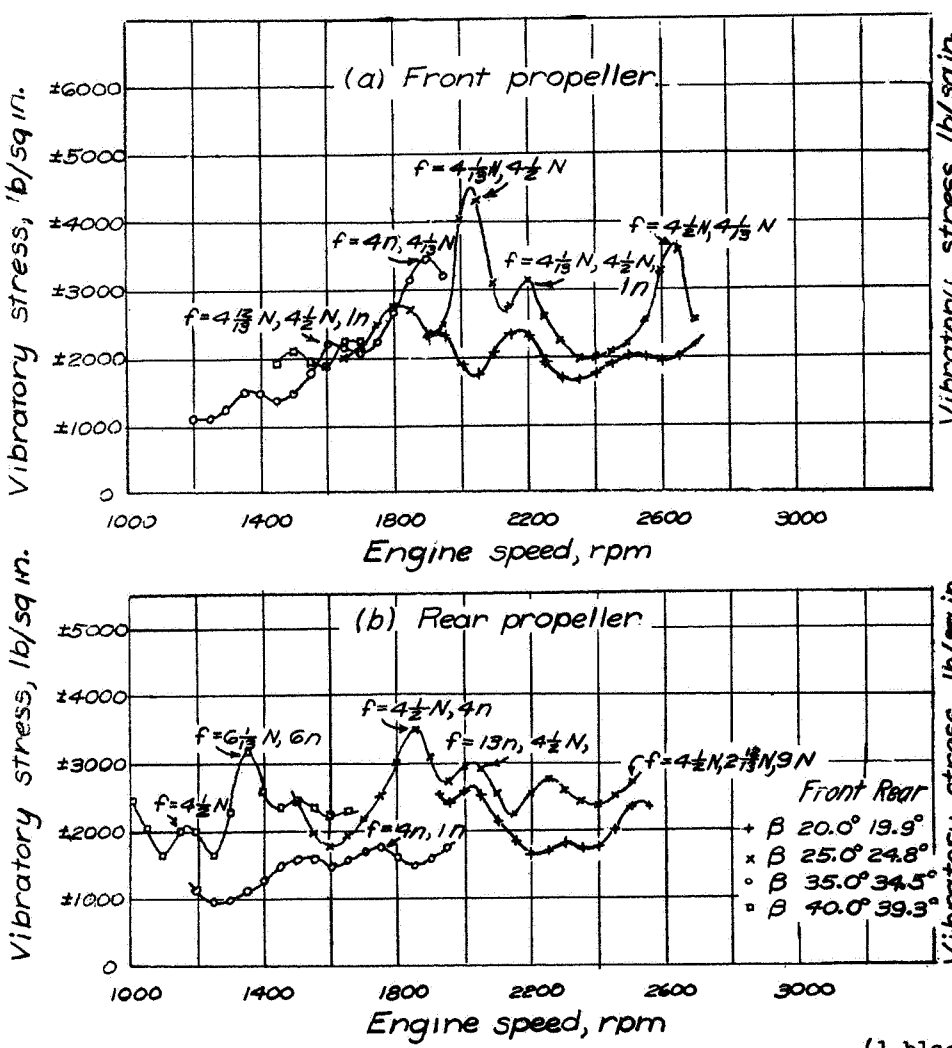

Figure 30.- Effect of blade angle upon vibratory tip stress, 9 in. from tip, for test 3. Tractor; 6 blades; aluminum alloy; bmep, 100 pounds per square inch

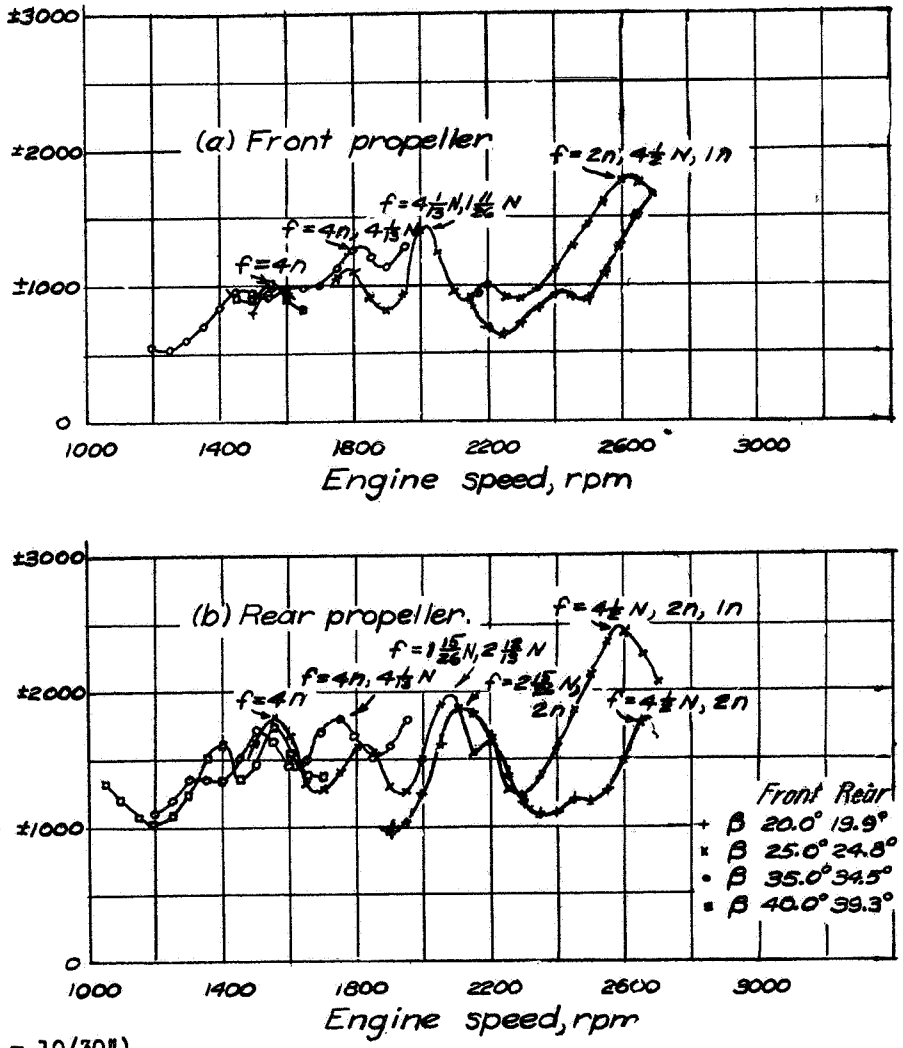

Figure 31.- Effect of blade angle upon vibratory shank stress at leading-edge position for test 3 Tractor; 6 blades; aluminum alloy; bmep, 100 pounds per square inch.

(1 block = 10/30")

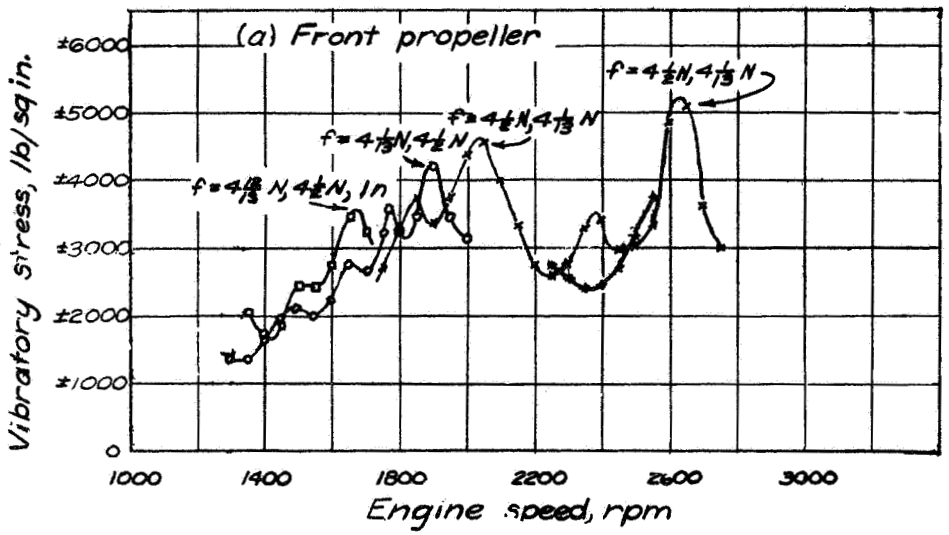

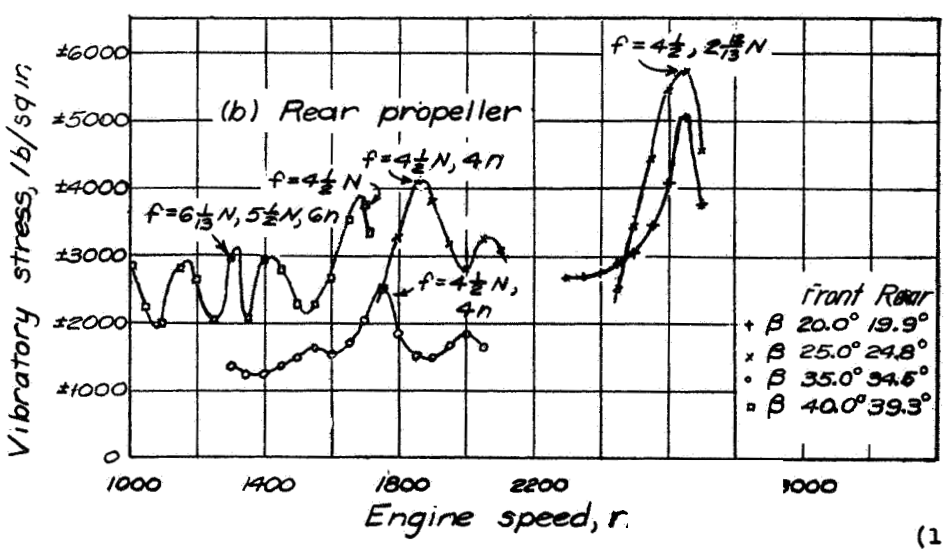

Figure 32.- Effect of blade angle upon vibratory tip stress, 9 in. from tip, for test 3. Tractor; 6 blades; aluminum alloy; bmep, 150 pounds per square inch.

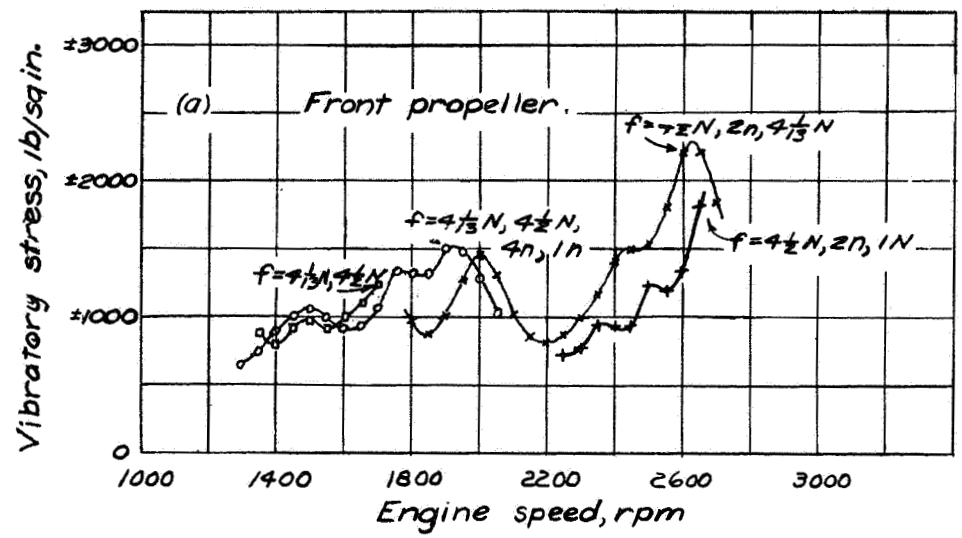

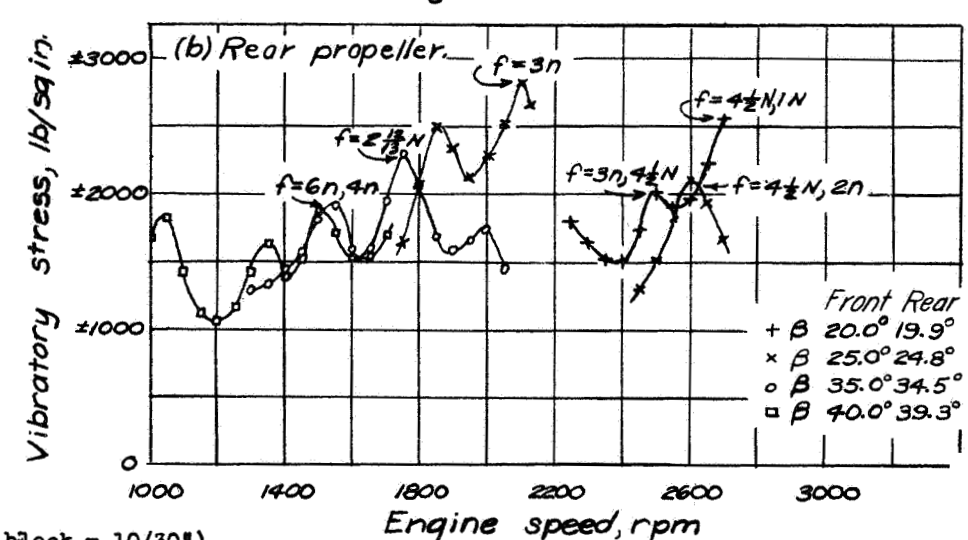

(1 block = 10/30")

Figure 33.- Effect of blade angle upon vibratory shank stress at leading-edge position for Test 3. Tractor; 6 blades; aluminum alloy; bmep, 150 pounds per square inch.

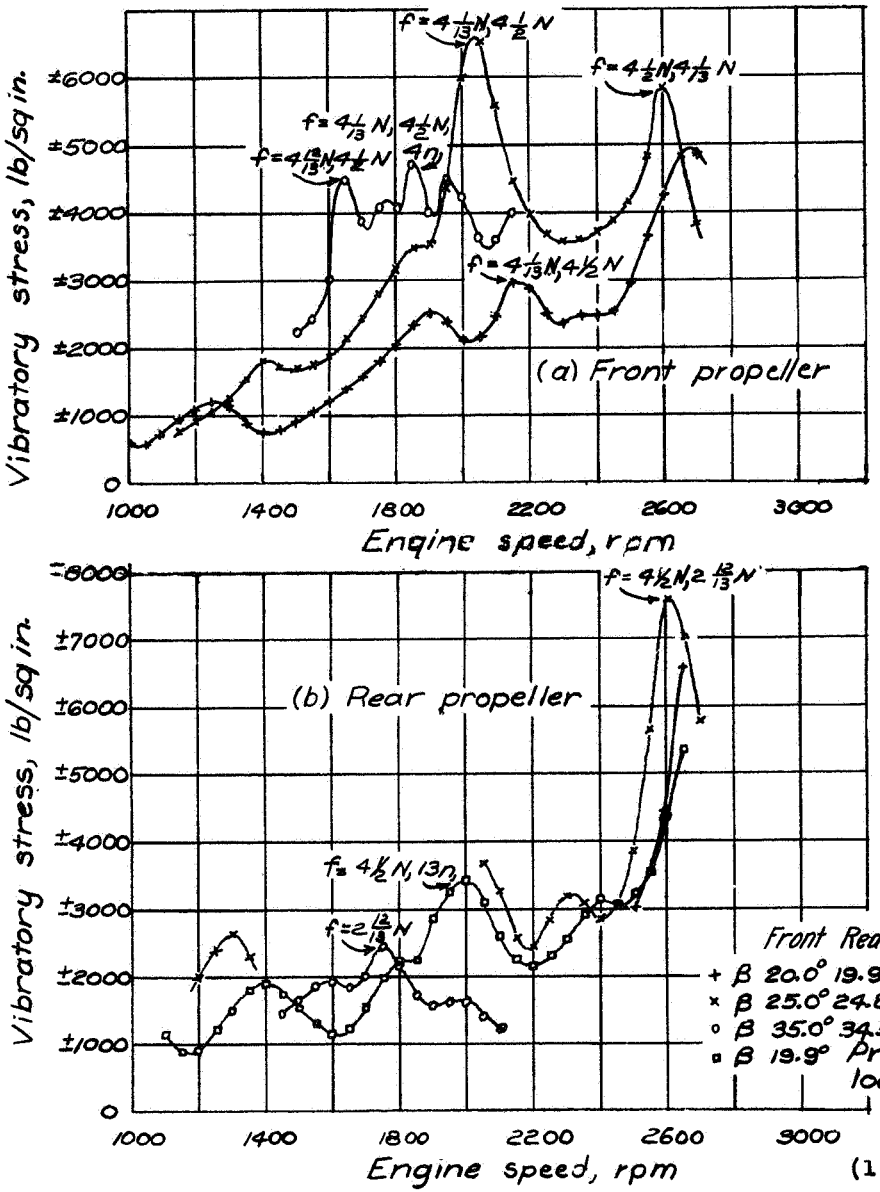

Figure 34.-Effect of blade angle upon vibratory tip stress, 9 in. from tip, for test 3. Tractor; 6 blades; aluminum alloy; bmep, 200 pounds per square inch.

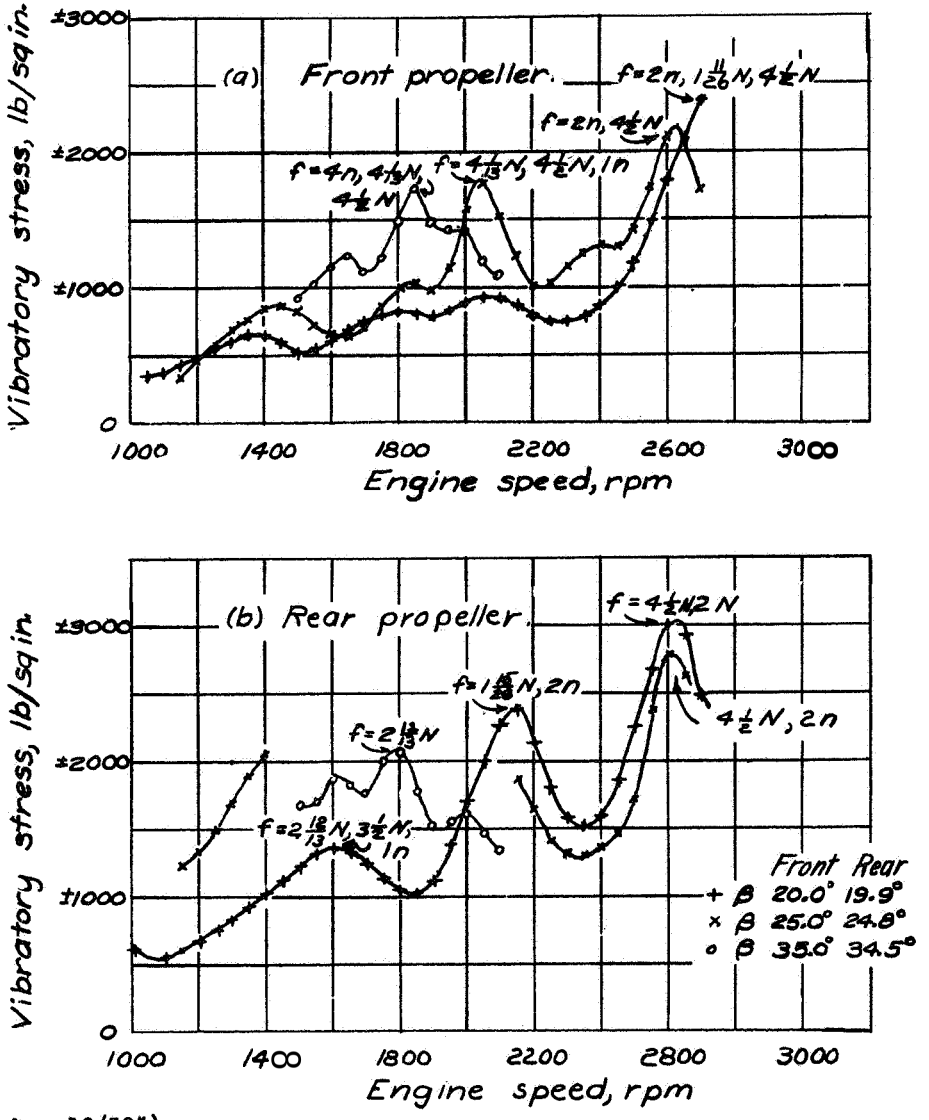

(1 block = 10/30")

Figure 35.-Effect of blade angle upon vibratory shank stress at leading-edge position for test 3. Tractor; 6 blades; aluminum alloy; bmep, 200 pounds per square inch.

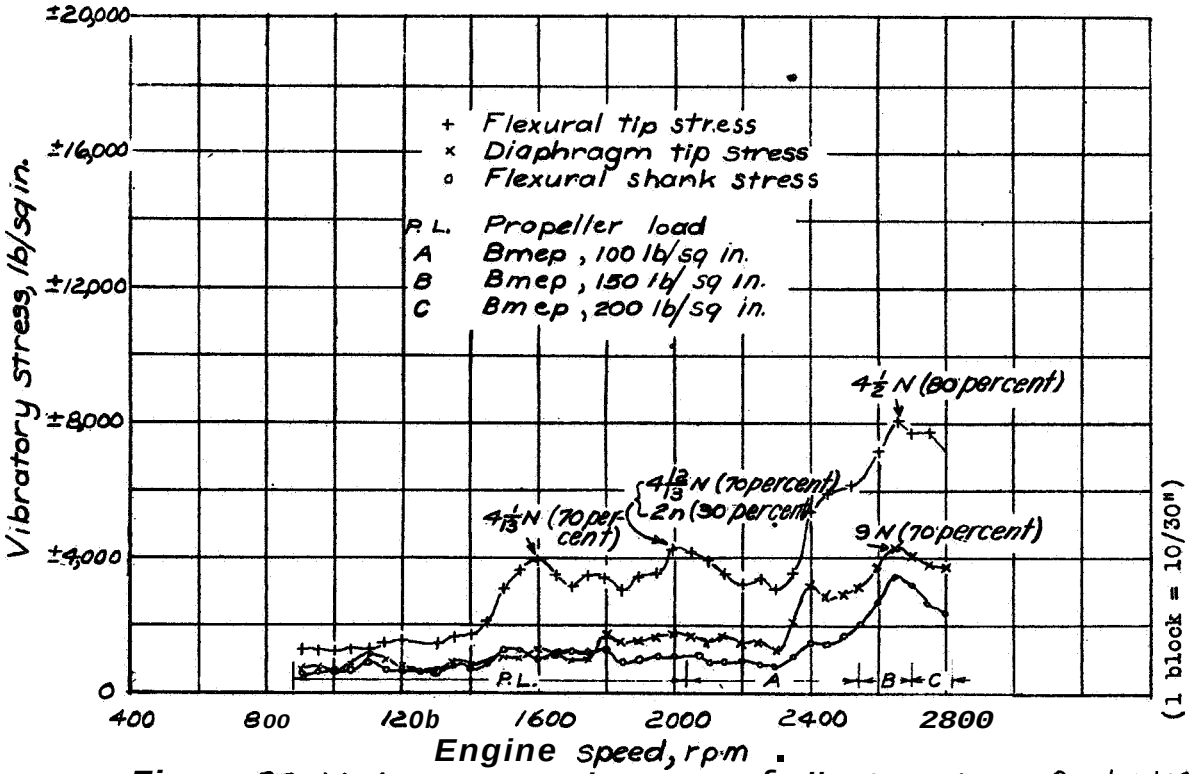

Figure 36.-Maximum composite curves of vibratory stress for test 4. Tractor; 8 blades; front propeller, hollow steel; $\beta = 26.4°$.

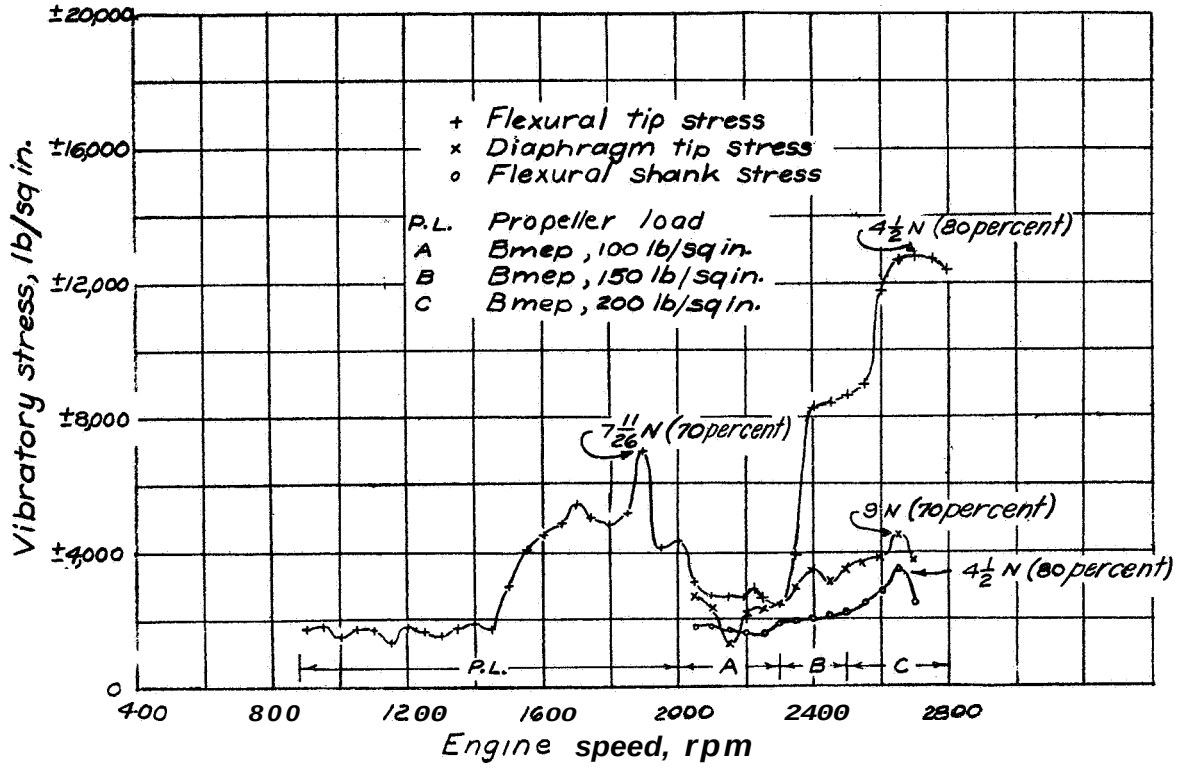

figure 37.-Maximum composite curves of vibratory stress for test 4. Tractor; 8 blades; rear propeller, hollow steel, $\beta = 25.9°$.

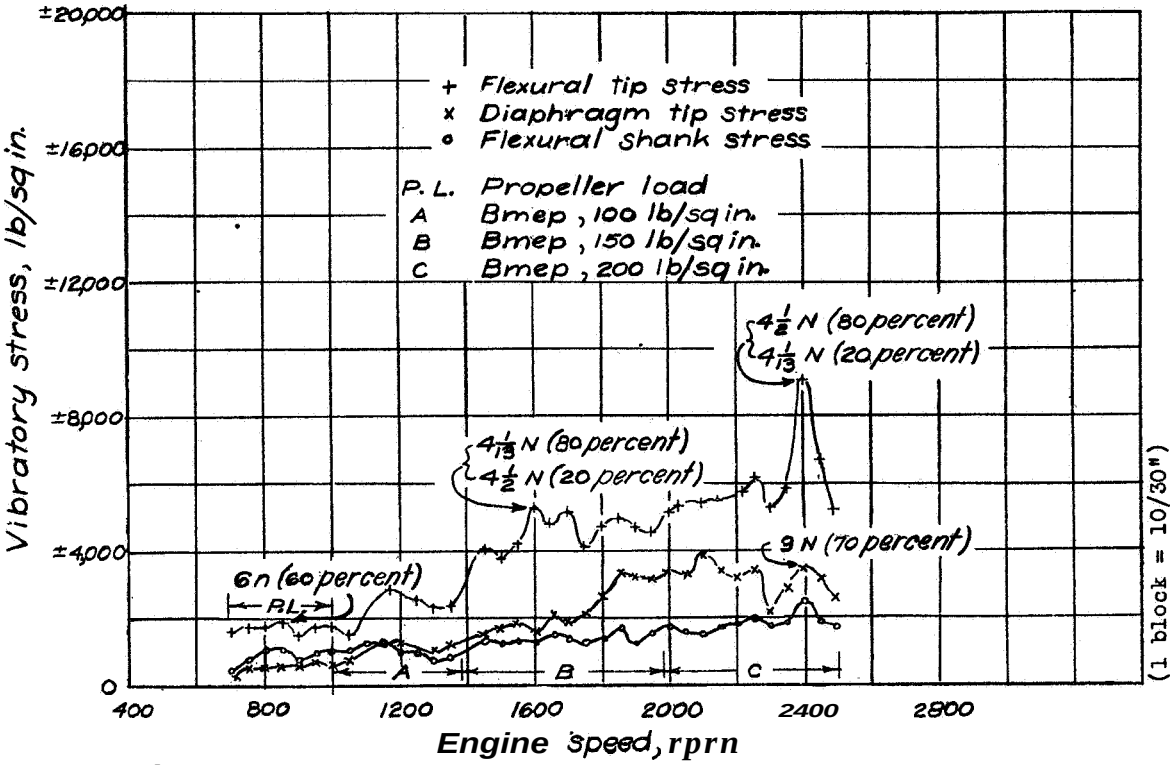

Figure 38.-Maximum composite curves of vibratory stress for test 4. Tractor; 8 blades, front propeller, hollow steel, β=38.7°.

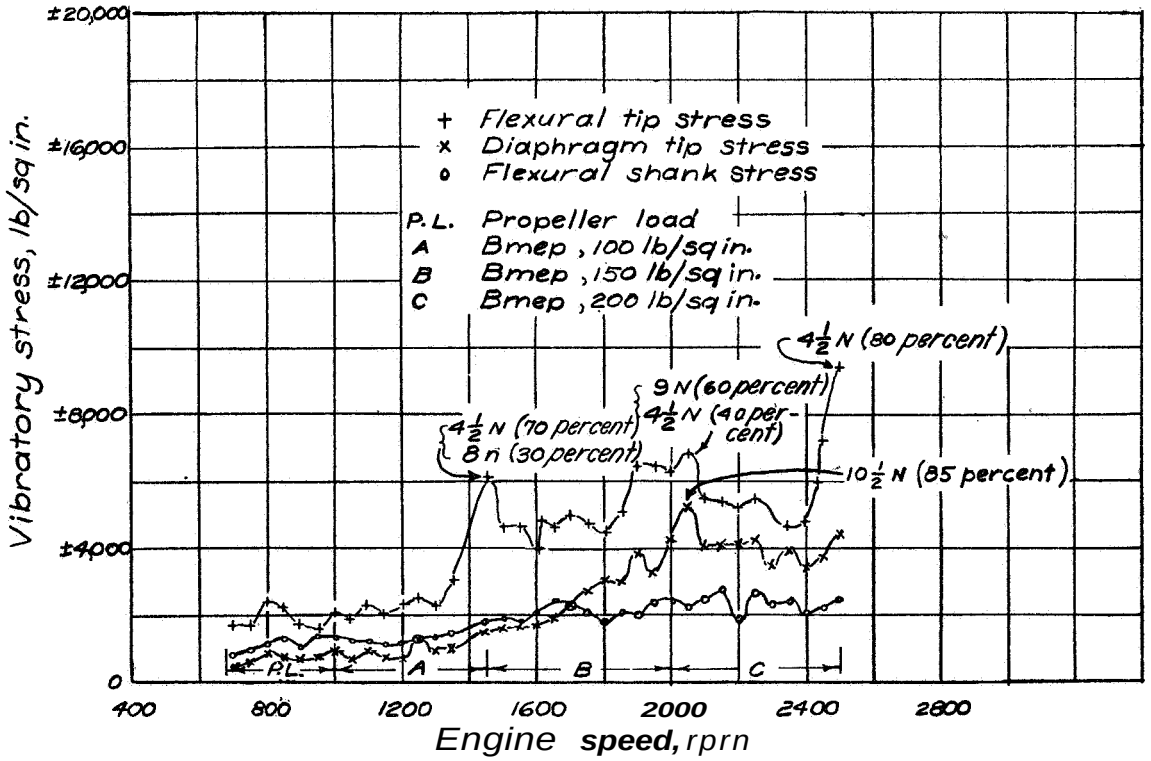

Figure 39.-Maximum composite curves of vibratory stress for test 4. Tractor; 8 blades, rear propeller, hollow steel, β=37.9°.

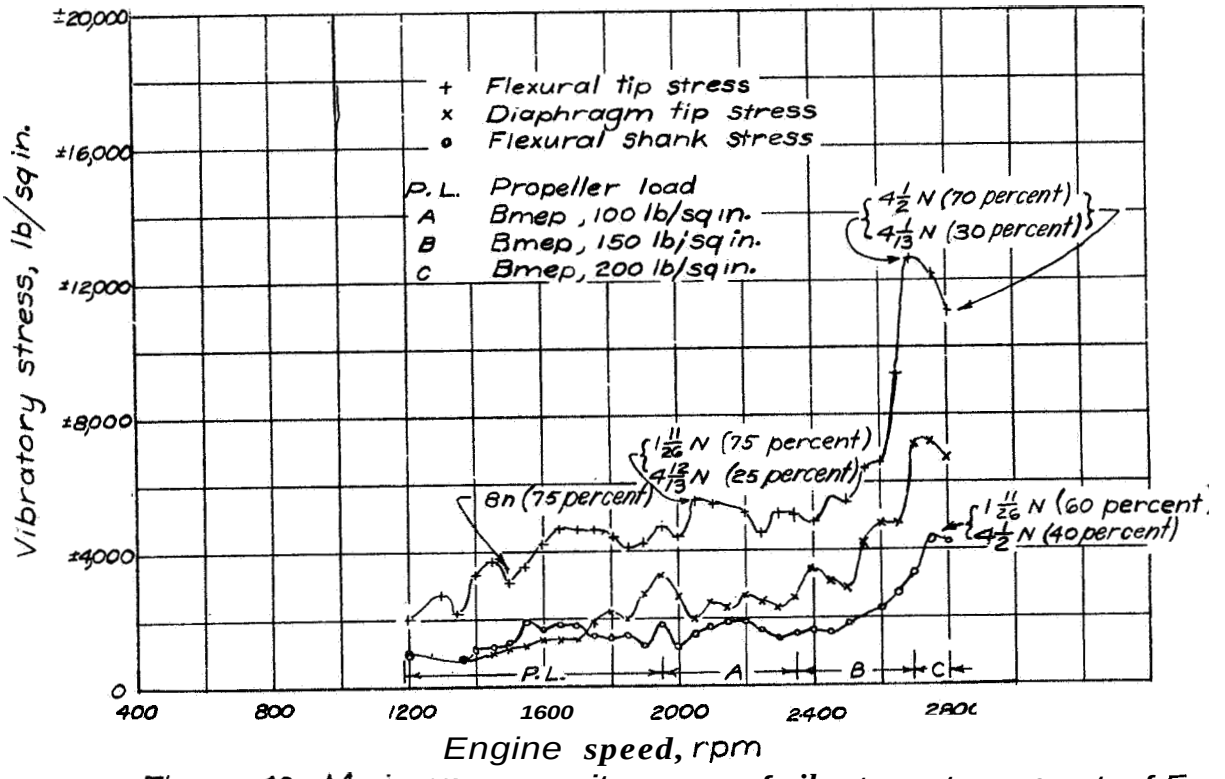

Figure 40.--Maximum composite curves of vibratory stress for test 5. Pusher; 7 blades, front propeller, 3-blade hollow steel, β=29.8°

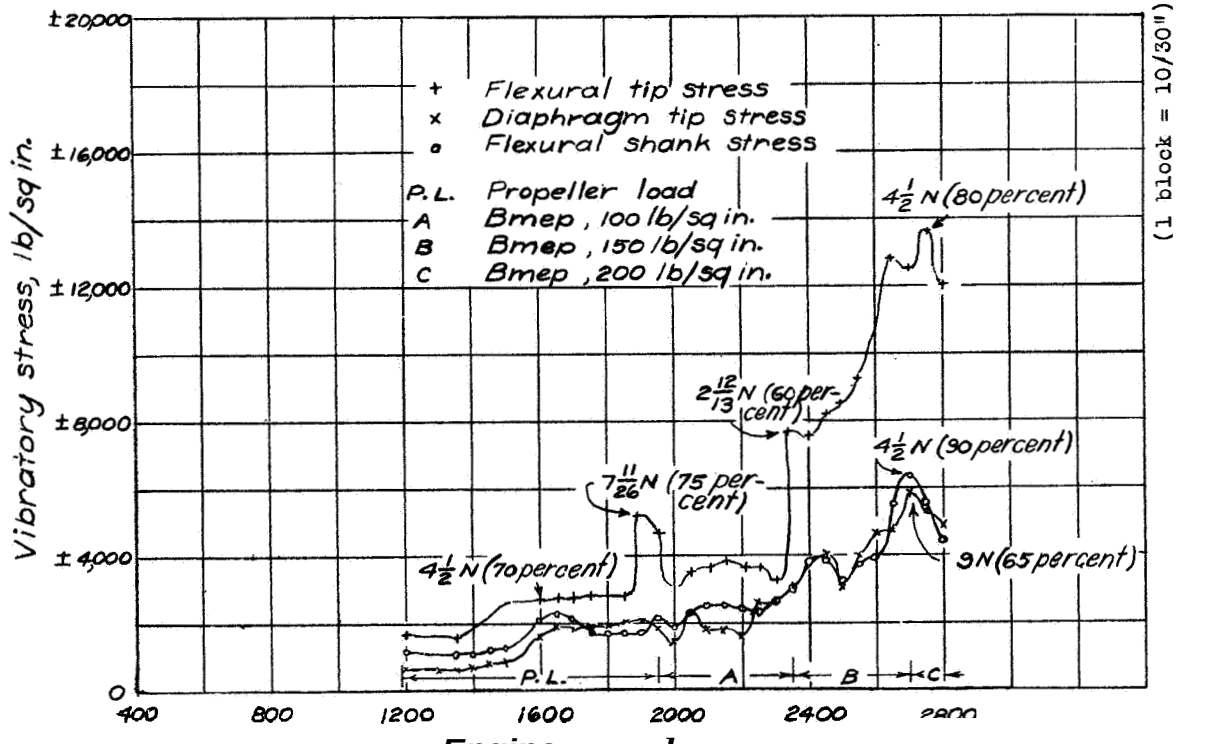

Figure 41.--Maximum composite curves of vibratory stress for test 5. Pusher; 7 blades, rear propeller, 4-blade hollow steel, β=26.1°

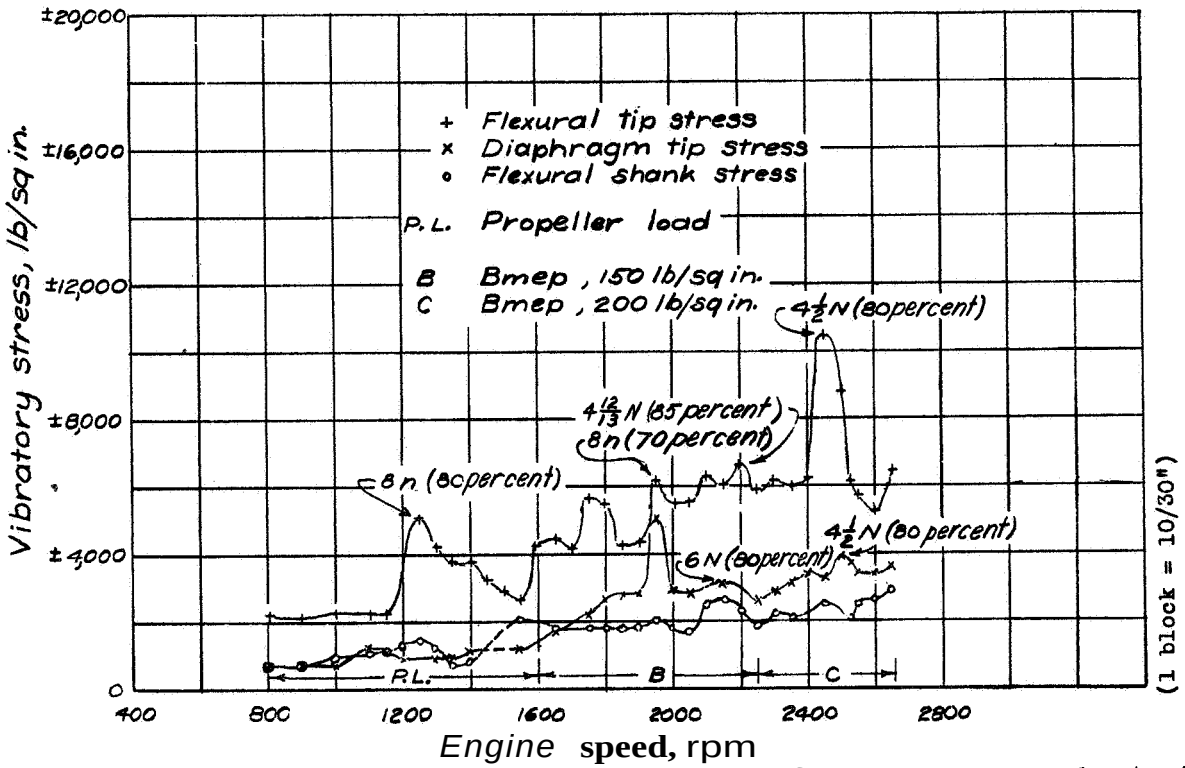

Figure 42 - Maximum composite curves of vibratory stress for test 5. Pusher; 7 blades; front propeller, 3-blade hollow steel, $\beta = 39.9°$

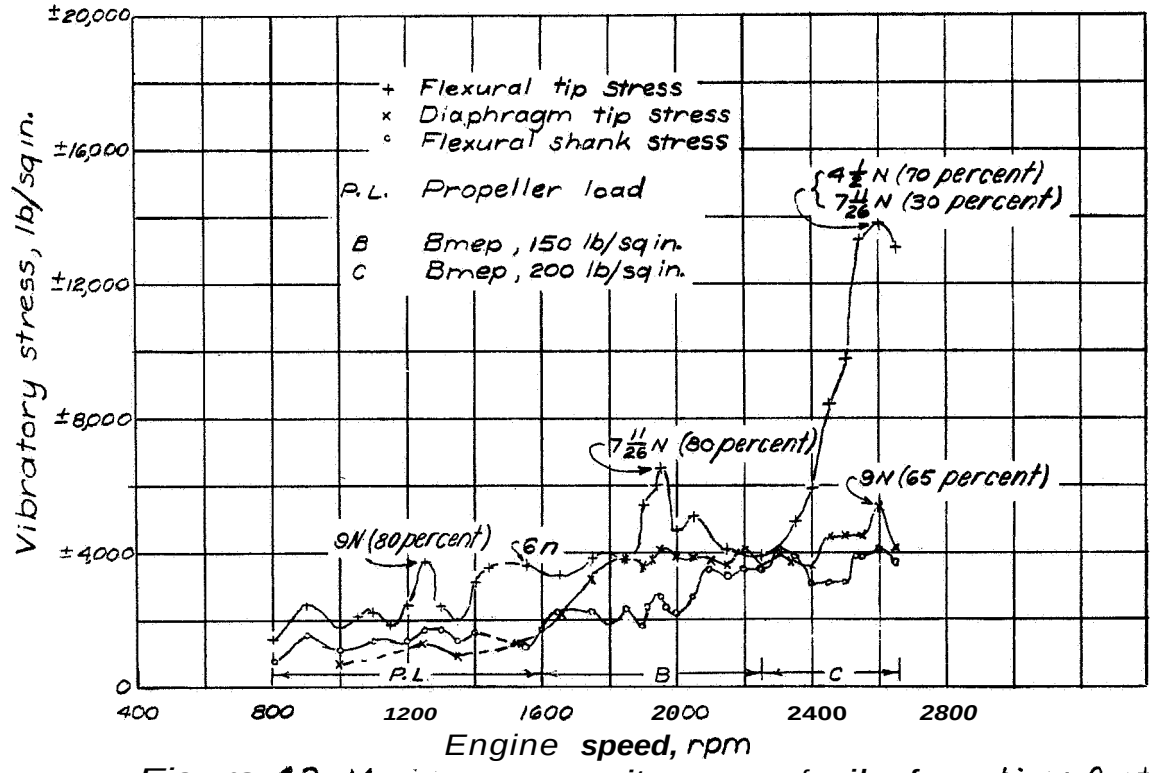

Figure 43.- Maximum composite curves of vibratory stress for test 5. Pusher; 7 blades; rear propeller, 4-blade hollow steel; $\beta = 37.8°$.

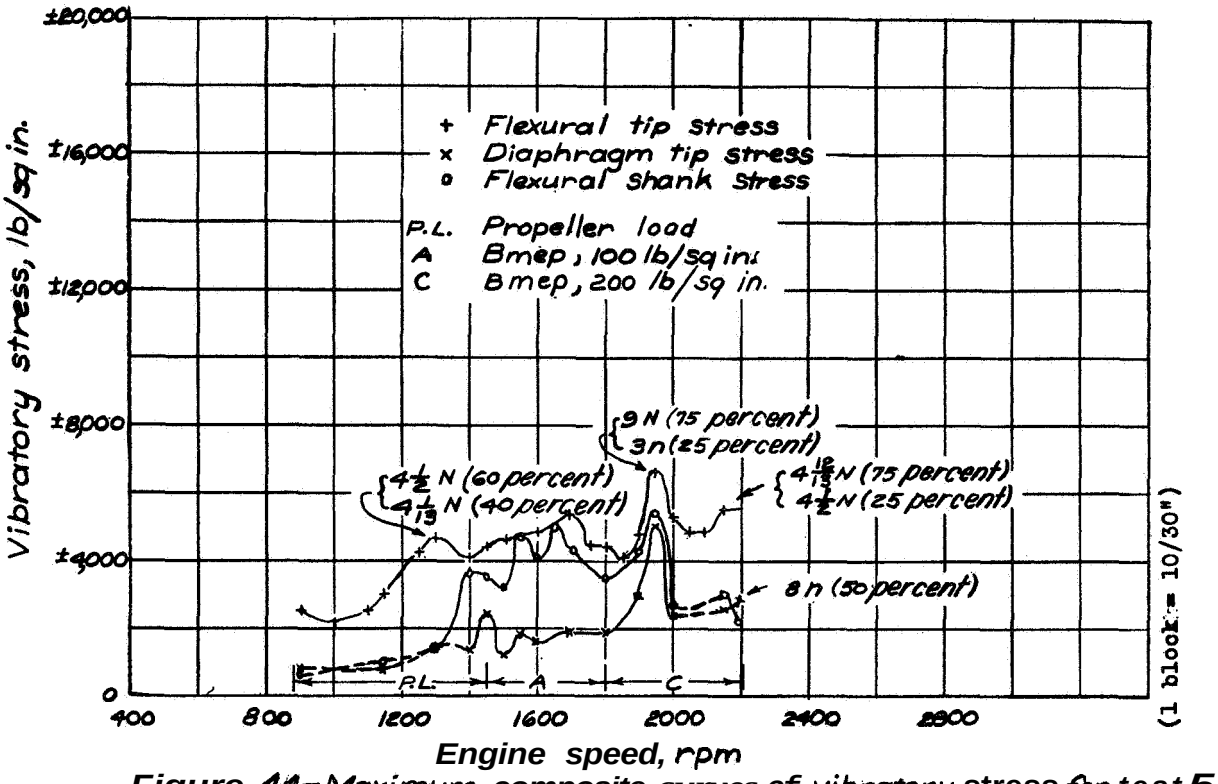

Figure 44-Maximum composite curves of vibratory stress for test 5. Pusher; 7 blades; front propeller, 3-blade hollow steel; β=45.3°.

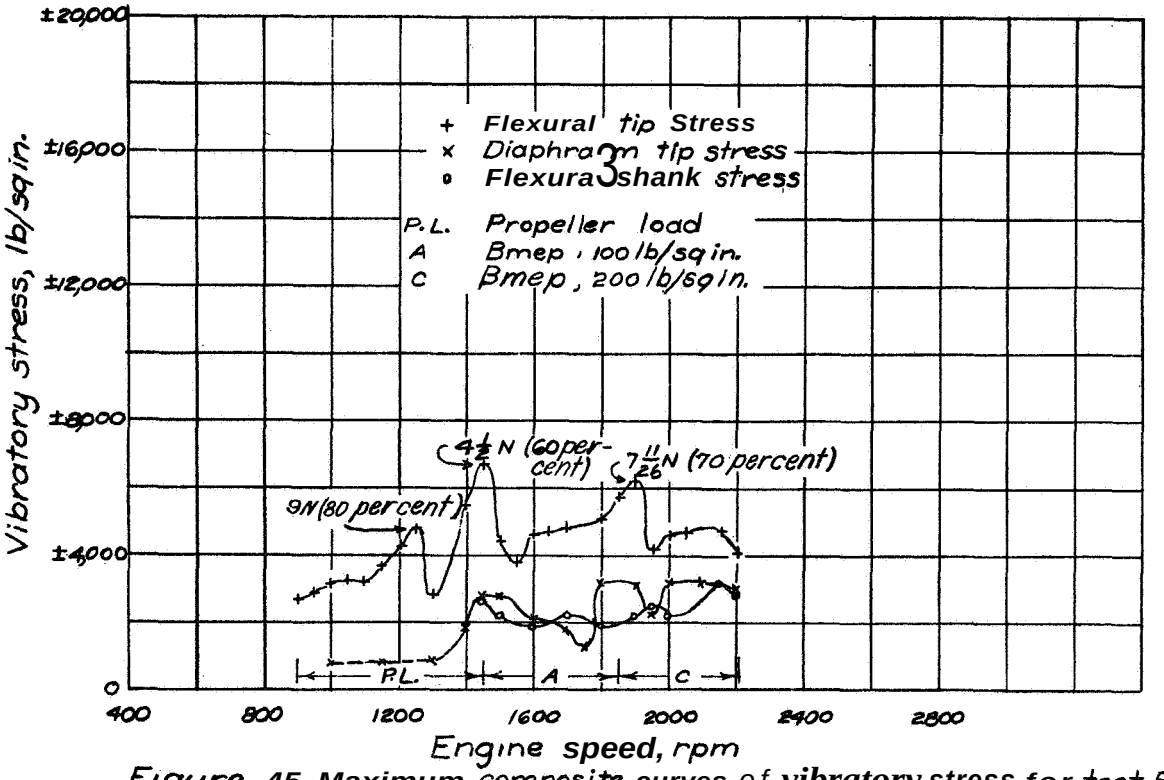

Figure 45-Maximum composite curves of vibratory stress for test 5. Pusher; 7 blades, rear propeller, 4-blade hollow steel; β=42.9°

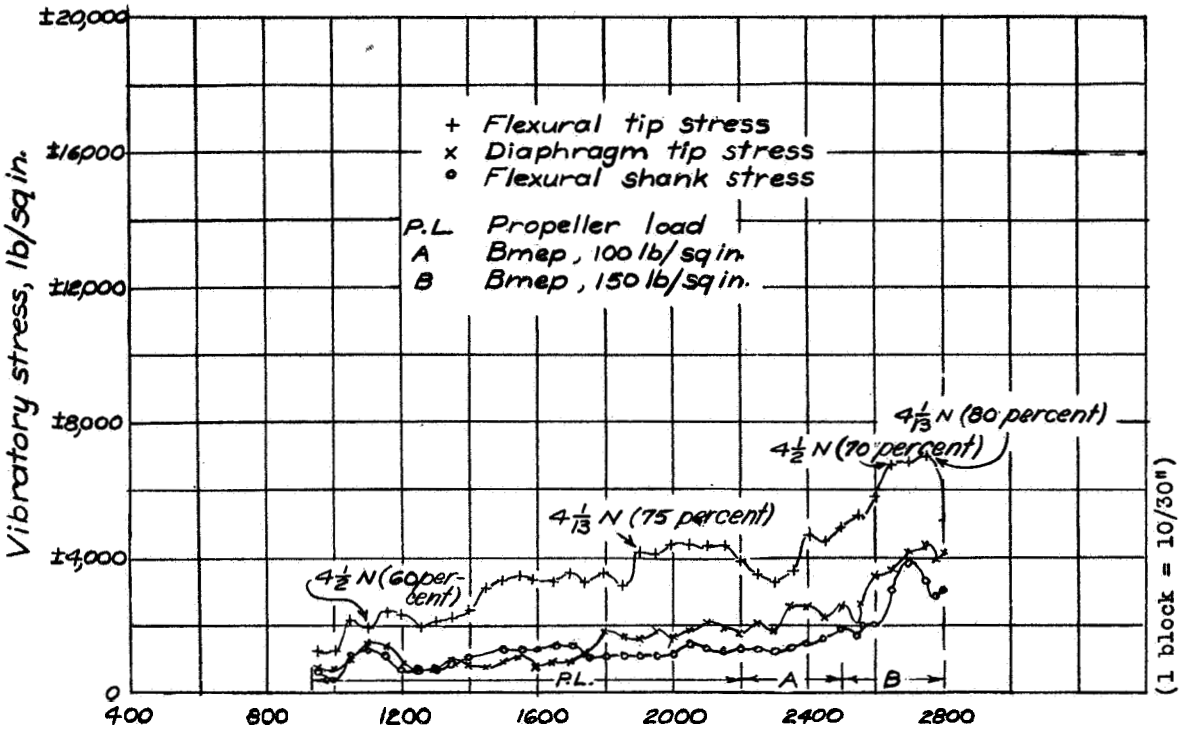

Figure 46.-Maximum composite curves of vibratory stress for test 6. Pusher; 8 blades: front propeller, hollow steel; β=26.6°.

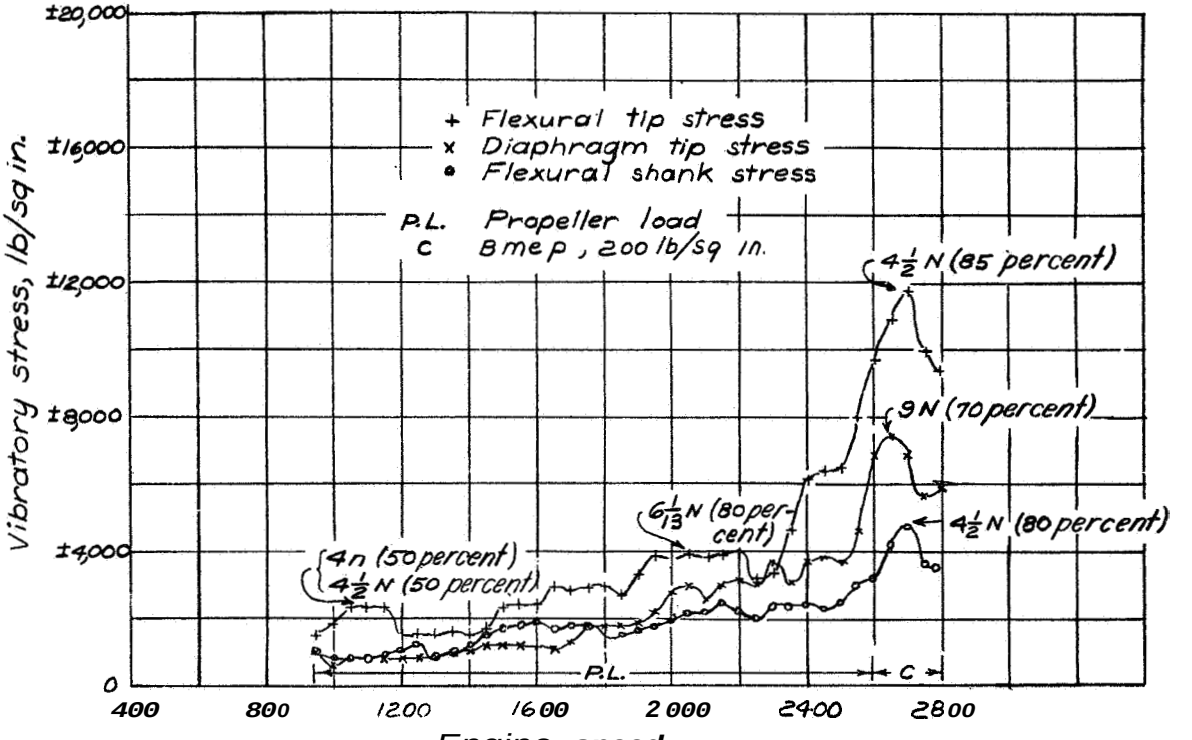

Figure 47-Maximum composite curves of vibratory stress for test 6. Pusher; 8 blades; rear propeller, hollow steel, β=26.3°.

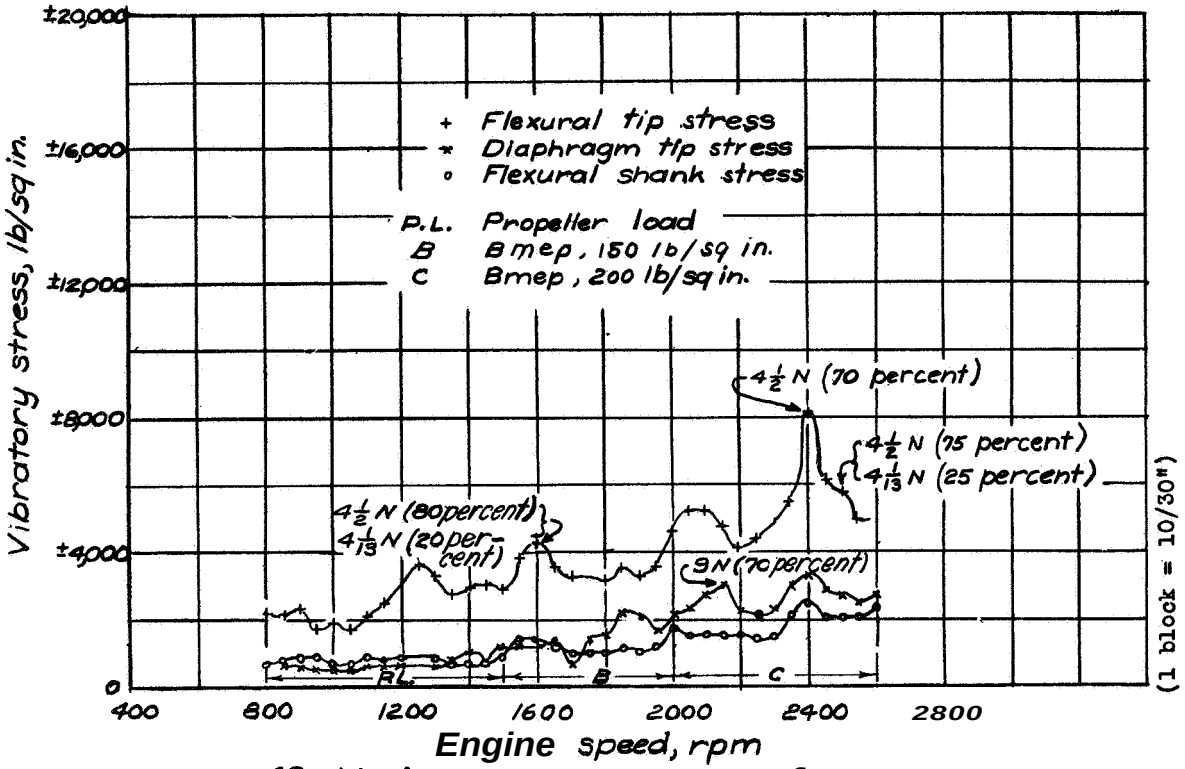

Figure 48.–Maximum composite curves of vibratory stress for test 6. Pusher; 8 blades; front propeller, hollow steel; β=38.0°.

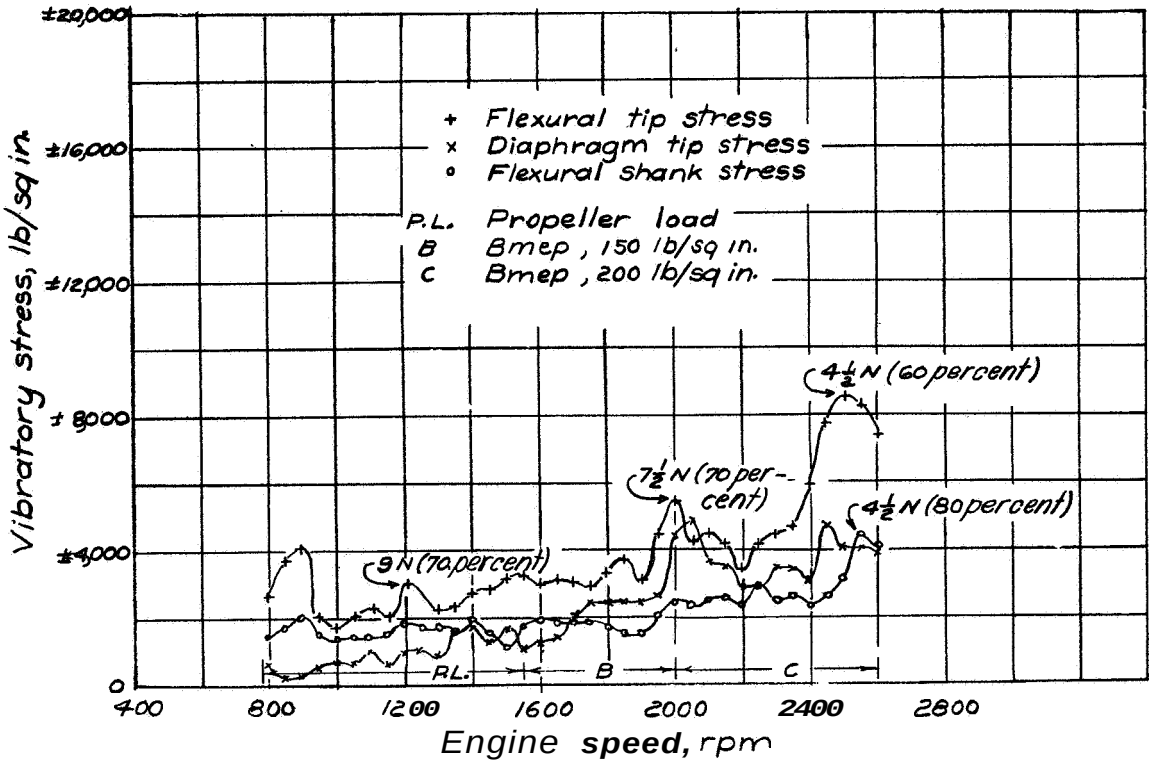

figure 49.–Maximum composite curves of vibratory stress for test 6. Pusher; 8 blades; rear propeller, hollow steel, β=37.5°

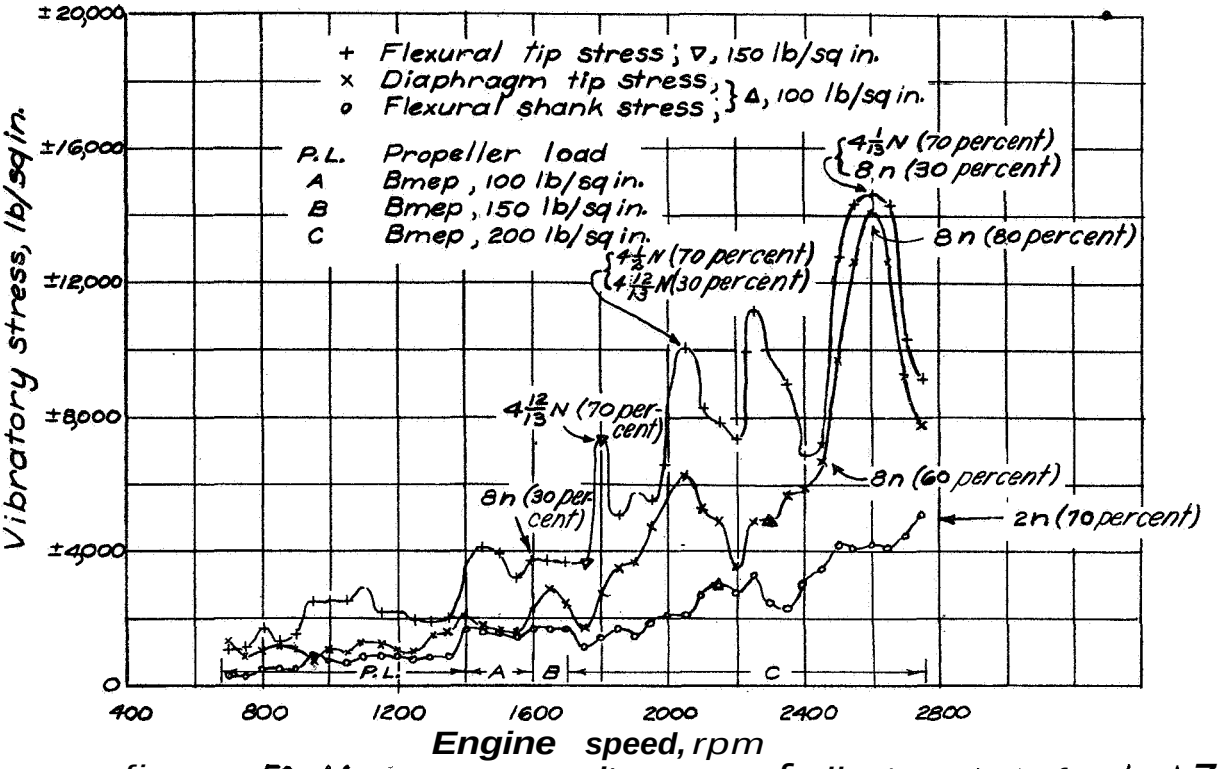

figure 50.-Maximum composite curves of vibratory stress for test 7. Pusher; 7 blades; Front propeller, 3-blade hollow steel; β=36.2°.

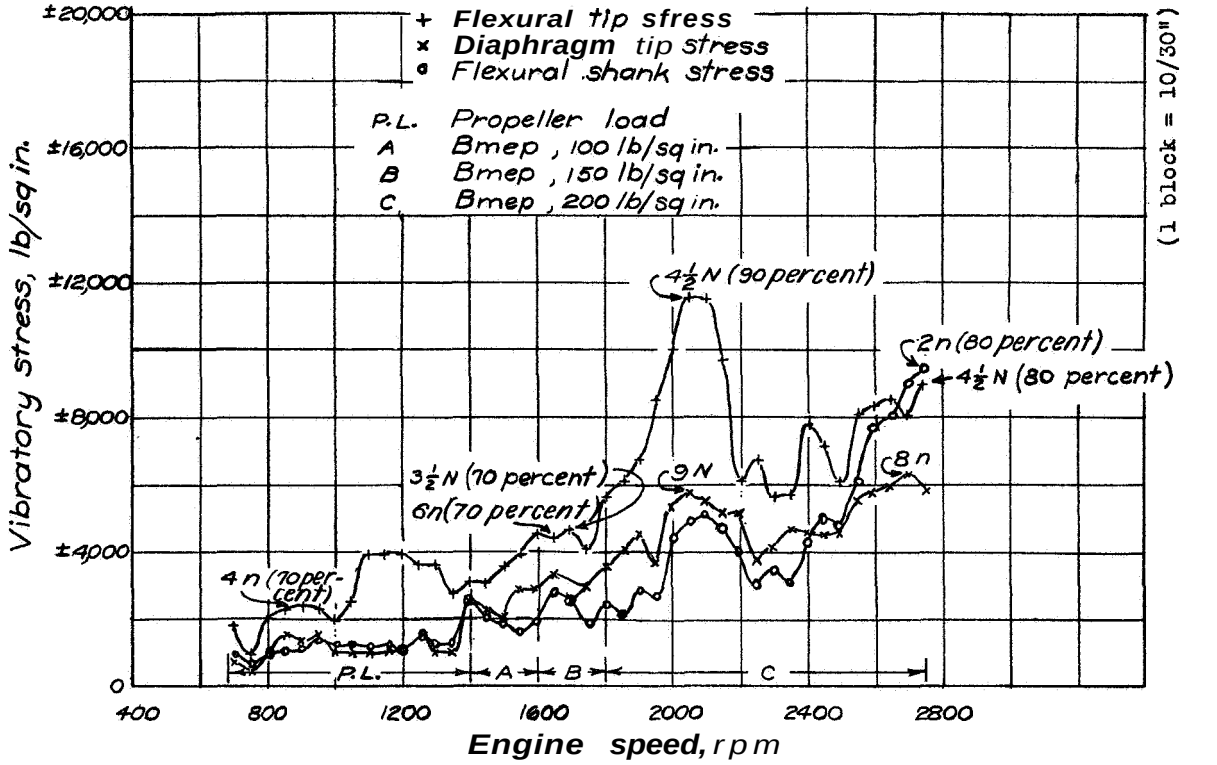

Figure 51.-Maximum composite curves of vibratory stress for test 7. Pusher; 7 blades; rear propeller, 4-blade hollow steel; β=35.0°.

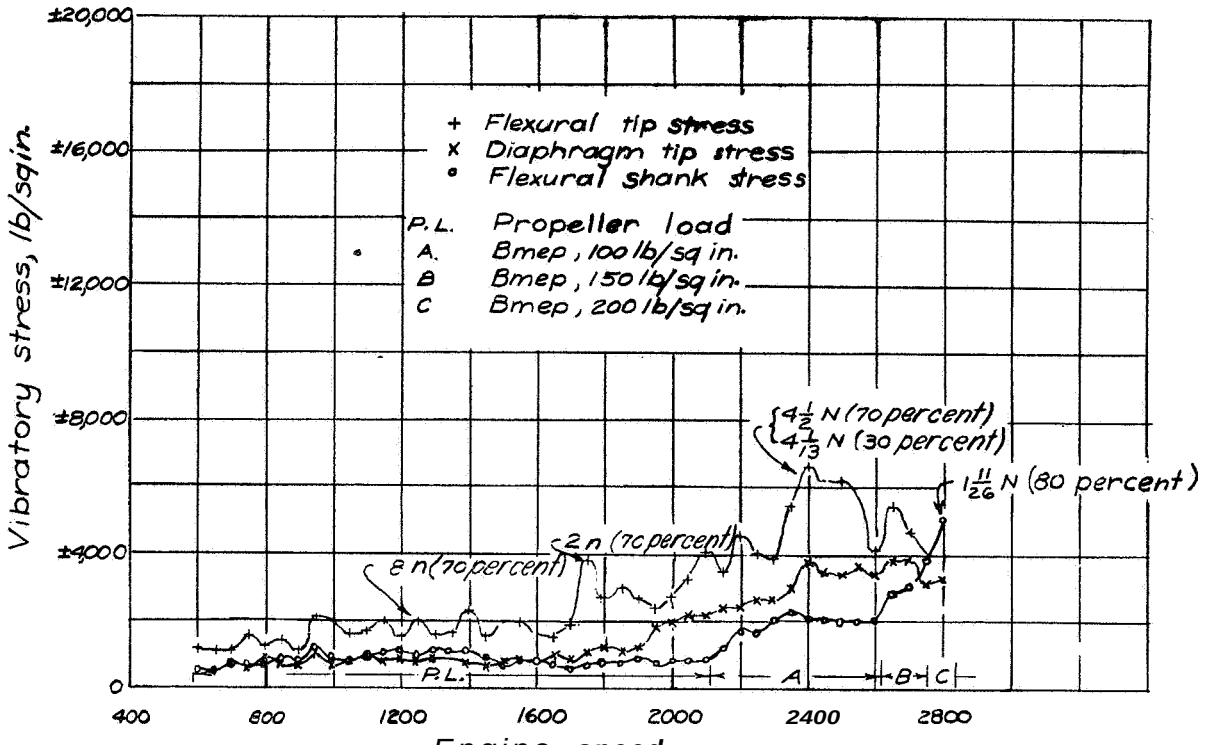

Figure 52.-Maximum composite curves of vibratory stress for test 8. Pusher, 8 blades; front propeller, hollow steel, β=22.1°

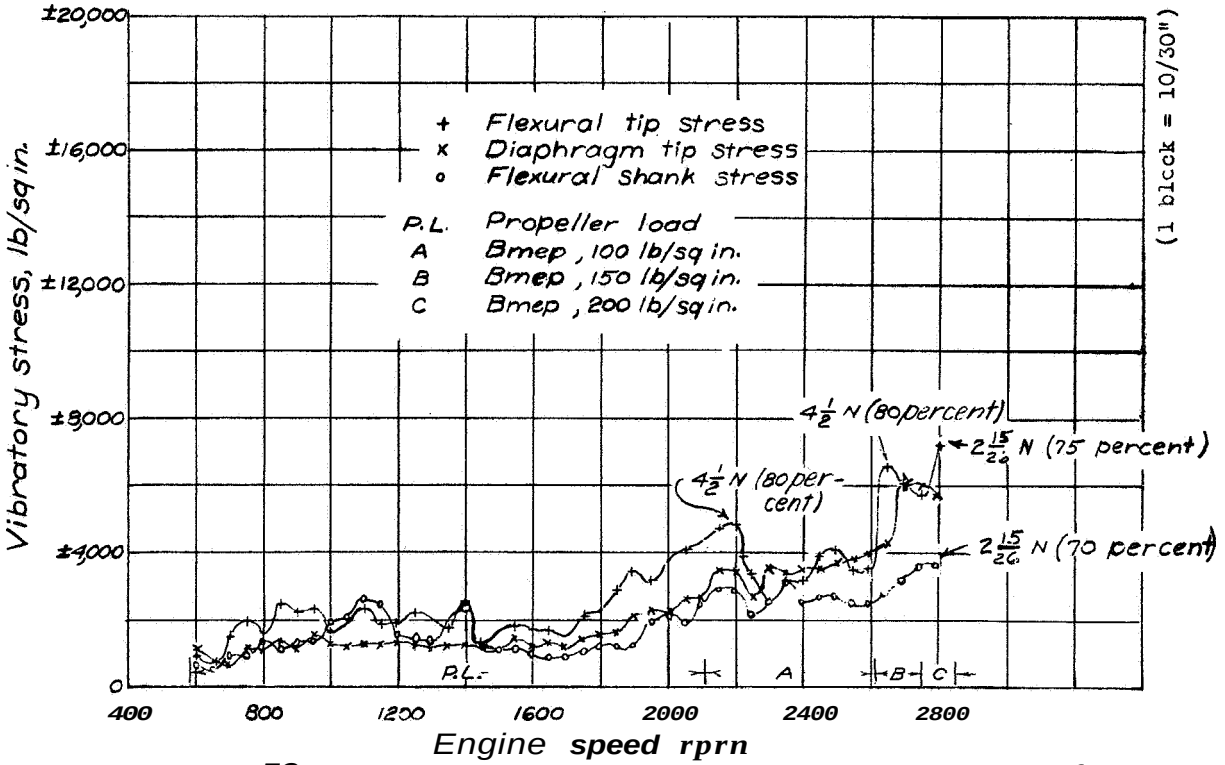

Figure 53.-Maximum composite curves of vibratory stress for test 8. Pusher; 8 blades; rear propeller, hollow steel, β=21.6"

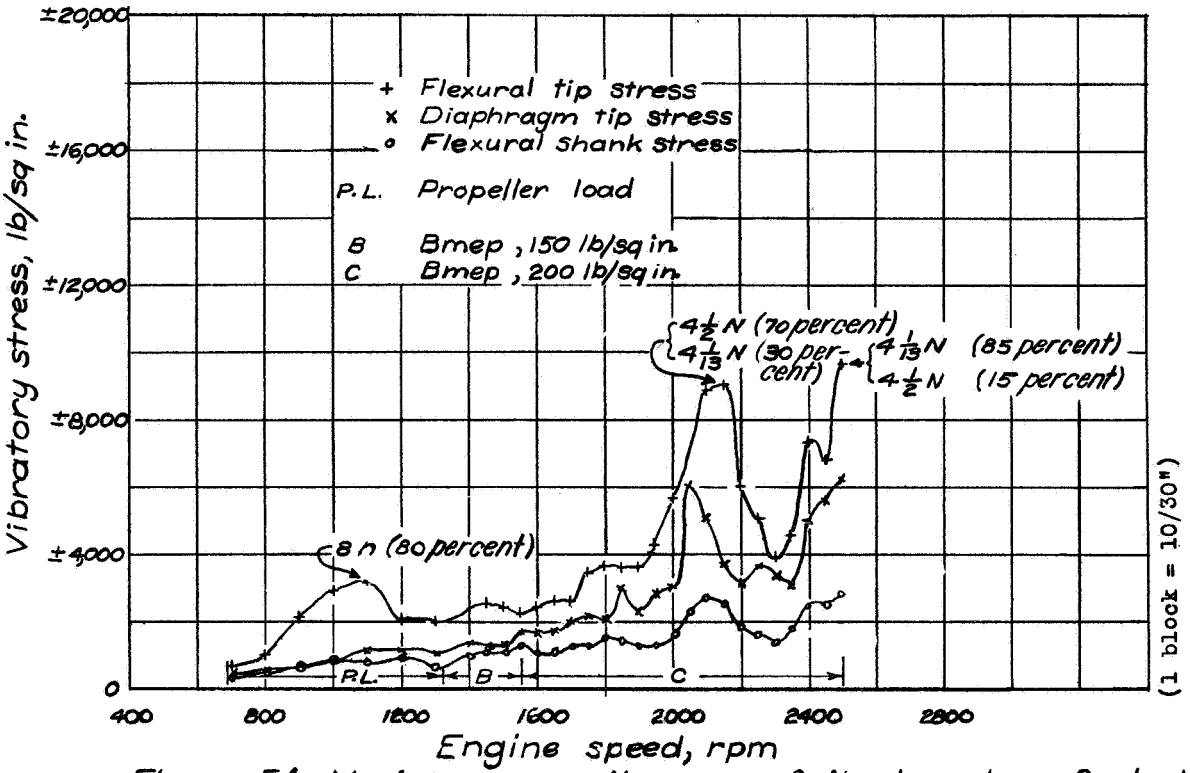

Figure 54.- Maximum composite curves of vibratory stress for test 8
Pusher; 8 blades; front propeller, hollow steel B=34.8°

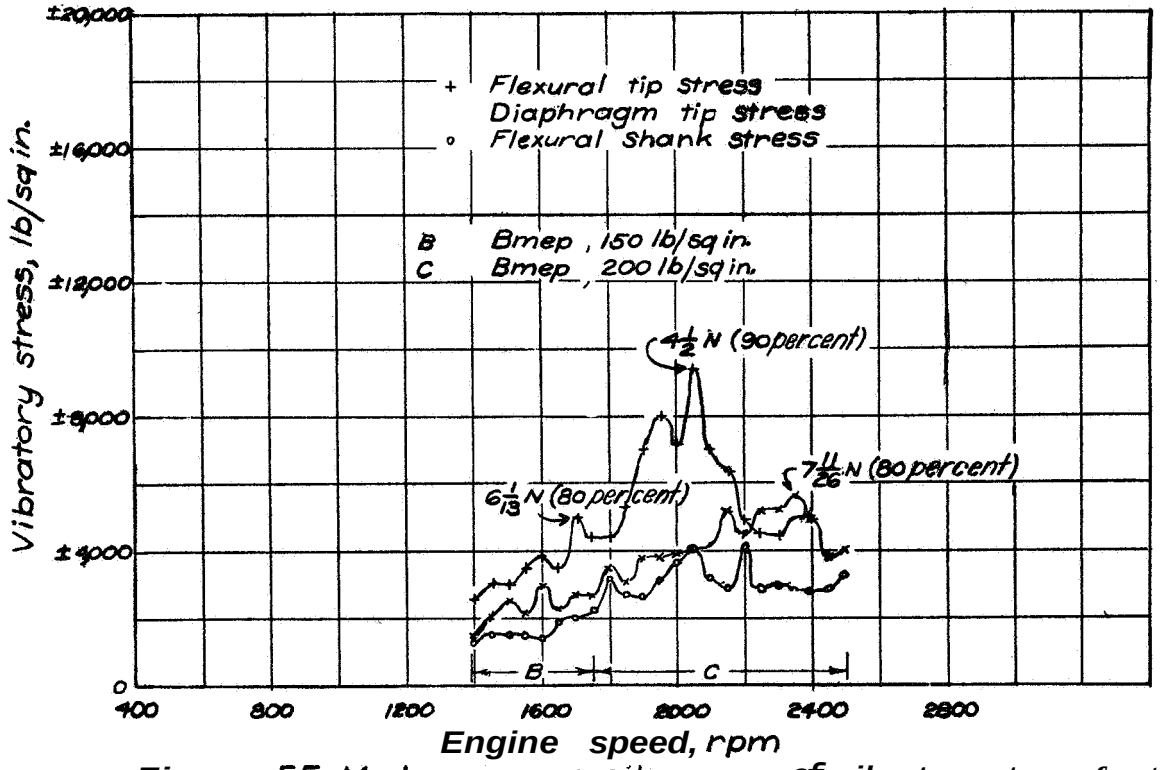

Figure 55.- Maximum composite curves of vibratory stress for test 8.
Pusher; 8 blades; rear propeller, hollow steel; β=35.0°